IDENTIFICATION OF WEED SPECIES AND GLYPHOSATE-RESISTANT WEEDS USING HIGH RESOLUTION UAS IMAGES

A Dissertation
Submitted to the Graduate Faculty
of the
North Dakota State University
of Agriculture and Applied Science

By

Alimohammad Shirzadifar

In Partial Fulfillment of the Requirements
for the Degree of
DOCTOR OF PHILOSOPHY

Major Department:
Agricultural and Biosystems Engineering

November 2018

Fargo, North Dakota

North Dakota State University
Graduate School

Title

IDENTIFICATION OF WEED SPECIES AND GLYPHOSATE-RESISTANT WEEDS USING HIGH RESOLUTION UAS IMAGES

By

Alimohammad Shirzadifar

The Supervisory Committee certifies that this ***disquisition*** complies with North Dakota State University's regulations and meets the accepted standards for the degree of

DOCTOR OF PHILOSOPHY

SUPERVISORY COMMITTEE:

Sreekala G. Bajwa
Chair

Peter Oduor

Kirk Howatt

Igathinathane Cannayen

Approved:

11/21/2018
Date

Sreekala G. Bajwa
Department Chair

ABSTRACT

Adoption of a Site-Specific Weed Management System (SSWMS) can contribute to sustainable agriculture. Weed mapping is a crucial step in SSWMS, leads to saving herbicides and protecting environment by preventing repeated chemical applications. In this study, the feasibility of visible and near infrared spectroscopy to classify three problematic weed species and to identify glyphosate-resistant weeds was evaluated. The canopy temperature was also employed to identify the glyphosate-resistant weeds. Furthermore, the ability of UAS imagery to develop accurate weed map in early growing season was evaluated. A greenhouse experiment was conducted to classify waterhemp (*Amaranthus rudis*), kochia (*Kochia scoparia*), and lambsquartes (*Chenopodium album*) based on spectral signature. The Soft Independent Modeling of Class Analogy (SIMCA) method on NIR (920-2500 nm) and Vis/NIR (400-2500 nm) regions classified three different weed species with accuracy greater than 90 %. The discrimination power of different wavelengths indicated that 640, 676, and 730 nm from red and red-edge region, and 1078, 1435, 1490, and 1615 nm from the NIR region were the best wavelengths for weed species discrimination. While, wave 460, 490, 520 and 670 nm from Vis range, and 760, 790 nm from NIR region were the significant discriminative features for identifying glyphosate-resistant weeds. Random Forest was able to detect glyphosate-resistant weeds based on spectral weed indices with more than 95% accuracy. Analysis of thermal images indicated that the canopy temperature of glyphosate-resistant weeds was less than susceptible ones early after herbicide application. The test set validation results showed the support vector machine method could classify resistant weed species with accuracy greater than 95 %. Based on the stepwise method the best times for discrimination of kochia, and waterhemp resistant were 46 and 95 hours after glyphosate application, respectively. In addition, a field study was proposed on

soybean field to identify weed species and glyphosate-resistant weeds using multispectral and thermal imagery. Results revealed that the object-based supervised classification method could classify weed species with greater than 90% accuracy in early growing season. Furthermore, the glyphosate-resistant kochia, waterhemp and ragweed were identified based on canopy temperature with 88%, 93% and 92% accuracy, respectively.

ACKNOWLEDGEMENTS

I am deeply grateful to all of those with whom I have had the pleasure to work during my Ph.D. curriculum. The Members of my Dissertation Committee have provided me extensive personal and professional guidance and taught me a great deal about both scientific research and life in general. I would especially like to thank my supervisor, prof. Sreekala Bajwa. As my teacher and mentor, she has guided me and encouraged me to carry on through these years and has contributed to this dissertation with a major impact. She has shown me what a good scientist (and person) should be. Thank you as well for guiding me, often with big doses of patience, through the subtleties of scientific writing. I extend my sincere thanks to Eng. John Nowatzki for his guidance, patience and valuable suggestions over the past four years.

Nobody has been more important to me in the pursuit of this project than the members of my family. A very special word of thanks goes for my parents, whose blessing and guidance are with me in whatever I pursue. Most importantly, I wish to thank my love who provides unending inspiration and always shows how proud she is of me.

DEDICATION

To my Parents

To my Love

Thank you for your unconditional love and encouragement.

TABLE OF CONTENTS

ABSTRACT iii

ACKNOWLEDGEMENTS v

DEDICATION vi

LIST OF TABLES xii

LIST OF FIGURES xiv

LIST OF ABBREVIATIONS xvii

LIST OF SYMBOLS xviii

1. INTRODUCTION 1

1.1. Motivation 1

1.1.1. Intellectual Merit and Broader Impact 5

1.1.2. Research Approach 6

1.2. Hypothesis and Objectives 7

1.2.1. Dissertation Objectives 7

1.3. Dissertation Structure 8

1.4. Literature Review 10

1.4.1. Herbicide Resistance 10

1.4.2. How Resistance Occurs 12

1.4.3. Mechanisms of Weed Resistance to Herbicides 13

1.4.4. Shikimate Accumulation 14

1.4.5. Plant Canopy Temperature 14

1.4.6. Alternatives to the Stress Indices 19

1.4.7. Weed Scouting 19

2. SIMCA ANALYSIS OF PLANT CANOPY SPECTRAL DATA 23

2.1. Abstract 23

2.2. Introduction 24
2.3. Materials and Methods 27
2.3.1. Greenhouse Experiment 27
2.3.2. Spectral Data Acquisition 29
2.3.3. Spectral Data Pre-Processing 30
2.3.4. SIMCA Analysis 32
2.3.5. Model Performance Evaluation 34
2.4. Results and Discussion 35
2.4.1. Overview of Canopy Reflectance 35
2.4.2. Spectral Pre-Processing 36
2.4.3. Classification by SIMCA 39
2.4.4. Model Distance 43
2.4.5. Discrimination Power Plot and Wavebands Selection 45
2.5. Conclusion 48
2.6. Acknowledgement 49
3. DEVELOPMENT OF SPECTRAL INDICES FOR IDENTIFYING GLYPHOSATE-RESISTANT WEEDS 50
3.1. Abstract 50
3.2. Introduction 51
3.3. Materials and Methods 53
3.3.1. Greenhouse Experiment 53
3.3.2. Herbicide Treatments 54
3.3.3. Spectral Signature Recording and Datasets 54
3.3.4. Development of Specific Indices for Identifying Glyphosate-Resistant Weeds 54
3.3.5. Feature Selection 56
3.3.6. Random Forest Classifier 57

3.3.7. Classifier Performance Evaluators 58
3.3.8. Vegetation Indices (VIs) 59
3.3.9. Software 59
3.4. Results and Discussion 60
3.4.1. Overview of Canopy Reflectance 60
3.4.2. Relief-F Analysis for Feature Selection 62
3.4.3. Relief-F Analysis for Feature Selection 63
3.4.4. Random Forest Analysis 64
3.4.5. Vegetation Indices (VI) 65
3.5. Conclusion 66
3.6. Acknowledgement 67
4. CAN CANOPY TEMPERATURE DIFFERENTIATE GLYPHOSATE-RESISTANT WEEDS IN CROP FIELDS? 68
4.1. Abstract 68
4.2. Introduction 69
4.3. Materials and Methods 72
4.3.1. Greenhouse Experiment 72
4.3.2. Thermal Images Acquisition 74
4.3.3. Measurement of Photosystem II Efficiency 78
4.3.4. Feature Selection with Stepwise Regression Analysis 78
4.3.5. SVM Classification 79
4.3.6. Non-Linearly Separable Binary Classification 80
4.3.7. Evaluation of SVM Classification 83
4.3.8. Software 84
4.4. Results and Discussion 84
4.4.1. Plant Canopy Temperature of Glyphosate-Resistant and Susceptible Weeds 84

4.4.2. Stepwise Regression Analysis for Feature Selection 87
4.4.3. Measurement of Photosystem II Efficiency 91
4.4.4. SVM Analysis 93
4.5. Conclusion 94
4.6. Acknowledgment 95
5. FIELD IDENTIFICATION OF WEED SPECIES AND GLYPHOSATE-RESISTANT WEEDS BASED ON UAS IMAGERY IN EARLY GROWING SEASON 96
5.1. Abstract 96
5.2. Introduction 97
5.3. Materials and Methods 100
5.3.1. Study Site and Field Experiment Design 100
5.3.2. Data Collection 102
5.3.3. Image Calibration 103
5.3.4. Image Mosaicking 103
5.3.5. Spectral Separability Analysis 104
5.3.6. Segmentation Procedure 106
5.3.7. Image Classification 106
5.3.8. Glyphosate-Resistant Weed Identification 108
5.4. Results and Discussion 111
5.4.1. Spectral Reflectance Separability 111
5.4.2. Crop and Weed Species Classification Accuracy 112
5.4.3. Glyphosate-Resistant and Glyphosate-Susceptible Weed Accuracy 117
5.5. Conclusions 120
5.6. Acknowledgment 121
6. SUMMARY AND CONCLUSIONS 122
6.1. Future Work 125

REFERENCES 126

LIST OF TABLES

Table		Page
2.1.	The test set validation results of the SIMCA analysis for classification of three weed species in the wavelength region of 400-920 nm, using different pre-processing methods.	40
2.2.	The test set validation results of the SIMCA analysis in the wavelength region of 920-2500 nm using different pre-processing methods.	41
2.3.	The test set validation results of the SIMCA analysis performed to classify three weed clusters using all spectral information (400-2500 nm) and different pre-processing methods.	42
2.4.	The summary of the SIMCA analysis performed to classify three weed clusters.	43
2.5.	The model distance value for the three weed clusters obtained from the best SIMCA model in 400-920 nm and 920-2500 nm wavelength regions.	44
3.1.	Selected discriminative wavebands for developing SWIs.	62
3.2.	SWIs for identifying glyphosate-resistant weeds.	63
3.3.	Confusion matrix of RF classification.	64
3.4.	Statistical measurements of the performance of RF.	65
3.5.	The most discriminative VI which identify glyphosate-resistant type of weed species.	66
3.6.	Statistical measurements of the performance of VI.	66
4.1.	The effect of glyphosate application on leaf water content of weed species.	87
4.2.	Model summary of stepwise regression for feature selection.	89
4.3.	Stepwise regression model developed from thermal signatures weeds.	91
4.4.	Confusion matrix of SVM classification.	93
4.5.	Statistical measurements of the performance of SVM.	94
5.1.	Summary of used cameras and flight procedures in the study.	102
5.2.	The input information used for segmenting field image into objects for object-based classification.	106

5.3. Atmospheric conditions during the period of data collection in Carrington (S1) and Mayville (S2) study sites. 109

5.4. Classification accuracy of weed species using different supervised classification algorithms at Carrington (S1) and Mayville (S2) study sites. 113

5.5. Mean values of canopy temperatures in Carrington (S1) and Mayville (S2) study sites. 117

5.6. Summary of glyphosate-resistant weed classification accuracy at Carrington (S1) and Mayville (S2) study sites. 120

LIST OF FIGURES

Figure Page

1.1. Structure of glyphosate molecule and its functional groups. 2

1.2. Glyphosate-resistant weeds distribution across the United States and its diversity trend around the world. 3

1.3. Dissertation overview and organization of the chapters. 8

1.4. How resistance occurs. (a) Herbicide application imposing a selection pressure on a mixed population. Light green: herbicide sensitive; dark green: herbicide resistant. (b) Repeated use of the same herbicide will repeat the selection process. 12

2.1. (a) Experimental set up in the NDSU greenhouse and the three weeds addressed in the study namely, (b) Waterhemp, (c) Kochia, and (d) Lambsquarters..... 28

2.2. The average canopy reflectance spectra of three weed species, including kochia, waterhemp, and lambsquarters in Vis/NIR wavelengths. 36

2.3. The PCA scores of the samples of kochia, lambsquarters, and waterhemp weed species obtained from the best pre-processing methods in the (a) 400-920 nm, (b) 920-2500 nm, and (c) the whole spectral region..... 38

2.4. The discrimination power plot for the three weed clusters obtained from the best SIMCA model in (a) 400-920 nm and (b) 920-2500 nm wavelength regions. 46

3.1. Flowchart showing the main steps involved in developing glyphosate-resistant weeds identification indices 55

3.2. Spectral signature of three-weed species in the range of 450-920 nm. 61

4.1. a) Experimental set up in the NDSU greenhouse showing cones of weed plants of the resistant and susceptible types. Three weeds addressed in this study were b) Waterhemp, c) Kochia, and d) Ragweed. 73

4.2. A cabinet sprayer, where weed plants are being sprayed with the recommended dose of glyphosate..... 74

4.3. A sample thermal image of the weed plants viewed in the IR Flash software. The average temperature for the various zones can be seen on the right-hand panel. 75

4.4. Thermal camera set up in the NDSU greenhouse, with a close-up of the thermal camera, and the plant racks placed on a table. 76

4.5. Relative humidity fluctuation during data collection in the greenhouse. 77

4.6. A visual illustration of resistant and susceptible weeds..... 77

4.7. A schematic illustration of the Support Vector Machine (SVM) classification method illustrating the hyperplane classifier between two classes (Bajwa & Kulkarni, 2011). 80

4.8. The difference between plant canopy temperature and ambient temperature (thermal signature) of resistant and susceptible three weed species (a) Waterhemp, (b) Kochia, and (c) Ragweed over time for the first 96 h after a glyphosate application. 85

4.9. The difference between plant canopy temperature and ambient temperature of resistant and susceptible three weed species vs. relative humidity: (a) Waterhemp, (b) Kochia, and (c) Ragweed. 86

4.10. Features selected by the stepwise regression process plotted for resistant and susceptible plants of a) Kochia, b) Waterhemp, and c) Ragweed. 90

4.11. Comparison of photosynthesis's performance measured from 1 to 4 days after glyphosate application on the weeds (Error bars represent the standard deviations). No significant difference was observed in the photosynthetic efficiency for different weed species in the first day. However, resistant weeds exhibited significantly higher photosynthetic efficiency than susceptible weeds 92

5.1. Field sites: a) Google Maps® inset showing the general location of the study sites with blown up views of fields at b) Carrington, c) Mayville. 101

5.2. A multispectral image illustrating the target classes in the two study sites: a) Carrington (false color image), b) Mayville (RGB image). 101

5.3. Calibrating RGB band Digital Numbers (DNs), in an empirical line correction approach. a) Blue band, b) Green band, c) Red band. 105

5.4. Flowchart of recognition algorithms applied for object classification and weed species detection and glyphosate resistant weeds. 110

5.5. Assessment of feasibility of field components classification in Carrington study site: a) Spectral signature, b) PC plane, and c) Scatterplot of spectral reflectance. Band number 1 through 4 are RGB, 670,710,730 nm. 111

5.6. Assessment of feasibility of field components classification in Mayville study site: a) Spectral signature, b) PC plane, and c) Scatterplot of spectral reflectance. Band number 1 through 4 are RGB, 670,710,730 nm. 112

5.7. Comparison of a) PBIA and b) OBIA classification algorithms in Carrington study site. 114

5.8. Comparison of a) pixel- and b) object-based classification algorithms in Mayville study site. 115

5.9. A thermal image of the waterhemp plants (Carrington study site) in IR Flash software. Zone 1(green) indicates Resistant waterhemp. And Zone 2 (red) indicates susceptible waterhemp. The average temperature for the various zones can be seen on the right-hand panel. 118

5.10. The thermal image of the ragweed plants (Mayville study site) in IR Flash software. Zone 1 (blue) # Resistant ragweed. Zone 2 (green) # susceptible ragweed. The average temperature for the various zones can be seen on the right-hand panel. 119

LIST OF ABBREVIATIONS

BLW.....Broadleaf weeds.

BSBC .....Best spectral band combination.

CCD .....Charge coupled device.

InGaAs .....Indium gallium arsenide.

LDA .....Linear discriminant analysis.

MSC .....Multiplicative scatter correction.

NIR.....Near infrared.

PCA.....Principal component analysis.

PCs .....Principal components.

PLS-DA.....Partial least squares discriminant analysis.

SIMCA.....Soft independent modeling of class analogy.

SNV.....Standard normal variate.

SSWMS.....Site-specific weed management system.

UAS.....Unmanned aerial system.

Vis/NIR .....Visible and near infrared.

VN.....Vector normalization.

LIST OF SYMBOLS

A.....Number of principal components in the model.

a_0 .....The average value of the sample spectra.

a_1 .....The standard deviation of the sample-spectra.

d_k .....Discrimination power of the variable k.

d (r, g).....The distance between r and g groups.

E .....Residual variance.

e_t .....The residual variance vector.

F .....The Fischer's F-test.

L .....Loadings matrix.

S^2_{total} .....The total residual variance.

S^2_u.....Residual variance for the tested sample.

T .....Scores matrix.

$t_i l_i^T$ .....The i^{th} orthogonal principal components.

t_u .....The estimate of the scores vector.

X_{cor} .....Corrected spectra.

$X_{i,\ fsd}$ .....The first-order derivative at wavelength i.

X_{org} .....Original sample spectra.

X_{ref}.....Total weight loss.

X_t.....Reference spectrum.

1. INTRODUCTION

1.1. Motivation

Weeds are the biggest threat to crop production because they cause significant yield loss in crops, limit crop rotation choices, and host insects and diseases (Cardina & Doohan, 2000; FAOSTAT, 2014; Slaughter et al., 2008). Potential yield loss due to uncontrolled weed growth is estimated to be 43% globally (Oerke, 2006). Weed management is an important aspect of agricultural production as the economic cost of not managing weeds with herbicide is estimated $21 billion approximately in the United States (Yontz, 2014). Herbicide application, which is the most common weed management strategy in the United States agriculture, provides a convenient, economical, and effective way to control weeds. However, the repeated and non-optimal application of herbicides results in herbicide resistance in weeds, excessive waste, herbicide residues in food, and environmental pollution with potential impact on human health, ecosystems, and quality and safety of agriculture products (Gil & Sinfort, 2005; Pimentel et al., 1992).

Among all different types of herbicides, glyphosate is the most applied herbicide in the world. Glyphosate or N-(phosphonomethyl) glycine is the aminophosphonic acid analog of the natural amino acid glycine. It was supposed to be first synthesized by Henri Martin in 1950. Glyphosate is widely used herbicides in agriculture, industrial weed control, forestry, and in outdoor residential applications in the United States. It was first registered for use in the United States in 1974. Glyphosate is a non-selective broad-spectrum, systemic, POST application herbicide, which prevents the plants from making certain proteins that are needed for plant growth. It comes in a number of chemical forms but most of the formulated products contain the isopropylamine salt. Glyphosate is a compound with an amphoteric and zwitterion structure

containing a basic secondary amino function in the middle of the molecule, monobasic-carboxylic and dibasic phosphonic acidic sites at both ends, hence having three functional groups, phosphonate, amino and carboxylic. A zwitterion is a neutral molecule with positive and negative electrical charges at different locations within the same molecule. It is different from simple amphoteric compounds that might only form either a cationic or anionic species depending on external conditions—a zwitterion simultaneously has both ionic states within the same molecule (Figure 1.1).

Figure 1.1. Structure of glyphosate molecule and its functional groups.

Recently, several species of glyphosate-resistant weeds are spreading across the United States and around the world, raising concerns about their potential impact on agriculture. Figure 1.2 presents the chronological increase in glyphosate-resistant weeds around world. Based on developed United States weed maps glyphosate-resistant weeds are in 35 states. Furthermore, the diversity of glyphosate-resistant weeds has been increasing sharply (Figure 1.2). However, weed mapping can be significant solution to choose the proper strategy against the formation and developing of herbicide-resistant weeds in agricultural fields.

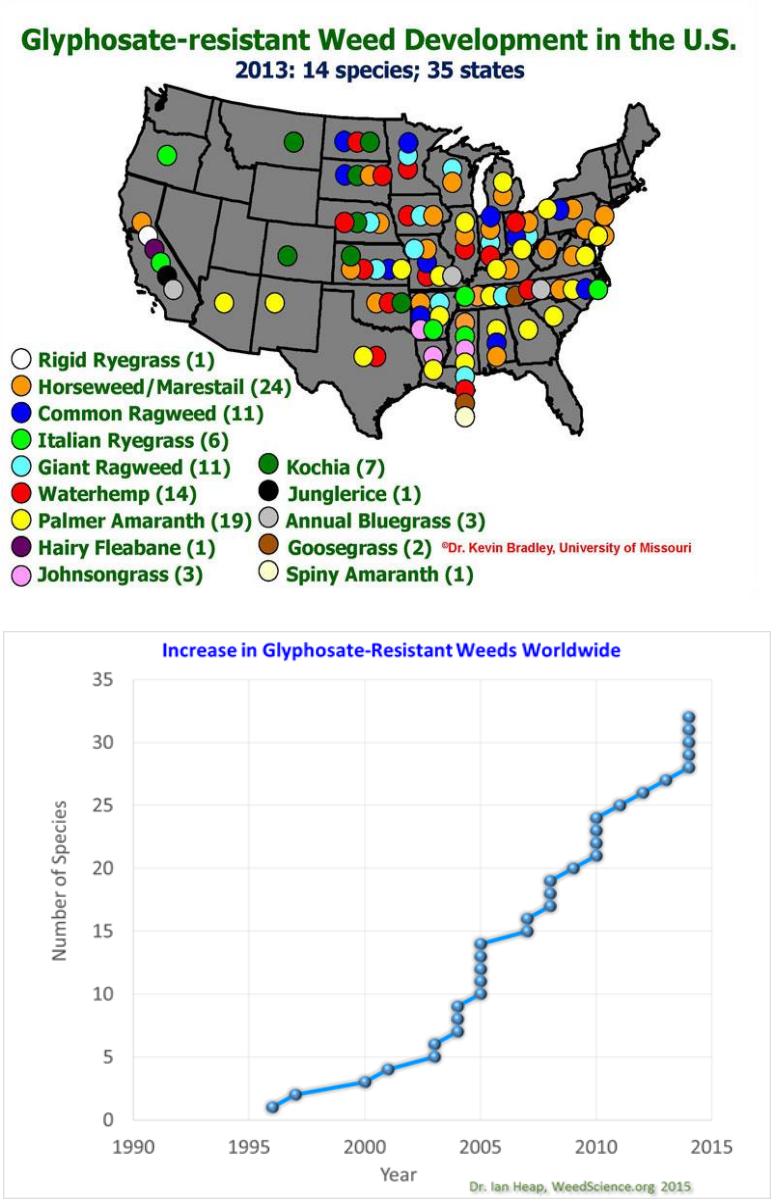

Figure 1.2. Glyphosate-resistant weeds distribution across the United States and its diversity trend around the world.

Weed distribution in fields is non-uniform, with field borders being the most infested by weed patches. Yet, herbicides are applied uniformly across the whole field. These problems can be reduced by more targeted methods of herbicide application. Therefore, there is a growing need to identify and map weed distribution in the field to reduce herbicide application. Adoption of a sustainable weed management strategy can improve the efficiency of herbicide application

without diminishing weed control. (Slaughter et al., 2008; Weis et al., 2008). Site-specific weed management (SSWM) is an efficient method that has been proposed to achieve satisfied weed control (Torres-Sánchez et al., 2013). In this procedure, farmers only apply the right amount of herbicide to the specific location at the right time. This application of Precision Agriculture (PA) can minimize chemical usage and herbicide resistance because it decreases the opportunity for selection of herbicide tolerant strains of weeds by minimizing the chance of survival through application of suboptimal concentrations of herbicide.

Weed scouting (early detection of weed) and quick target spraying (applying herbicide only on the weeds instead of soil and crop) are two critical key components of a SSWM. Several approaches were reported for weed identification with sensing technologies, visual texture, and spectral characteristics of plants (Pantazi et al., 2016; Tian, 2002).

Discrimination between weeds and crop plants is the first step needed to apply SSWM (Gutjahr & Gerhards, 2010). Visible wavelengths remote sensing is one method of acquiring information for SSWM application (Peña et al., 2013). However, the use of satellite imagery for weed detection at the early stages of weed growth is limited by the lack of spatial and spectral resolution of the satellite sensors to detect small plants (Peña et al., 2013). UASs or drones are an alternative means of collecting high spatial and temporal resolution Vis and NIR imagery (Garcia-Ruiz et al., 2015). They are easily deployed, relatively low-cost and have a flexible payload capability that allows them to be fitted with lightweight sensors such as multispectral cameras (Von Bueren et al., 2015).

Multispectral remote sensing refers to the collection of reflected, emitted or back-scattered energy from an object of interest in multiple bands (regions) of the electromagnetic spectrum. The bands are sensitive to different features of the object, so they can be used to detect

weeds and crop, and to classify weed plants based on difference in spectral signatures (Garcia-Ruiz et al., 2015). Image processing techniques potentially can be used to discriminate the weed species from the crop plants and thereby produce an accurate weed map from the multispectral imagery (Lee et al., 2010).

This research has the potential to demonstrate a procedure for identifying spectrally unique signatures from the weed species and glyphosate-resistant weeds, introducing canopy temperature to discriminate glyphosate-resistant versus susceptible weeds and employing them as the basis for multispectral and thermal imagery to map weeds in the field.

1.1.1. Intellectual Merit and Broader Impact

Despite the satisfactory results of weed versus crop classification based on spectral reflectance, this technique has not been used, to the best of our knowledge, to discriminate weed species using the Vis/NIR spectrometers. Since processing the huge spectral dataset is complicated, selecting the optimal statistical analysis method is a crucial step in the classification of weed species accurately in efficient time. Furthermore, if resistant weeds can be mapped without having to scout the fields, it would contribute to the effectiveness of weed management. Timely identification of resistant weeds is the first step in managing them effectively, as the farmers can then make decisions for appropriate alternate weed management methods. Currently, there is no cost-effective method to identify the distribution of herbicide resistant weeds on large fields. We developed a method and an algorithm to identify major glyphosate-resistant weeds in the field using UAS imagery. Therefore, this study was conducted with the objective developing and validating a method in the greenhouse to identify resistant from susceptible weeds in selected weed species, using canopy temperature and spectral signature early after herbicide

application. We introduce the concept of thermal signature in this study for detecting resistant weeds in greenhouse conditions.

Remote sensing will provide an inexpensive and more efficient method for mapping weed infestations than ground surveys. Early and easier detection of herbicide resistant weeds would allow growers to effectively manage these weeds by applying another herbicide or using manual method before the plant seeds and spreads. Herbicide resistance in weeds is becoming an increasing problem, with serious implications to crop yield and weed management costs. With the rapid adoption of glyphosate-resistant crops, glyphosate use increased more than six-fold from 1992 to 2002 (Gianessi & Reigner, 2006). With this adoption there has been tremendous increase in the incidence of glyphosate-resistant weeds in the United States and around the world. Identifying weed species and resistant biotypes and mapping their distribution in a field is a first step in managing these weeds in the field. Farmers will benefit greatly from identifying resistant weeds and weed species in their fields by implementing integrated weed management practices early in development to prevent it from becoming more devastating within a short time period.

1.1.2. Research Approach

This study focused on the classification of three common glyphosate-resistant weed species considering spectral signature of weeds. Spectral weed species indices were developed using discriminative wavelengths to identify glyphosate-resistant weeds. Furthermore, this study introduced a new concept for identifying glyphosate-resistant weeds based on plant canopy temperature early after glyphosate application. Classifying weed species and identifying glyphosate-resistant weeds using UAS images in early growing season was the final goal of this project.

1.2. Hypothesis and Objectives

1.2.1. Dissertation Objectives

The long-term goal of this project was to develop a method for identifying herbicide resistant weeds. The project was divided into four objectives and the study had the following sub-objectives:

1.2.1.1. Sub-Objectives

1. To develop a methodology for classifying weed species and detecting glyphosate-resistant weeds from susceptible ones based on spectral reflectance.
2. To develop the spectral weed indices for detecting glyphosate-resistant weeds early after spraying.
3. To evaluate glyphosate-resistant weeds identification based on plant canopy temperature early after herbicide application.
4. To employ the proper image processing method for weed mapping in early growing season.

1.2.1.2. Dissertation Hypothesis

1. There is a significant difference between spectral signature of weed species, and also between glyphosate-resistant weed and susceptible one.
2. Machine learning methods can find the wavebands which are useful to classify weed species and to identify glyphosate-resistant weeds with high accuracy.
3. Canopy temperature of susceptible weeds increase after herbicide application compared to glyphosate-resistant weeds.

4. There is an image processing method that can be used for accurate classifying weed species in early growing season, when there are a lot of mixed pixels in the acquired images.

1.3. Dissertation Structure

This manuscript-based dissertation divided into six chapters; Chapter one includes a general introduction and literature review. Chapters two to five include the main findings of this dissertation, and chapter six contains an overall discussion of the research related to the sub-objectives outlined above. A schematic for the organization of the dissertation is presented in Figure 1.3.

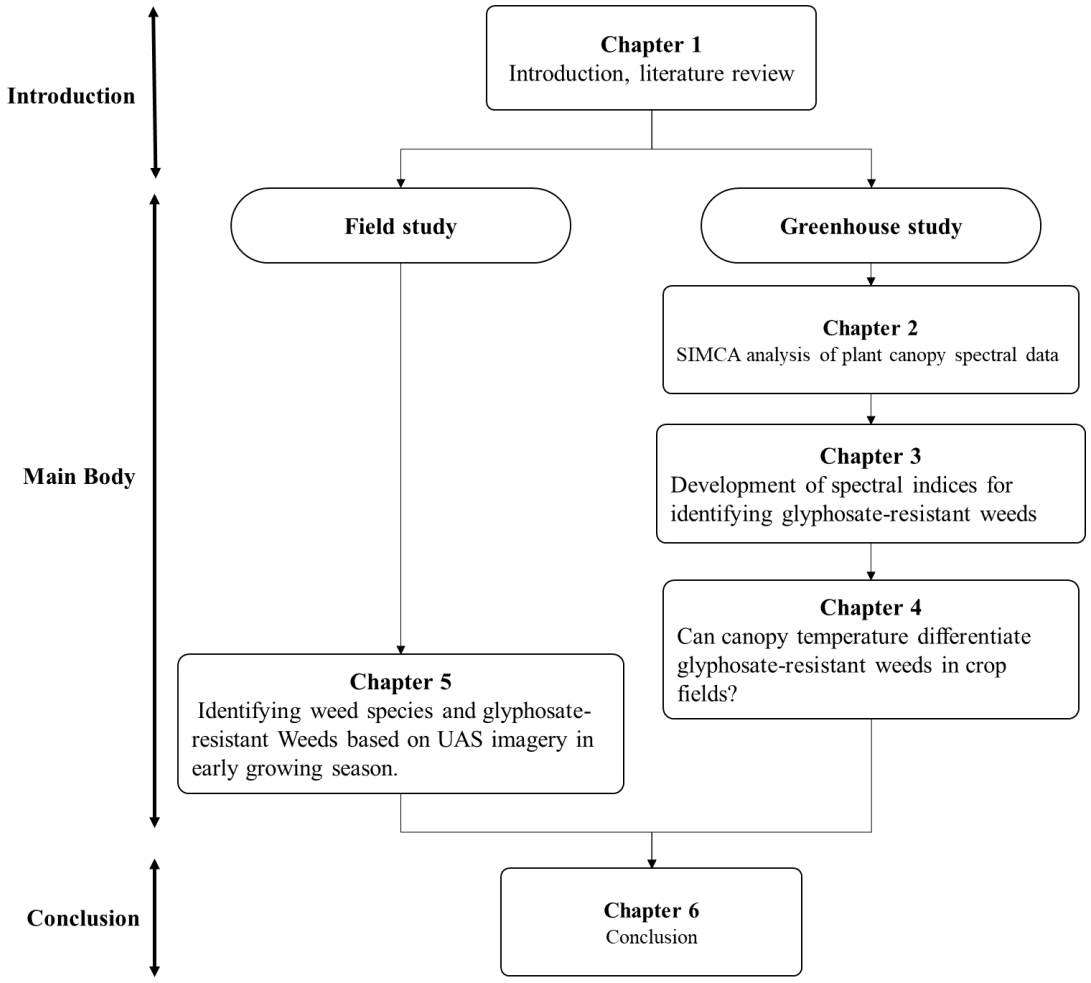

Figure 1.3. Dissertation overview and organization of the chapters.

Chapter 1 offers a comprehensive introduction and literature review on the importance of weed species classification approach. Particularly, the application of different techniques on detecting the glyphosate resistance status in weed species is discussed. This chapter identifies the current challenges in identifying resistant weeds. The objectives and hypothesis of the dissertation are also defined in chapter one.

Chapter 2 presents a paper published in *Biosystem Engineering 171 (2018), 143-154*. This chapter provides a comprehensive greenhouse study on the application of soft independent modelling of class analogy (SIMCA) analysis of plant canopy spectral data to classify weed species.

Chapter 3 is based on a greenhouse study which is evaluating the feasibility of spectral weed indices (SWIs) to identify glyphosate-resistant weeds early after herbicide application. In this study Relief-F algorithm was employed to select the significant and most relevant wavelengths describing the detrimental effect of glyphosate application for three different weed species.

Chapter 4 reports a case study to assess the application of plant canopy temperature after glyphosate application as an indicator for glyphosate resistant weeds. In this work the stepwise regression and support vector machine (SVM) methods were used to analyze the discriminative time features to classify resistant weeds based on canopy temperature.

Chapter 5 is based on a field study validating the potential application of high resolution multispectral and thermal UAS images in classification of weed species and glyphosate-resistant weeds at early phenological stage. Six classification algorithms were used to identify three different weed species in a soybean field and a field which was naturally infested by different

weed species. Thermal infrared imagery was also used to assess the canopy temperature variance within the weed species to identify the glyphosate- resistance status in detected weeds

Chapter 6 includes significant conclusions and recommendation for further research on weed species classification methods and weed mapping.

1.4. Literature Review

1.4.1. Herbicide Resistance

Herbicides are effective and popular for weed control which can be so helpful to increase crop yield and quality (Harker et al., 2013). Development of herbicide-resistant crops has resulted in significant positive changes to agronomic practices, while repeated and intensive use of herbicides with the same mechanisms of action has caused the evolution of herbicide-resistant weeds. Upward trend of developing herbicide resistant weeds is a critical problem in all around the world which effect on the yield crops (Evans & Diggle, 2008). The result of one survey in the US indicated that farmers and neighbors who successfully managed glyphosate-resistant weeds in corn and soybean crop improved their profits by more than 20% (Livingston et al., 2015). Glyphosate or N-(phosphonomethyl) glycine is a widely used herbicides in agriculture and forestry for industrial weed control, and in outdoor residential applications in the US. It is a non-selective broad-spectrum, systemic, post-herbicide that prevents the plants from making certain proteins that are vital for plant growth (Jayasumana et al., 2014). Two glyphosate resistance mechanisms have been identified in naturally occurring glyphosate-resistant weeds namely, reduced target-site affinity for glyphosate and reduced translocation of glyphosate to meristematic regions (Pollegioni et al., 2011).

Herbicide resistance was reported by Ryan in 1970. The first herbicide-resistant weed was common groundsel (*Senecio vulgaris*) that was shown to be resistant to atrazine and

simazine after the herbicides had been applied once or twice annually for 10 years in Washington State. Herbicide resistance might be occurred prior to this date while it was interpreted as a poor weed control. Survey herbicide resistance has been continued by Weed Science Society of America's Herbicide Resistant Weeds Committee. In 1986, over 50 weeds were resistant to triazines, and over 107 resistant biotypes had evolved around the world. Rapid developing resistance to atrazine and other classes of herbicide cause the phenomenon of resistance has become major problem in agriculture.

Inherited ability of a weed population (biotype) to survive and reproduce after exposure to an herbicide dose (rate) that would control an unselected (sensitive) population. Inherent in this definition are three important points:

1. Herbicide resistance is inheritable, so it is a characteristic coded for in the plant genome. At least some of the progeny of that plant will either be resistant or will carry the resistance trait. This distinguishes herbicide resistance from other causes of poor herbicide efficacy, perhaps caused by environmental factors including their effect on spray effectiveness, plant physiology and biochemistry.
2. Herbicide - resistant plants survive herbicide treatment and can successfully complete their life cycle by flowering and producing seed. This does not mean that resistant individuals will not show symptoms of herbicide damage, but that they are not killed by herbicides. In many cases some herbicide damage may be observed but it does not lead to plant death.
3. A normal population is a population of the species that when treated with an optimum dose of an herbicide, under ideal conditions, all individuals within it are killed. This population will be one that has never been exposed to an herbicide. Such ‘wild - type’

populations are not always available to the researcher, so populations that have demonstrated 100% susceptibility are often used in research, regardless of their field history. To determine baseline sensitivity for an herbicide acting on a distinct species, several normal populations are ideally used.

1.4.2. How Resistance Occurs

Selection pressure*:* repeated and intensive use (frequency and number of acres treated) on the same field site of herbicides with similar modes of action has imposed selection for increased resistance within species that formerly had been susceptible. The plants that are susceptible are killed. The resistant population survives and reproduce, so year upon year (if the same herbicides are used) the percentage of resistant individuals in a population will increase and comes to dominate (Figure 1.4).

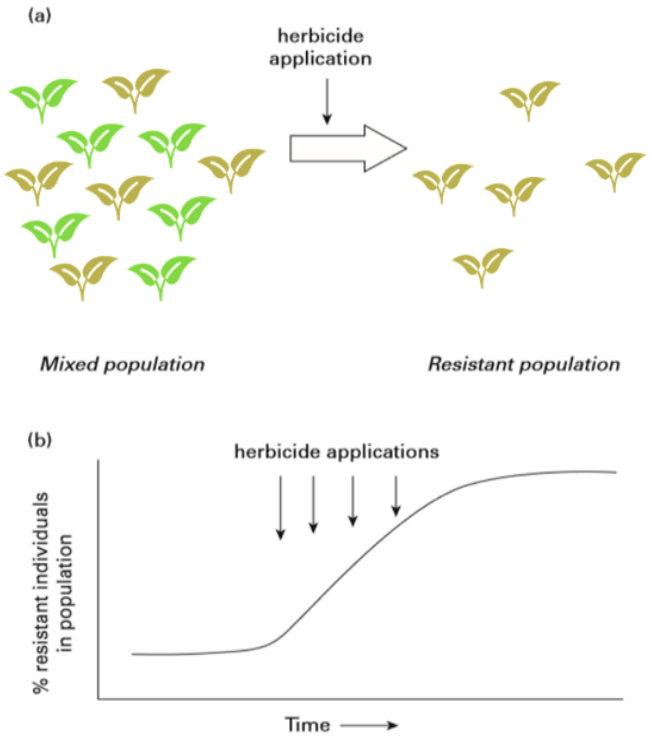

Figure 1.4. How resistance occurs. (a) Herbicide application imposing a selection pressure on a mixed population. Light green: herbicide sensitive; dark green: herbicide resistant. (b) Repeated use of the same herbicide will repeat the selection process.

Since the introduction of herbicide resistant crop (Genetically Modified Organisms, GMOs) and the dramatic decrease in herbicide price, herbicide has been widely used for weed control. This significantly increased the number of acres where herbicide is used and greatly increased the potential for selecting herbicide-resistant weeds.

1.4.3. Mechanisms of Weed Resistance to Herbicides

There are two common mechanisms of weed resistance to herbicides including target site resistance, enhanced metabolism resistance and enhanced compartmentalization. Herbicides have distinct target sites where they disrupt biochemical processes leading to cell, tissue and plant death (Evans & Diggle, 2008). Most target sites are enzymes and the interaction between herbicide and target site can be disrupted if there is a change in the primary structure of the enzyme protein molecule. Where this occurs, the herbicide may no longer be effective in blocking the action of the target site and the plant will not die, but exhibit herbicide resistance. Plants possess a host of enzymes for the metabolism of xenobiotics and unwanted substances (Pollegioni et al., 2011). It is these detoxifying enzymes that modify or break down herbicides once they enter a plant cell. The rate at which these enzymes carry out this task will determine whether a plant lives or dies and is the main contributor to herbicide selectivity between crops and weed species. If an individual weed biotype within a population has the ability to metabolize an herbicide at an increased rate, then it may survive an herbicide treatment. Such biotypes are described as possessing enhanced metabolism resistance.

Both target- and non-target-site-based resistance mechanisms are responsible for glyphosate resistance. Two glyphosate resistance mechanisms have been identified in naturally occurring glyphosate-resistant weeds, reduced target-site affinity for glyphosate and reduced translocation of glyphosate to meristematic regions. Alterations in the EPSPS gene sequence,

specifically at the amino acid P106, have been reported in several glyphosate-resistant weeds. Glyphosate translocation is mostly restricted within the treated leaves, resulting in significantly less translocation throughout the whole plant. The absorption pattern of glyphosate is similar up to 24 hours after herbicide application in resistant susceptible while after this time, resistant plants absorb more herbicide than susceptible weeds (Alcántara-de la Cruz et al., 2016).

1.4.4. Shikimate Accumulation

Shikimate accumulation following glyphosate application has been employed to recognise glyphosate-resistance plants (Corrêa et al., 2016). Quantifying shikimate accumulation in suspected glyphosate- resistant and known susceptible plants can determine whether suspected plants are resistant and can provide data concerning the resistance mechanism. If the resistance mechanism is a mutated target site with a lower affinity for glyphosate, the shikimate accumulation will be lower in the resistant plants than in the known susceptible weeds because of less pathway blockage. If both resistant and susceptible plants accumulate shikimate at the same rate, then pathway blockage is similar, and the target site is inhibited. Resistant and susceptible weeds did not differ in shikimate accumulation at 3 days after treatment, but accumulation slowed between 2 and 3 days after treatment for the resistant populations, while continuing to rise in the susceptible population.

1.4.5. Plant Canopy Temperature

Several studies indicated the reduction of the photosynthetic rate following glyphosate treatment. (Gomes et al., 2017; Mateos-Naranjo et al., 2009; Yanniccari et al., 2012; Zobiole et al., 2012). Glyphosate can influence photosynthesis by inhibiting chlorophyll biosynthesis (Radwan & Fayez, 2016) or inducing chlorophyll degradation (Gomes et al., 2016), decreasing stomatal conductance (Yanniccari et al., 2012). Evaporation of water during photosynthesis

diurnal phase has cooling effect on the plants. However, warmer canopy can happen because of reduced evapotranspiration rates that are often associated with reduced leaf stomatal size openings and prevent plant water lose, after glyphosate application. Plant canopy temperature depends on the radiation and environmental factors such as air temperature, humidity, wind speed, time of day, clear or cloudy sky, and soil conditions (soil type, soil water content, etc.) as well as stomatal aperture. Equation 1.1 exhibits the plant canopy temperature (T_{canopy}) as a function of leaf energy balance (Costa et al., 2013).

$$T_{canopy} - T_{air} = \frac{\left[r_{HR}(r_{aw} + r_s)\gamma R_{ni} - \rho c_p r_{HR} VPD\right]}{\left[\rho c_p\{\gamma(r_{aw} + r_s) + s r_{HR}\}\right]} \quad (1.1)$$

Where T_{canopy} denotes plant canopy temperature (K), T_{air} is air temperature (K), r_{HR} represents parallel resistance to heat and radiative transfer (s m^{-1}), r_{aw} is boundary layer resistance to water vapor (s m^{-1}), γ is the psychrometric constant (Pa K^{-1}), R_{ni} is net isothermal radiation (the net radiation for a plant at air temperature) (W m^{-2}), ρ is density of the air (kg m^{-3}), c_p is specific heat capacity of air (J kg^{-1} K^{-1}), s represents the slope of curve relating saturating water vapor pressure to temperature (Pa K^{-1}), and VPD denotes air vapor pressure deficit (Pa).

Considering Equation 1.1, T_{canopy} is dependent not only on T_{air}, but also on, R_{ni}, VPD, and wind speed (Jones, 1999). Based on energy balance equation, the canopy to air temperature difference ($T_{canopy} - T_{air}$) depends on VPD under non-limiting soil water conditions, a crop transpires at the potential rate (i.e. evapotranspiration is the maximum it can be, but maximum evapotranspiration increases with increasing VPD). Thus, there is a linear relationship between $T_{canopy} - T_{air}$ and VPD when water availability is not limiting, and sky is clear. This linear relationship is known as the theoretical non-water-stressed baseline which provides the minimum possible value of $T_{canopy} - T_{air}$ at a given VPD (Costa et al., 2013). If the goal is to measure the

increase of stress in a crop over time, on the other hand, it is essential to normalize T_{canopy} in relation to references to account for changing meteorology.

Many researches have been conducted to normalize the data to account for environmental variation and resolve this problem. The first normalization technique for environmental difference was a function of T_{air}, achieved by adding differences between T_{canopy} and T_{air} as an indicator of stress in plant. T_{canopy} rises as a result of plant stress (Ben-Gal et al., 2009). The stress degree day is the summation of differences in temperature between the crop canopy and the ambient air along a specific time. In this technique, if T_{canopy} is lower than T_{air}, then plants are expected to be well watered. In contrast, if T_{canopy} is greater than the T_{air}, then plants are assumed to be drought stressed. While this index represents an improvement over the use of T_{canopy} alone, since it allows T_{air} changing, it does not reflect fluctuations in VPD, solar radiation, or wind speed. The $T_{canopy} - T_{air}$ for a non-transpiring crop is insensitive to VPD and can be estimated if wind speed and net solar radiation are known. This sets the 'upper limit' to T_{canopy} – Tair used the idea of 'upper and lower' baselines, to create a crop water stress index (CWSI):

$$CWSI = \frac{\left(T_{canopy} - T_{air}\right) - \left(T_{canopy} - T_{air}\right)_{nwsb}}{\left(T_{canopy} - T_{air}\right)_{ul} - \left(T_{canopy} - T_{air}\right)_{nwsb}} \quad (1.2)$$

Where $T_{canopy} - T_{air}$ is the measured difference in temperature, $(T_{canopy} - T_{air})_{nwsb}$ is the estimated difference at the same VPD under non-limiting soil water conditions (non-water stressed baseline), and $(T_{canopy} - T_{air})_{ul}$ is the non-transpiring upper limit.

CWSI allows to relate crop's temperature to the maximum and minimum values possible under similar environmental conditions. The higher the CWSI, the greater the crop stress is assumed to be (Testi et al., 2008). This index does not account for changes in T_{canopy} due to irradiance and wind speed, and the non-water-stressed baseline is not necessarily the same under

different radiation conditions. Finally, the non-transpiring upper limit also varies, with a wide range of values being reported (Ben-Gal et al., 2009).

Rather than using actual empirical crop temperatures as references for calculation of CWSI, an alternative method is to replace the non-water-stressed baseline and the non-transpiring upper limit, respectively with the T_{canopy} from which there is maximum transpiration and the T_{canopy} from which there is no transpiration, measured in the same environment and at the same time as the crop of interest. The fact that these 'references' are in the same environment as T_{canopy} means that there is no need for theoretical estimations of baselines, as they will be exposed to the same VPD, R_{ni}, and wind speed as the canopy of interest. The temperatures of the references are referred to as T_{wet} and T_{dry}, respectively. Therefore, crop water stress index which include these reference temperatures was developed as following form (Costa et al., 2013).

$$CWSI = \frac{(T_{canopy} - T_{wet})}{(T_{dry} - T_{wet})} \tag{1.3}$$

This version of CWSI inversely correlates with leaf water potential. To ensure that there are suitable references in each thermal image, plant's leaves can be sprayed with water (T_{wet}) and covered in Vaseline to artificially close stomata (T_{dry}). A particularly helpful feature of the use of wet and dry reference temperatures is that they can readily be used for the derivation of indices that do not require detailed environmental information. It is a useful index for screening purposes, and in other cases where absolute estimates of stomatal conductance may not be required.

(I_G) is the index of stomatal conductance where the index is proportional to stomatal conductance (for a constant boundary layer conductance) and is calculated using Equation 1.4:

$$I_G = \frac{(T_{dry} - T_{canopy})}{(T_{canopy} - T_{wet})} \quad (1.4)$$

For most values of stomatal conductance (gs), I_G is linearly proportional to gs, as has now been demonstrated under a wide range of conditions. This index uses the same references as the second form of CWSI (Equation 1.3) but gives low values in stressed crops and higher values with increasing gs.

As the inclusion of wet and dry reference surfaces in every image can sometimes be logistically difficult, an alternative to the above indices is to use an actual non-water-stressed plant and a stressed plant as extremes and relate the temperature of the crop of interest to these. This is suitable for example where the crop is scarcity irrigated and hence anticipated to have a T_{canopy} intermediate between those extremes. Since the reference crops, however, cannot usually be included in every image, there is the problem that meteorological conditions can change between imaging the reference crop and the crop of interest. (Costa et al., 2013) interpolated the temperatures of the reference crops between a series of images to estimate their temperature at the precise time when the crops were imaged.

The above indices are appropriate where only leaves are being examined (i.e. either the crop completely covers the soil, or only leaves are selected to obtain T_{canopy}). An alternative index called the water deficit index (WDI) was established for applications where soil and crop temperatures could not be separated (Costa et al., 2013). This index employs the variation between the temperature of the surface (which includes vegetation and bare soil) and the temperature of the air – (T_s – T_{air}) – along with an index of vegetation cover. At 100% vegetation cover, the values of WDI will fall within the same limits of the CWSI.

1.4.6. Alternatives to the Stress Indices

An alternative to the application of stress indices is to approximate gs from T_{canopy}. This requires that T_{air} and VPD, net radiation, and wind speed are measured at the same time as T_{canopy}. Berni et al. (2009) estimated CWSI using meteorological data rather than references to obtain T_{wet} and T_{dry}. CWSI was strongly inversely correlated with leaf water potential. Ben-Gal et al. (2009) compared approximation of CWSI using meteorological data with estimation using $T_{dry} = T_{air} + 5$ °C (which is rather arbitrary) and T_{wet} being the temperature of a wet cloth. The two methods gave similar results, and the authors suggested using meteorological data is preferable, to avoid the need of a wet reference in every image. This approach, however, means that the reference temperatures are not obtained at the same environmental conditions as T_{canopy}, since a full set of meteorological data cannot be collected at each plant of interest.

1.4.7. Weed Scouting

Weed scouting is a key component of integrated weed management programs, particularly if there are resistant weeds involved. Many of the proposed automatic weed identification methods use a variety of visual characteristics of the plants, and sensing technologies (Lin, 2010). Three general characteristics used for plant species identification are biological morphology, spectral characteristics, and visual texture (Hong et al., 2012). The ability for non-contact detection, simple measurement process, fast response, high reliability, and low power consumption make a spectral discrimination method a simple and easy application procedure that can be used in real-time application systems (Rogalski, 2003; Wang et al., 2001). Plants reflect NIR radiation and absorb the visible wavelengths. Weed mapping is challenging because of the similarity in reflectance between the weed species. Hyperspectral sensing may provide a way to identify differences between weed species. NIR, red-edge and Green regions

are the optimal regions for discrimination between different species (Wilson et al., 2014). The position and magnitude of the red-edge zone depends on the amount and type of chlorophyll pigmentation in the leaf (Blackburn, 2006). Reflectance from the NIR and red-edge regions produces the most accurate discrimination of aquatic weeds in the US (Everitt et al., 2011). Leaf structure and the processes that occur in it affect the spectral reflectance from it. Spectral reflectance of plant species at canopy or single leaf scale at specific stages is unique and known as the spectral signature. The spectral signature of weed species and glyphosate-resistant weeds can be a useful tool for weed identification.

In previous studies, researchers demonstrated many spectral reflectance analysis techniques to distinguish weeds from soil background (Scotford & Miller, 2005). Spectral reflectance was successfully employed to identify weeds versus crops when there was a maximum phenological distinction between crop and weeds (López Granados et al., 2008). Identifying critical wavelengths that can effectively discriminate between crops, weeds, and soil is another step in identifying weeds from crops or bare ground (Andújar et al., 2013).

Three main steps in the spectral characterization of weed species include developing spectral data pre-processing or reduction methods, building a proper classification model, and validating the best combination of pre-processing with a classification model. Many processing methods have been used to distinguish the reflectance of weeds from crop plants. These include Artificial Neural Network (ANN), Principal Component Analysis (PCA) and Stepwise Linear Discriminant Analysis (SLDA) (Eddy et al., 2014). To discriminate between crop versus weeds, a SLDA procedure identified four bands of 572.7, 676.1, 801.4, and 814.6 nm as most suitable for discrimination weeds from maize or sugar beet crop (Vrindts et al., 2002). This method discriminated sugar beet from weeds with 90% accuracy. A combination of two methods, ANN

and PCA, produced the most accurate classification in discriminating between weeds and crop plants (Liu et al., 2010) . Maximum Likelihood Classification (MLC) and ANN were tested to distinguish between redroot pigweed and wild oats in Southern Alberta, Canada. The results showed that ANN was more accurate for redroot pigweed and wild oats species (Eddy et al., 2008). A partial least squares discriminant analysis (PLS-DA) model was used to classify soil, wheat, broadleaf weed, and grass weed with 85% accuracy (Shapira et al., 2013).

Two different classification methods such as PCA and Linear Discrimination Analysis developed from a select group of vegetation indices and the best spectral band combination (BSBC) successfully classified soybean, six broadleaf weeds (BLW), and soil (Gray et al., 2009). The classification accuracy varied from less than 50% for PCA to greater than 50% for LDA, and 80% for BSBC. Qin et al. (2013) applied the soft independent modeling of class analogy (SIMCA) method on visible and infrared spectroscopy to identify cabbage versus weeds with the highest accuracy of 98%. PCA and SLDA have been used to select wavelengths to separate different plant species (Yang & Everitt, 2010). These methods increased classification accuracy by 10%. SLDA was used to select the significant bands to distinguish weeds from crop plants (de Castro et al., 2012). The comparison of spectral reflectance between two crops and five weed species was tested and produced 90% accuracy using SLDA and LDA (Smith & Blackshaw, 2003). The combination of PLS and LDA to identify weeds in wheat showed good discrimination (Rabatel et al., 2011). The glyphosate-resistant and susceptible Palmer amaranth weeds were discriminated successfully around the wavebands 676 and 730 nm based on hyperspectral imaging (Reddy et al., 2014a).

In the other study, PLS-DA analysis of plant spectra used to select multispectral camera filters. Researchers acquired sugar beet and thistle weed spectral reflectance to discriminate

weeds versus crop by using UAS. Spectral responses of a multi-band camera equipped with the filter configuration proposed by the PLS-DA models were simulated (Garcia-Ruiz et al., 2015). Applications of remote sensing using UASs have increased recently in precision agriculture (Laliberte et al., 2010). UASs are capable of capturing imagery in high risk situations. They can also be flown below clouds and in light rain. (Berni et al., 2009). A further big advantage is that they are not limited by physiological conditions that would affect human pilots of light planes. FieldCopter is a UAS that can carry multispectral sensors for crop monitoring (Van der Wal et al., 2013). It can fly and capturing imagery in more than 70% of weather conditions compared to satellite imagery. The spectral and spatial resolution of the images depends on the sensors carried by the UAS.

The type of sensor should be matched to the type of information to be collected. For instance, discriminating weed species and pests or detecting the occurrence of specific diseases needs multispectral or thermal camera (Berni et al., 2009). The multispectral camera which has more bands than RGB camera but less than hyperspectral (which has hundreds of bands) can collect higher spatial resolution imagery than satellite sensors and at a lower cost (Torres-Sánchez et al., 2013). Good imagery depends on the UAS, sensor types, and flight plan (Espinoza et al., 2015). In Italy, the first research using UASs for mapping was successful in vineyard plant vigor based on NDVI (Primicerio et al., 2012). A multi-spectral camera and a spectroradiometer were used to capture imagery and record the hyperspectral reflectance data respectively. Hyperspectral and multispectral data can be used to detect spectral differences between weeds and crop plants(Garcia-Ruiz et al., 2015). The weed species reflect unique spectral signatures that can potentially be processed to produce a weed map.

2. SIMCA ANALYSIS OF PLANT CANOPY SPECTRAL DATA[1]

2.1. Abstract

Adoption of a site-specific weed management system (SSWMS) can contribute to sustainable agriculture. Weed classification is a crucial step in SSWMS that could lead to saving herbicides by preventing repeated chemical applications. In this study, the feasibility of visible and near infrared spectroscopy to discriminate three problematic weeds was evaluated. A greenhouse experiment was conducted to classify three common weed species: waterhemp (Amaranthus rudis), kochia (Kochia scoparia), and lambsquarters (Chenopodium album). Soft independent modeling of class analogy (SIMCA) method was used to classify these weed species based on canopy spectral reflectance. Five different pre-processing methods were evaluated to remove the irrelevant information from spectral reflectance. Analysis of data indicated that the second derivative pre-processing method applied to NIR (920-2500 nm) spectra was the best to discriminate three weed species with 100% accuracy for 63 test samples. The SIMCA model on NIR wavebands exhibited the highest discrimination power ratio. The results showed the model distance value for most developed classes in NIR range was more than 3, which indicated its superior ability to discriminate weed species with low risk of misclassification. Furthermore, the discrimination power of different wavelengths obtained from the best models indicated that 640,

[1] The material in this chapter was co-authored by Alimohammad Shirzadifar, Sreekala Bajwa, Seyed Ahmad Mireei, Kirk Howatt, and John Nowatzki. Content in this chapter was published in Journal of Biosystems Engineering 171 (2018): 143-154. Alimohammad Shirzadifar had primary responsibility for performing the samples preparation and all of the tests. Alimohammad Shirzadifar also drafted and revised all versions of this manuscript. Sreekala Bajwa and Kirk Howatt helpe in conducting greenhouse experiments and they served as proofreader. Seyed Ahmad Mireei helped in data processing and interpreting the results. Sreekala. Bajwa and John Nowatzki supervised the project.

676, and 730 nm from the red and red-edge region, and 1078, 1435, 1490, and 1615 nm from the NIR region were the best wavelengths for weed discrimination.

Keywords: Spectral Reflectance, Soft independent modeling of class analogy, Weed classification.

2.2. Introduction

Weeds are the biggest threat to crop production because they cause significant yield loss in crops, limit crop rotation choices, and host insects and diseases (Cardina & Doohan, 2000; FAOSTAT, 2014; Slaughter et al., 2008). Weed management is an important aspect of agricultural production as the economic cost of not managing weeds with herbicide is estimated as $21 billion approximately in the US (Yontz, 2014).

Herbicide application, which is the most common weed management strategy in US agriculture, provides a convenient, economical, and effective way to control weeds. However, repeated and non-optimal use of herbicides results in herbicide resistance in weeds, excessive waste, herbicide residues in food, and environmental pollution with potential impact on human health, ecosystems, and quality and safety of agriculture products (Gil & Sinfort, 2005; Pimentel et al., 1992).

Weed distribution in fields is non-uniform (Pantazi et al., 2016; Slaughter et al., 2008), with field borders being the most infested by weed patches. Yet, herbicides are applied uniformly across the whole field. Therefore, there is a growing need to identify and map weed distribution in the field to reduce herbicide application by applying only the best herbicide option in the areas that need application. Adoption of a sustainable weed management strategy, such as site-specific herbicide application, can improve the efficiency of herbicide application without diminishing

weed control and can play an important role in reducing spraying cost and the pollution of non-target sensitive environments (Slaughter et al., 2008; Weis et al., 2008).

Weed scouting (early detection of weed) and quick target spraying (applying herbicide only on the weeds instead of soil and crop) are two critical key components of a site-specific weed management system (SSWM). Several approaches were reported for weed identification with sensing technologies, visual texture, and spectral characteristics of plants (Pantazi et al., 2016; Tian, 2002). The sensor-based systems include ultrasonic (Andújar et al., 2012), X-ray (Haff et al., 2011), and optoelectronic (Andújar et al., 2011; Biller, 1998) sensors, remote sensing method (Thorp & Tian, 2004), machine vision systems (Burgos-Artizzu et al., 2011; Christensen et al., 2009; Piron et al., 2011; Weis & Sökefeld, 2010), and ground-level hyperspectral imaging (Hadoux et al., 2014; Sui et al., 2008; Vrindts et al., 2002). The ability for non-contact detection, simple measurement process, fast response, high reliability, and low power consumption make a spectral discrimination method a simple and easy application procedure that can be used in real-time application systems (Rogalski, 2003; Wang et al., 2001). Hyperspectral sensors can capture subtle differences in reflectance obtained from plant species (He et al., 2015).

Spectral reflectance of plant species at canopy or single leaf scale at specific stages is unique and known as the spectral signature. The spectral signature of weed species can be a useful tool for weed identification. Weeds' distinctive colors, phenological stages, and vegetation indices can enhance the differences between weed species as a distinguishing factor to classify weeds (López Granados et al., 2008). In previous studies, researchers demonstrated many spectral reflectance analysis techniques to distinguish weeds from soil background (Scotford & Miller, 2005). Spectral reflectance was successfully employed to identify weeds versus crops

when there was a maximum phenological distinction between crop and weeds (López Granados et al., 2008). Identifying critical wavelengths that can effectively discriminate between crops, weeds, and soil is another step in identifying weeds from crops or bare ground (Andújar et al., 2013). Three main steps in the spectral characterization of weed species include developing spectral data pre-processing or reduction methods, building a proper classification model, and validating the best combination of pre-processing with a classification model. To discriminate between crop versus weeds, a stepwise discriminant analysis procedure identified four bands of 572.7, 676.1, 801.4, and 814.6 nm as most suitable for discrimination weeds from maize or sugar beet crop (Vrindts et al., 2002). This method discriminated sugar beet from weeds with 90% accuracy. A partial least squares discriminant analysis (PLS-DA) model was used to classify soil, wheat, broadleaf weed, and grass weed with 85% accuracy (Shapira et al., 2013). In the other study, PLS-DA analysis of plant spectra was used to select multispectral camera filters. Researchers acquired sugar beet and thistle weed spectral reflectance to discriminate weeds versus crop by using unmanned aerial vehicles (UAV). Spectral responses of a multi-band camera equipped with the filter configuration proposed by the PLS-DA models were simulated (Garcia-Ruiz et al., 2015). The red-edge region was reported as the best region to identify vegetation classes. Two different classification methods such as principal component analysis (PCA) and linear discriminant analysis (LDA) developed from a select group of vegetation indices and the best spectral band combination (BSBC) successfully classified soybean, six broadleaf weeds (BLW), and soil (Gray et al., 2009). The classification accuracy varied from less than 50% for PCA to greater than 50% for LDA, and 80% for BSBC. Qin et al. (2013) applied the soft independent modeling of class analogy (SIMCA) method on visible and infrared spectroscopy to identify cabbage versus weeds with the highest accuracy of 98%.

Despite the satisfactory results of weed versus crop classification based on spectral reflectance, this technique has not been used, to the best of our knowledge, to discriminate weed species using the Vis/NIR spectrometers. Since processing the huge spectral dataset is complicated, selecting the optimal statistical analysis method is a crucial step in the classification of weed species. SIMCA is an ideal class modeling technique for the classification of spectral data because it does not assume a specific distribution of variables, and each class model is created independently (Brereton, 2003).

This study focuses on the classification of three weed species waterhemp (*Amaranthus rudis*), kochia (*Kochia scoparia*), and lambsquarters (*Chenopodium album*). Among these species, waterhemp and kochia have been reported as glyphosate-resistant weeds in North Dakota, US. Lambsquarters was studied because it should be controlled carefully due to different herbicide application rate needs (Zollinger, 2016). The objective of this research was to evaluate the feasibility of visible and near infrared (Vis/NIR) spectroscopy for discriminating the three-weed species. Furthermore, the supervised pattern recognition, SIMCA method and appropriate pre-processing corrections were evaluated for their influence on classification performance.

2.3. Materials and Methods

2.3.1. Greenhouse Experiment

A greenhouse experiment was conducted with three weed species to test the hypothesis that canopy reflectance is a good tool for weed identification. The weed species considered in this study were waterhemp (*Amaranthus rudis*), kochia (*Kochia scoparia*), and lambsquarters (*Chenopodium album*), which are major weeds of concern in the upper great plains of the Midwestern US. These weed biotypes were raised in March 2016 at the North Dakota State University greenhouse from locally collected seeds. Bulked weed seeds (110 seeds for each

species) were planted in labeled SC7 cones with a cell diameter of 3.81 cm (1.5") and a depth of 21 cm (5.5"). Cone-tainers contained a commercial potting mix (Metro-Mix 360; Sun Gro Horticulture, Bellevue, WA). The tall, cone-shaped design and internal vertical anti-spiral ribs allow the roots to grow deep and straight. Plants were irrigated at 10 am daily in each individual cell, which had a center drainage hole at the bottom and four side-drain holes on the tapered end. Cone cells were arranged randomly in 70×30.5×17.15 cm (24"×12"×6.75") cone-tainer racks, that could hold 98 cells (Figure 2.1a).

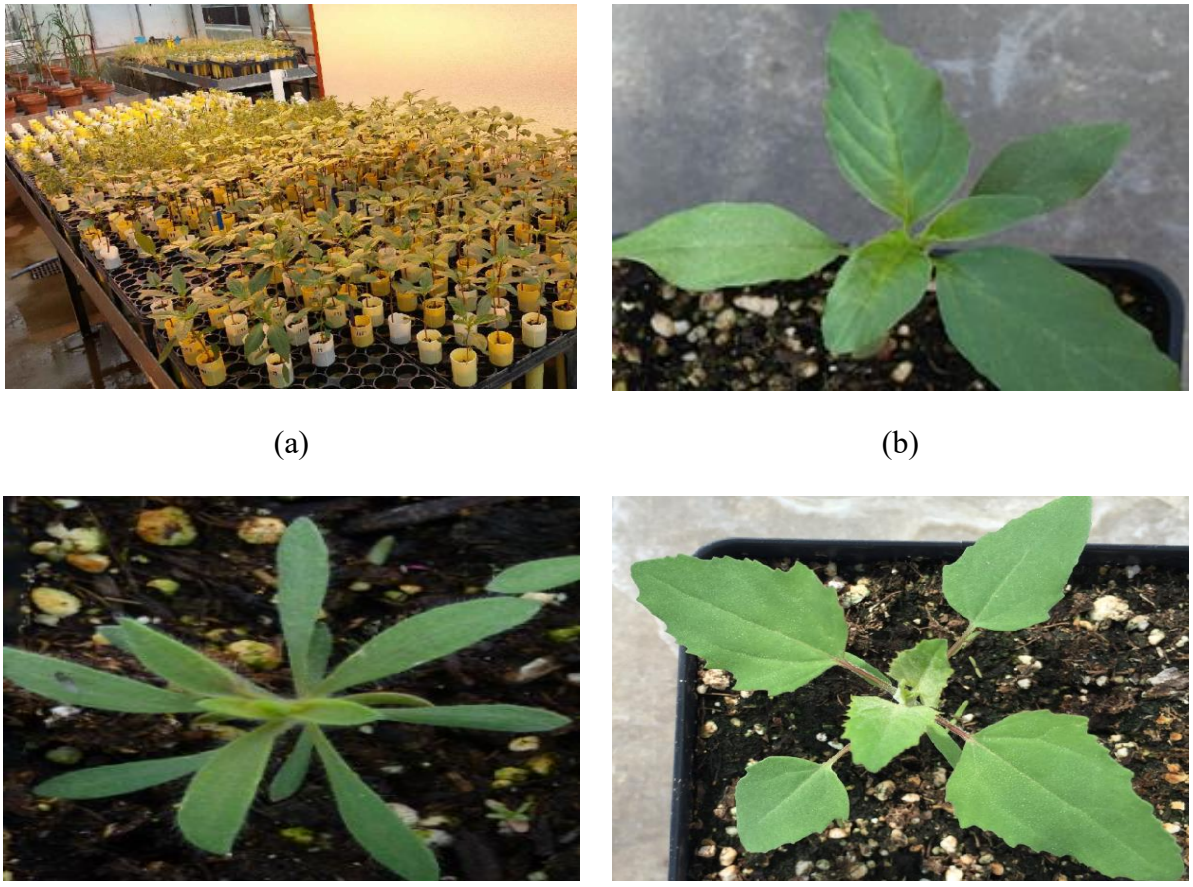

(a) (b)

(c) (d)

Figure 2.1. (a) Experimental set up in the NDSU greenhouse and the three weeds addressed in the study namely, (b) Waterhemp, (c) Kochia, and (d) Lambsquarters.

The greenhouse was maintained at 28/22 ± 3 °C day/night temperatures, with natural light supplemented by sodium vapor lamps to provide a 12 h photoperiod. Three weeks after

germination, when plants were less than 8 cm (3") tall, samples were selected for the reflectance measurement. Reflectance spectra were measured from canopies of 88 of waterhemp, 108 of kochia, and 56 of lambsquarters plants.

Waterhemp plants are characterized by oval leaves with a prominent mid-vein, reddish tinted underside and shiny and smooth surface (Figure 2.1b). Kochia leaves were elliptic, dull green above, purplish on the underside and covered in soft hairs (Figure 2.1c). Lambsquarters had narrow leaves with no mid-vein, dull green to gray color with a mealy coating on both surfaces (Figure 2.1d).

2.3.2. Spectral Data Acquisition

A USB2000 Vis/NIR spectrometer (MODEL+XR1-ES, Ocean Optic Inc. Dunedin, Florida, USA) was used to acquire spectral reflectance characteristics of the weed plants when they were less than 8 cm tall. At this time, the plants had 4 to 6 leaves for waterhemp and lambsqurters and 8 to 10 leaves for kochia. The spectrometer consisted of two individual systems, including a UV-Vis-NIR (USB 2000 sensor) spectrometer that measured reflectance in the 200-920 nm range, and an NIR spectrometer (NIRQuest512-2.5 sensor) that measured reflectance in the 920-2500 nm range. The USB 2000 sensor was equipped with a 2048-element linear silicon CCD array that collected data at 2 nm band interval. The maximum integration time of 1 ms was helpful to avoid saturating the detector under bright light conditions. The NIR spectrometer had a 6 nm spectral resolution and used a Hamamatsu indium gallium arsenide (512-element InGaAs array) detector with a 25 μm slit. An HL-2000 family tungsten halogen lamp with an integrated fan was used as a Vis/NIR light source.

To calculate the relative reflectance of each sample and eliminate the interference by the optical system, the reference and dark spectra were recorded before sample spectra acquisition.

The reference spectra were collected at the beginning of each of 20 sample measurements using a Polytetrafluoroethylene made reference panel. The reference panel was able to reflect more than 95% of the light from 250-2200 nm, respectively. The integration time for reflected spectra of samples was set to 110 ms. Two reflectance spectra were acquired over each plant canopy by rotating the plant by 180°. The spectral data were collected by pointing the fiber optic probe at the plant canopy from nadir at 6 cm above the top of plant canopy. This distance was enough to acquire the spectrum of each plant sample according to the field of view of the sensor. The average of two obtained spectra were then calculated and used for representing the canopy reflectance of each weed plant sample.

2.3.3. Spectral Data Pre-Processing

The canopy reflectance spectra were pre-processed before performing feature selection and classification. The raw Vis/NIR spectra of solid samples include irrelevant information due to light scattering, distance variation of sample and detector, and physical properties of samples such as surface irregularities. Typically, the most effective pre-processing method is selected by trial and error. In this study, five pre-processing methods were evaluated: (1) multiplicative scatter correction (MSC), (2) standard normal variate (SNV), (3) vector normalization (VN), (4) first derivative and (5) second derivative.

The MSC performs a linear transformation of each spectrum in two steps, estimation of the correction coefficients (additive and multiplicative contributions) by Equation 2.1 in the first step and calculating the corrected spectra (Equation 2.2) in the second step.

$$X_{org} = b_0 + b_{ref,1}X + e \tag{2.1}$$

$$X_{corr} = \frac{X_{org} - b_0}{b_{ref,1}} = X_{ref,1} + \frac{e}{b_{ref,1}} \tag{2.2}$$

Where X_{org} is one original sample spectra measured by the NIR instrument, X_{ref} is a reference spectrum used for pre-processing the entire dataset, e is the un-modeled part of X_{org}, X_{corr} is the corrected spectra, and b_0 and $b_{ref,1}$ are scalar parameters.

The SNV correction was performed by subtracting the average spectra from each observed spectrum, and then dividing it by the standard deviation of the spectra sample Equation 2.3.

$$X_{corr} = \frac{X_{org} - a_0}{a_1} \tag{2.3}$$

Where a_0 is the average value of the sample spectra to be corrected, a_1 is the standard deviation of the sample-spectra.

The principal of object-wise standardization correction is similar to SNV while, for normalization, a_0 is set equal to zero. Since SNV and normalization do not involve the least square fitting in their parameter estimation, they can be sensitive to noisy entries in the spectra. To enhance the absorbance and reflectance peaks in the spectra, the first and second derivatives were computed from the raw data using Savitzky-Golay algorithm. The derivatives are capable of removing both additive and multiplicative effects in the spectra. First and second derivatives are mainly used to resolve peak overlap and eliminate constant and linear baseline drift between the samples. Spectral derivatives can be calculated by obtaining the differences between two consecutive points (Equation 2.4). Some common disadvantages of applying derivatives are noise enhancement and difficult spectral interpretation.

$$X_{i,fsd} = X_i - X_{i-1} \tag{2.4}$$

Where $X_{i,\ fsd}$ denotes the first-order derivative at wavelength i, this technique removes only the baseline of the spectra.

2.3.4. SIMCA Analysis

The pre-processed data were then transformed into the principal components (PCs) with Principal Component Analysis (PCA) to test the possibility of discriminating weed species. PCA is the oldest and most common latent variable projection method (Jackson, 2004; Wold et al., 1987). The data matrix X is decomposed into several PCs that explained the highest variance in the data on each successive component under the constraint of being orthogonal to the previous PCs Equation 2.5. The result is a bilinear model, a product of scores (T) and loadings (L) matrices. Since each object gets a score value on each PC, objects can be presented in score plots which can reveal patterns, such as clusters, trends, and outliers in the data. In the same manner, variables can be presented in loading plots. Since each variable gets a loading value on each PC, loading plots monitor covariance among variables and can be used to interpret patterns observed in the score plot, scores, and loadings.

$$X = TL^T + E = t_1 l_1^T + t_2 l_2^T + t_3 l_3^T + \cdots + t_A l_A^T + E \quad (2.5)$$

Where X is the original n samples (rows) × p wavelengths (columns) data matrix, T is a n×A matrix known as the scores matrix, A is the number of principal components in the model, L is a p×A matrix known as the loadings matrix, superscript T indicates the transpose of L, E is a n×p matrix that represents the residual variance, $t_i l_i^T$ are the ith orthogonal principal components that make up the model.

The final step in data processing was the classification of weed species with SIMCA model. SIMCA is a supervised classification technique in which a PCA is developed for each class individually within its calculated boundary. In this study, three weed classes were modeled by PCA using 75% of samples representative of the class population variance as the training class. Cross-validation was performed by a leave-one-out procedure to define the optimum

number of PCs to avoid over- or under-fitting in models. Finally, the rest of the 25% of observations in each weed species were used to validate the selected PC-based SIMCA models (X_t in Equation 2.6). In order to classify the weed plants, after transforming the test data to the latent variable (computed PCA sub-models as a $\hat{t}_u$t in Equation 2.6) space, a nearest neighbor classification strategy was used (computing the residual variance in Equation 2.6).

Equations (2.6) to (2.9) illustrate how the spectra of each tested weed specify to weed classification in SIMCA model. Equation 2.6 calculates the residual variance. The total residual variance for all the n samples in the PCA model can be calculated by Equation 2.8. These two variances allow us to perform a Fischer's F-test Equation 2.9 that forms the ultimate basis of the SIMCA classification method. The tested weed sample belongs to the class representing matrix *X*, if S^2_u and S^2_{total} are statistically the same based on the F test (Davis et al., 2015).

$$e_t = X_t - \hat{t}_u L^T \tag{2.6}$$

$$s_u^2 = \sum_{j=1}^{p} \frac{e_{uj}^2}{p - A} \tag{2.7}$$

$$s_{total}^2 = \left(\frac{1}{n - A - 1}\right) \sum_{i=1}^{n} \left(\sum_{j=1}^{p} \frac{e_{uj}^2}{p - A} \right)_i \tag{2.8}$$

$$F = \frac{s_u^2}{s_{total}^2} \tag{2.9}$$

Where X_t is tested spectra, $\hat{t}_u$ is the estimate of the scores vector, and e_t is the residual variance vector, S^2_u is residual variance for the tested sample, *A* is the number of principal components in the model, S^2_{total} is the total residual variance for all the n samples, and *F* is the Fischer's F-test.

The ability of SIMCA analysis to classify three weed species was evaluated using all the wavelengths as variables as well as just the visible or near infrared wavelengths. Pre-processing

of data and SIMCA analysis were all performed with the Unscrambler V10.4 (CAMO AS, Trondheim, Norway) software package.

2.3.5. Model Performance Evaluation

Model performance was evaluated by three performance parameters: discrimination power, model distance, and classification accuracy. The results of SIMCA analysis allow us to evaluate the discrimination power of the individual wavelength (Esbensen et al., 2002). The discrimination power depends on the number of weed samples that were inside each class, the standard deviation of distance between the samples, the class centroid, and the number of variables that made the specific class. Equations (2.10) to (2.14) show the discrimination power (d_k) computational steps.

$$d_k^{(r,g)} = \sqrt{\frac{S_{k,r}^2(g) + S_{k,g}^2(r)}{S_{k,r}^2 + S_{k,g}^2}} \tag{2.10}$$

$$S_{k,r}^2 = \sum_{i=1}^{n_r} \frac{e_{ik}^2}{(n_r - A_r - 1)} \tag{2.11}$$

$$S_{k,r}^2(g) = \sum_{i=1}^{n_r} \frac{e_{kf}^2(g)}{n_r} \tag{2.12}$$

$$S_{k,g}^2(r) = \sum_{i=1}^{n_g} \frac{e_{kf}^2(r)}{n_g} \tag{2.13}$$

$$S_{k,g}^2 = \sum_{i=1}^{n_g} \frac{e_{ik}^2}{(n_g - A_g - 1)} \tag{2.14}$$

Where $d_k^{(r, g)}$ symbolizes the discrimination power of the variable k in terms of r and g classes, k=1, 2…, p is the number of variables, i=1, 2..., n is the number of observations.

Discrimination power indicates the independent variables that are most useful in describing the difference between the classes. If the discrimination power equals 1, classes cannot be discriminated, while the discrimination power value greater than 1 indicates classes can be successfully discriminated. A discrimination power value of 3 or greater means that the relevant variable is of vital importance in discriminating the classes.

Model distance (Equation 2.15) shows the distance between two classes.

$$d(r.g) = \sqrt{\frac{\sum_{k=1}^{p}(S_{k,r}^2(g) + S_{k,g}^2(r))}{\sum_{k=1}^{p}(S_{k,r}^2 + S_{k,g}^2)}} \quad (2.15)$$

Where *d (r, g)* is the distance between *r* and *g* groups.

Model distance could be useful in comparing different models. A distance larger than 3 indicates good class separation and low risk of misclassification in the model. No classification can be made if the model distance is less than 1 and the discrimination of the classes can be made successfully if the value is more than 3.

2.4. Results and Discussion

2.4.1. Overview of Canopy Reflectance

Mean raw reflectance data of kochia, waterhemp, and lambsquarters are illustrated in Figure 2.2. The jump in the spectra around the wavelength of 1000 nm was occurred due to the changing of the spectrometer system. This jump was constant for all samples and no adverse effects were seen in the performance of classification models. The canopy reflectance for three weed species were different in the red and red-edge regions and also in several parts of the NIR region. These regions related primarily to chlorophyll and water content of selected weed species, respectively. These distinguishable differences in canopy reflectance of the weed spices

indicated the possibility to classify them based on their spectral signature in Vis/NIR wavelengths (Figure 2.2).

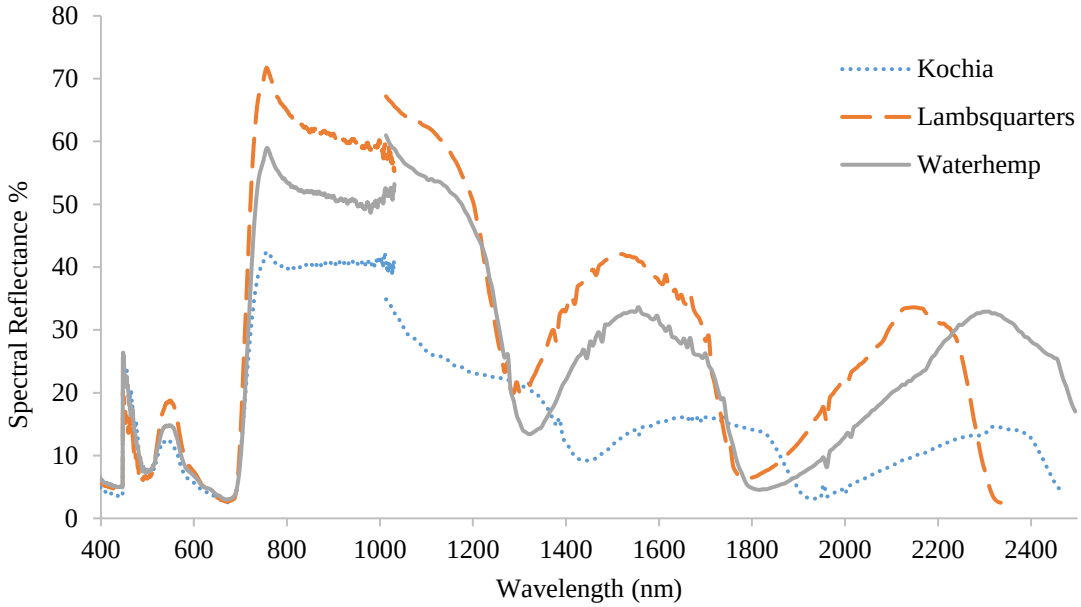

Figure 2.2. The average canopy reflectance spectra of three weed species, including kochia, waterhemp, and lambsquarters in Vis/NIR wavelengths.

2.4.2. Spectral Pre-Processing

In general, the pre-processing method significantly influenced the separation of the clusters. However, among different pre-processing methods, SNV could better separate the weed species clusters in 400-920 nm and whole spectral (400-2500) ranges, while 2nd derivative could better discriminate the weed species in 920-2500 nm spectral range, based on visual inspection. Figure 2.3 illustrates the scatter plot of the PCA scores in the first two PC spaces obtained from best pre-processing methods in the 400-920 nm (Figure 2.3a), 920-2500 nm (Figure 2.3b), and the whole spectral region (Figure 2.3c). As shown, among different ranges, the spectral range of 920-2500 resulted in the best discrimination between the weed clusters (Figure 2.3b), where, despite the relative overlap between the kochia and lambsquarters samples, waterhemp samples were successfully separated from other weed species. It should also be noted that this

discrimination was carried out with two PCs that only described 52% of total spectral data variance (40% for PC1 and 12% for PC2). It was expected that spectral reflectance analysis can lead to better results when more PCs are used. Figure 2.3b also depicts that the major part of waterhemp samples was located on the positive side of the PC2 axis, while the kochia and lambsquarters samples were scattered on the negative side of PC2 with a tendency to the origin region. The other wavelength regions, however, could only result in a slight separation between weed species in the first two PC spaces, as shown in Figure 2.3a and c. The overlap of weed species in the 400-920 nm (Figure 2.3a) may be due to the similar spectral characteristics of the weed species in the visible range which include the main part of 400-920 nm (Figure 2.2) since the leaf of the weed species had similar color features (Figure 2.1). Regarding Figure 2.3c, no significant improvement in the separation of clusters was achieved when using all spectral data. In general, the total variance described by two PCs were less than the respective models when using 400-920 nm (Figure 2.3a) and 920-2500 nm (Figure 2.3b) spectral information. This was due to the larger number of input variables to the PCA models. Therefore, more PCs may be needed to achieve a better discrimination power.

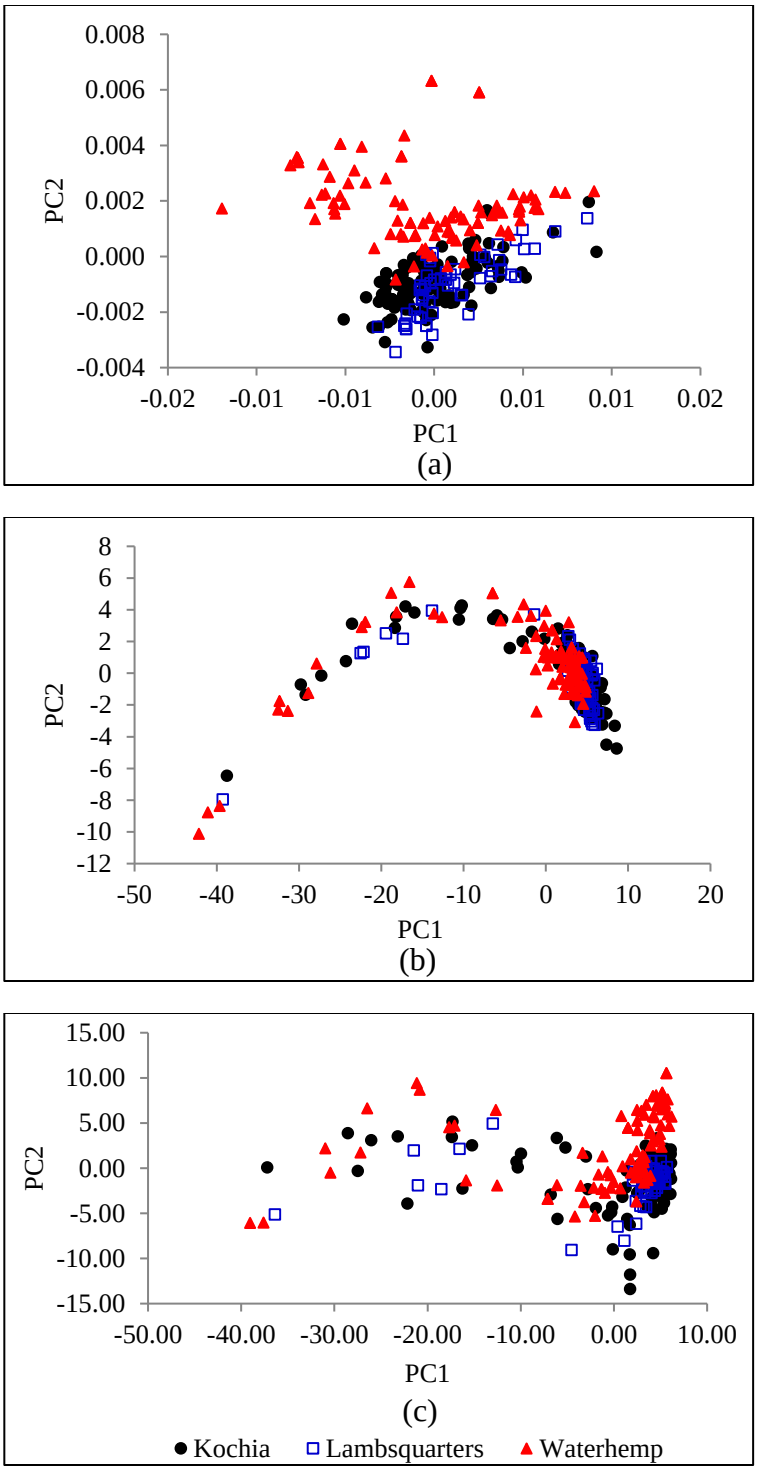

Figure 2.3. The PCA scores of the samples of kochia, lambsquarters, and waterhemp weed species obtained from the best pre-processing methods in the (a) 400-920 nm, (b) 920-2500 nm, and (c) the whole spectral region.

2.4.3. Classification by SIMCA

Table 2.1 summarizes the test set validation results of the SIMCA analysis performed to discriminate three weed clusters in the wavelength region of 400-920 nm, using different pre-processing methods. The number of PCs necessary to obtain the best SIMCA models was between 1 and 10 and depends on the class and pre-processing method. As expected, among different pre-processing methods, the best results were obtained by SNV with a total accuracy of 88.89%. Interestingly, 92.59% and 100% of kochia and lambsquarters samples, respectively, were successfully discriminated. This was expected because after a close investigation of Figure 2.3a, it was concluded that the kochia and lambsquarters groups were more accurately classified than the waterhemp group. However, the relatively poor discrimination of waterhemp samples (77.27%) reduced the total accuracy to 88.89%, due to the significant overlap of waterhemp samples with the two other weed samples (Figure 2.3a).

The test set validation results of the SIMCA analysis performed to classify three weed clusters in the wavelength region of 920-2500 nm using different pre-processing methods were shown in Table 2.2. As expected from Figure 2.3b, the 2^{nd} derivative pre-processing resulted in the best discrimination power. The developed SIMCA model could successfully discriminate all three weed clusters (Total accuracy of 100%). The optimum number of PCs necessary to achieve this model was 12, 10, and 14 for kochia, lambsquarters, and waterhemp classes, respectively (Table 2.2). The 1st derivative pre-processing resulted in the next best model in the range of 920-2500 nm and the related SIMCA model could successfully classify all the kochia and lambsquarters samples (classification accuracy of 100%). However, only one waterhemp sample was misclassified as kochia (classification accuracy of 95.45%) and caused the total accuracy to be 98.41% (Table 2.2).

Table 2.1. The test set validation results of the SIMCA analysis for classification of three weed species in the wavelength region of 400-920 nm, using different pre-processing methods.

Spectral Pre-processing	Class variable	PCs	Kochia	Lambsquarters	Waterhemp	Accuracy (%)	Weighed accuracy (%)
Raw	Kochia (n=27)	4	25	0	2	92.59	76.19
	Lambsquarters (n=14)	4	1	13	0	92.86	
	Waterhemp (n=22)	3	12	0	10	45.45	
Normalization	Kochia (n=27)	3	21	2	4	77.78	84.13
	Lambsquarters (n=14)	5	1	13	0	92.86	
	Waterhemp (n=22)	4	3	0	19	86.36	
MSC	Kochia (n=27)	2	26	0	1	96.30	80.95
	Lambsquarters (n=14)	2	2	12	0	85.71	
	Waterhemp (n=22)	1	9	0	13	59.09	
SNV	Kochia (n=27)	3	25	0	2	92.59	88.89
	Lambsquarters (n=14)	5	0	14	0	100.00	
	Waterhemp (n=22)	3	5	0	17	77.27	
1st Derivative	Kochia (n=27)	7	27	0	0	100.00	87.30
	Lambsquarters (n=14)	5	3	11	0	78.57	
	Waterhemp (n=22)	5	5	0	17	77.27	
2nd Derivative	Kochia (n=27)	13	26	1	0	96.30	85.71
	Lambsquarters (n=14)	15	3	11	0	78.57	
	Waterhemp (n=22)	10	5	0	17	77.27	

Table 2.2. The test set validation results of the SIMCA analysis in the wavelength region of 920-2500 nm using different pre-processing methods.

Spectral Pre-processing	Class variable	PCs	Kochia	Lambsquarters	Waterhemp	Accuracy (%)	Weighed accuracy (%)
Raw	Kochia (n=27)	4	26	0	1	96.30	87.30
	Lambsquarters (n=14)	2	1	11	2	78.57	
	Waterhemp (n=22)	2	4	0	18	81.82	
Normalization	Kochia (n=27)	2	24	0	3	88.89	85.72
	Lambsquarters (n=14)	2	2	10	2	71.43	
	Waterhemp (n=22)	2	2	0	20	90.91	
MSC	Kochia (n=27)	4	25	1	1	92.59	88.89
	Lambsquarters (n=14)	3	1	12	1	85.71	
	Waterhemp (n=22)	3	1	2	19	86.36	
SNV	Kochia (n=27)	2	27	0	0	100.00	83.55
	Lambsquarters (n=14)	2	0	14	0	100.00	
	Waterhemp (n=22)	1	2	4	16	72.73	
1st Derivative	Kochia (n=27)	3	27	0	0	100.00	98.41
	Lambsquarters (n=14)	2	0	14	0	100.00	
	Waterhemp (n=22)	2	1	0	21	95.45	
2nd Derivative	Kochia (n=27)	12	27	0	0	100.00	100.00
	Lambsquarters (n=14)	10	0	14	0	100.00	
	Waterhemp (n=22)	14	0	0	22	100.00	

MSC: multiplicative scatter correction; PCs: principal components; SNV: standard normal variate.

Despite the satisfactory results of the 920-2500 nm wavelength region for classifying the weed clusters, the total spectral data (400-2500 nm) were also used to possibly find more simple and robust models. Table 2.3 summarizes the test set validation results of the SIMCA analysis performed to classify three weed clusters using all spectral information (400-2500 nm) and different pre-processing methods.

Table 2.3. The test set validation results of the SIMCA analysis performed to classify three weed clusters using all spectral information (400-2500 nm) and different pre-processing methods.

Spectral Pre-processing	Class variable	PCs	Kochia	Lambsquarters	Waterhemp	Accuracy (%)	Weighed accuracy (%)
Raw	Kochia (n=27)	4	25	0	2	92.59	87.30
	Lambsquarters (n=14)	3	2	11	1	78.57	
	Waterhemp (n=22)	4	3	0	19	86.36	
Normalization	Kochia (n=27)	4	25	1	1	92.59	85.71
	Lambsquarters (n=14)	4	3	11	0	78.57	
	Waterhemp (n=22)	4	4	0	18	81.82	
MSC	Kochia (n=27)	4	26	1	0	96.30	92.06
	Lambsquarters (n=14)	3	2	12	0	85.71	
	Waterhemp (n=22)	4	2	0	20	90.91	
SNV	Kochia (n=27)	5	27	0	0	100.00	96.82
	Lambsquarters (n=14)	4	1	13	0	92.86	
	Waterhemp (n=22)	5	1	0	21	95.45	
1st Derivative	Kochia (n=27)	28	27	0	0	100.00	79.36
	Lambsquarters (n=14)	26	6	8	0	57.14	
	Waterhemp (n=22)	19	7	0	15	68.18	
2nd Derivative	Kochia (n=27)	10	27	0	0	100.00	95.23
	Lambsquarters (n=14)	9	1	11	2	78.57	
	Waterhemp (n=22)	11	0	0	22	100.00	

MSC: multiplicative scatter correction; PCs: principal components; SNV: standard normal variate.

Despite the better results in comparison with the wavelength region of 400-920 nm (Table 2.1), no improvement in prediction power occurred when using all spectral information as compared with the wavelength region of 920-2500 nm. This can be due to the additional and unnecessary information for distinguishing between three classes that was imported to the built SIMCA models. The best model (in the range of 400-2500 nm), however, was obtained by the SNV pre-processing method that could successfully discriminate 100%, 92.86%, and 95.45% of kochia, lambsquarters, and waterhemp samples, respectively (Table 2.3).

The total accuracy of 96.82% of whole spectra was obviously worse than the best model obtained in the spectral region of 920-2500 nm (100%) but better than the best obtained model in the 400-920 spectral region (Table 2.4).

Table 2.4. The summary of the SIMCA analysis performed to classify three weed clusters.

Spectral Range	Spectral pre-processing	Weighted accuracy (%)
400-920 nm	SNV	88.89
920-2500 nm	2^{nd} Derivative	100.00
400-2500 nm	SNV	96.82

SNV: standard normal variate.

2.4.4. Model Distance

Table 2.5 depicts the model distance values for the three weed clusters obtained from the best SIMCA model in the 400-920 nm and 920-2500 nm (Table 2.3) wavelength regions. These values are usually used to estimate the distance between the models for specific target classes or to quantify the possible differences between them (Equation 2.15). A useful way to interpret these values is that a model distance greater than 3 indicates the models are significantly different (Esbensen et al., 2002). As shown in Table 2.5, only the distance between lambsquarters and waterhemp models had this criterion (model distance greater than 3) and the

other distances were less than 3, indicating the high risk of misclassification in the developed model. Especially in discrimination of kochia from waterhemp, the low model distance of 1.65 caused 5 waterhemp samples from a total of 22 to be misclassified as kochia (Table 2.1), indicating high similarity of kochia to waterhemp sample in using the 400-920 nm spectral region. For discriminating of lambsquarters from waterhemp, however, due to the high model distance of 3.29 between lambsquarters and waterhemp classes (Table 2.1), no confusion between these two-weed species occurred when 400-920 nm spectral range was used as the input to the SIMCA model.

Table 2.5. The model distance value for the three weed clusters obtained from the best SIMCA model in 400-920 nm and 920-2500 nm wavelength regions.

	Model distance	
Class combination	400-920 nm	920-2500 nm
Kochia-lambsquarters	2.693	3.928
Kochia-waterhemp	1.653	4.157
Waterhemp-lambsquarters	3.288	6.246

In contrast to 400-920 nm, the 920-2500 nm region resulted in satisfactory model distances, where surprisingly all three model distances between the weed clusters were greater than 3 (Table 2.5). Hence, the developed SIMCA model could significantly differentiate between all weed clusters (Table 2.2). The maximum model distance was provided between the waterhemp and lambsquarters classes (a model distance of 6.25), indicating the high potential of SIMCA analysis for discriminating these two-weed species. Moreover, the kochia and waterhemp model distance in using 920-2500 nm range was 4.16, which resulted in no confusion between these two clusters (Table 2.2).

2.4.5. Discrimination Power Plot and Wavebands Selection

In order to investigate which variables were the most important in discriminating the models, the discrimination power values of the best models (in both ranges of 400-920 nm and 920-2500 nm) were plotted against wavelength variables (Equation 2.10). Figure 2.4 illustrates this plot for the best SIMCA models obtained from 400-920 nm (Figure 2.4a) and 920-2500 nm (Figure 2.4b) spectral ranges. On the whole, the variables that have a discrimination power value greater than 3 could be considered useful in the overall classification. As shown in Figure 2.4a, no variable was found in the 400-920 nm that could satisfy this criterion for all three weed clusters simultaneously. However, for discriminating the kochia from lambsquarters, the wavelength variables around 640, 676, and 725 nm (wavebands of (635-650 nm), (670-683 nm), and (720-733 nm)) resulted in discrimination power values greater than 3. The wavelength variables around 730 nm (waveband of 701-731 nm) could also satisfy the criterion of wavelength selection for discriminating the lambsquarters from waterhemp (Figure 2.4a).

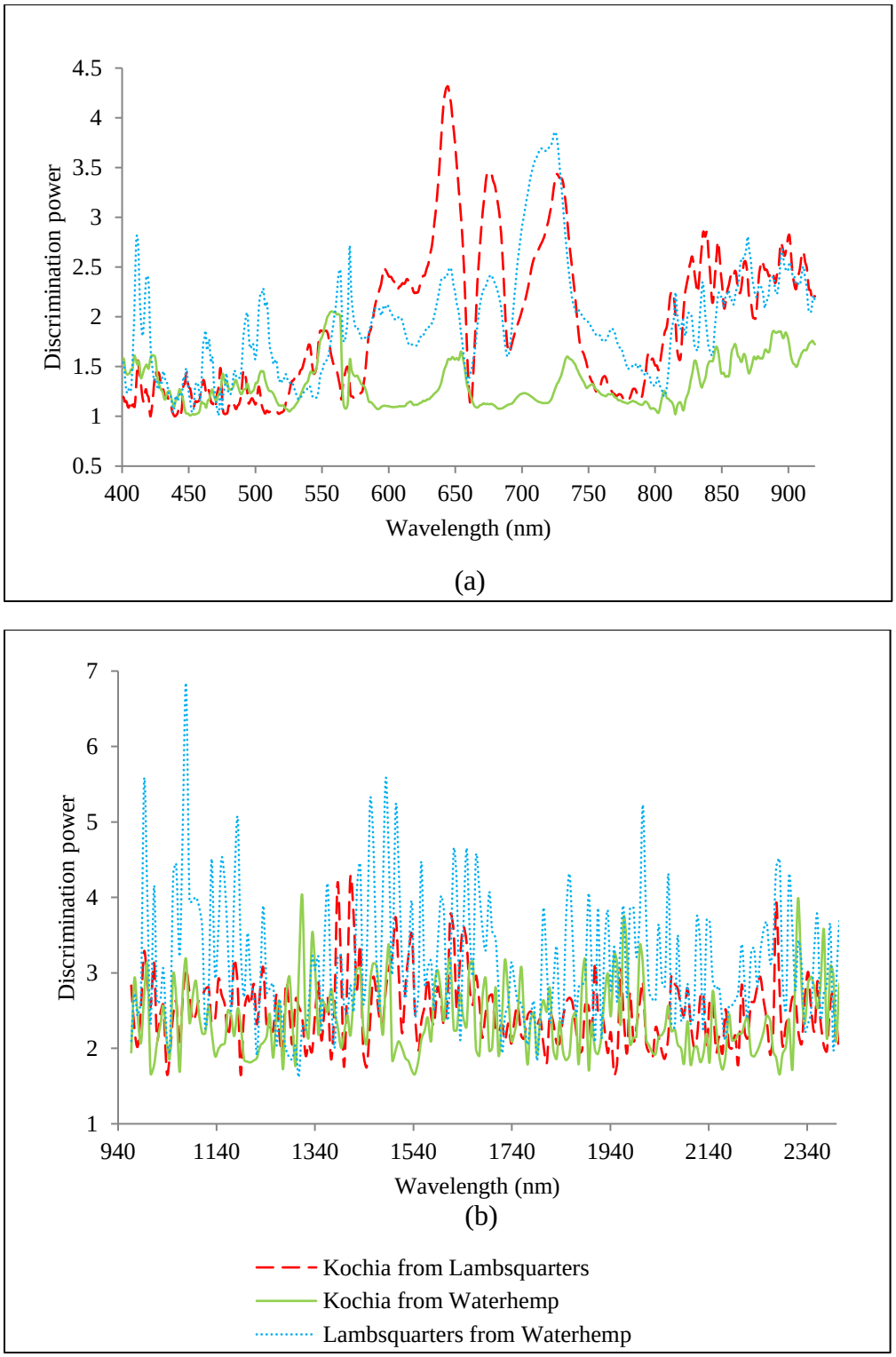

Figure 2.4. The discrimination power plot for the three weed clusters obtained from the best SIMCA model in (a) 400-920 nm and (b) 920-2500 nm wavelength regions.

This was in agreement with findings obtained for differentiating the glyphosate resistant and susceptible weeds (Palmer amaranth) using hyperspectral imaging, where the wavebands around 676 and 730 nm presented the best separation ability (Reddy et al., 2014a). The wavelengths around 640 and 676 nm are normally attributed to the chlorophyll absorption bands, while the wavelengths around 730 nm (the red edge) corresponded to C-H fourth overtone associated with the carbohydrate content of the leaves (Yang et al., 2012). Therefore, it can be concluded that the chlorophyll and carbohydrate contents of weed leaf can be considered as the helpful factors for distinguishing the weed species.

For the 920-2500 nm spectral region, (Figure 2.4b), the number of wavelength variables with the high discriminatory power was relatively more than those obtained in the 400-920 nm spectral region. However, only four wavelengths of 1078, 1435, 1490, and 1615 nm achieved the discrimination power values greater than 3 for classifying the three weed species simultaneously. Yet, the available literature does not investigate the exact biochemical composition of leaves in the studied weed species. Therefore, accurate chemical analyses are needed to characterize the specific components in the weed leaves and better discern differences in chemical composition among the weed species.

Nevertheless, by applying the partial least squares (PLS) regression for determining wavelength regions, Lehmann et al. (2015) related the wavelength regions around 1078, 1435, and 1615 nm to the tannin concentration of the different exotic-invasive shrub species. They also showed that these wavelength regions had a better classification performance for discrimination of Mediterranean native plants and shrub species than using all wavelengths. Generally, the wavelengths around 1078 nm is close to the second overtone of N-H functional group and it was

found to have a high correlation to tannin concentration in plant tissues (Lehmann et al., 2015) which precipitates proteins and other organic compounds including amino acids and alkaloids.

Moreover, the wavelengths around 1490 nm are close to the first overtone of N-H functional group or first overtone of O-H functional group found in cellulose structures (Burns & Ciurczak, 2007). Therefore, it may be attributed to the protein content of weed leaves or water content of plant. The high discrimination power values at the wavelengths in the vicinity of 1435 nm can be related to the possible differences in the water content of weed species, since the wavelengths around 1435 nm correspond to the strong absorption of the water content of the leaves (first overtone of O-H functional group). Moreover, the high discriminatory power of wavelengths around 1615 can be attributed to the differences in carbohydrate content of three studied weed species (Burns & Ciurczak, 2007). Similar to the 400-920 nm spectral region, it seems that the water and carbohydrate contents of weed leaves play an important role in the classification of three weed species studied in this work.

2.5. Conclusion

The greenhouse study described in this paper proved the potential of Vis/NIR spectroscopy to discriminate three selected weed species. The SIMCA classification method discriminated three weed species, namely waterhemp (*Amaranthus rudis*), kochia (*Kochia scoparia*), and lambsquarters (*Chenopodium album*) with 100% accuracy. This research study demonstrated the feasibility of SIMCA supervised classification method combined with a second-derivative pre-processing method. Based on the test set validation results, SIMCA models on Vis, NIR and Vis-NIR regions classified three different weed species with more than 90 percent accuracy. The derivatives correction was more effective to obtain high accuracy classification compared to the other pre-processing methods evaluated in this study. This

expected result confirmed that in the greenhouse, the derivatives correction played a more important role than the scattering filters due to the consistency of light. Based on distance model results, the SIMCA model on NIR bands showed the lowest risk of misclassification. Furthermore, the discrimination power of different wavelength variables obtained from the best models indicated that the red and red-edge (640, 676, and 730 nm) and NIR (1078, 1435, 1490, and 1615 nm) regions had the best wavelengths for weed discrimination.

2.6. Acknowledgement

We thank Sandy Johnson and Mark Ciernia of NDSU greenhouse for help with the greenhouse experiment, the North Dakota Department of Commerce Research ND program for providing grant support (grant number: FAR0024073).

3. DEVELOPMENT OF SPECTRAL INDICES FOR IDENTIFYING GLYPHOSATE-RESISTANT WEEDS[1]

3.1. Abstract

Glyphosate as the most common and widely-used herbicide in agricultural crops has resulted in the explosion of resistant weeds around the world. The objective of this study was to evaluate the feasibility of spectral weed indices (SWIs) to identify glyphosate-resistant weeds 72 h after herbicide application. A greenhouse experiment was conducted on three common weed species, namely, waterhemp (*Amaranthus rudis*), kochia (*Kochia scoparia*) and ragweed (*Ambrosia artemisiifolia L.*) including resistant and susceptible types to collect canopy spectral reflectance after glyphosate spraying. Relief-F algorithm selected the significant and most relevant wavelengths and two band normalized differences from 450 to 920 nm describing the detrimental effect of glyphosate application for each weed species, separately. To generate hyperspectral indices for detecting resistant weeds from susceptible plants the best weighted combination of single wavelength and a normalized wavelength difference was searched exhaustively by testing all possible combinations. The performance of optimized SWIs on resistant weeds identification were assessed by employing a machine learning Random Forest (RF) method. The RF classification model achieved a classification accuracy of 96%, 97% and 100% for resistant kochia, waterhemp and ragweed, respectively. A comparison between developed SWIs and introduced spectral-based vegetative indices (VIs) in previous published

[1] The material in this chapter was co-authored by Alimohammad Shirzadifar, Sreekala Bajwa, and John Nowatzki. Alimohammad Shirzadifar performed the experiments and processed the experimental data. Alimohammad Shirzadifar also drafted and revised all versions of the manuscript. Sreekala Bajwa aided in interpreting the results and worked on the manuscript. Sreekala Bajwa and John Nowatzki supervised the work.

works indicated that generated SWIs were accurate enough to identify glyphosate-resistant weeds based on spectral signature.

Keywords: Glyphosate-resistant weed, Spectral weed indices, vegetative indices, Hyperspectral reflectance, weed classification.

3.2. Introduction

Weeds are ubiquitous to most crops, proliferating each year on every farm around the world. Particularly, weeds in crop fields are considered as a significant problem due to weed competition on crop yield (Yadav et al., 2018). In general, mechanical and chemical methods are two common weed management. The existing manual weed management options are no longer feasible due to large scale crop fields and unavailability of manual labours in peak season (Rao et al., 2018). Furthermore, overreliance on the some commonly used chemical herbicide has resulted in the occurrence of several herbicide-resistant weed species, leading to an increased need for herbicide application (Colbach et al., 2017).

Glyphosate is a non-selective, systemic herbicide, extremely toxic to a variety of sensitive plant species. The application of glyphosate is dramatically growing, while the resistance to glyphosate is the most common genetic modification (GM) in crops (Bonny, 2016), suggesting the importance of the weed management as an important factor in precision agriculture (Shirzadifar et al., 2018).

General information on weed species is essential, so that farmers can minimize the environmental impacts of weed control via reducing the repeated application of herbicides (Aiello et al., 2018). Recent advances in sensors opened up the possibility of using machine vision methods to identify different weed species, providing precision weed control (Singh et al., 2016).

Weed management can be implemented through the application of spectral reflectance imaging, in which, the reflectance spectra at each point of the farm is measured and the weed species is identified for each point via spectral signature recognition rather than shape analysis method (Westwood et al., 2018). Spectral signature basically includes recording and identifying a set of repeatable spectral features for distinct targets (Ferguson & Rundquist, 2018).

In the case of weed species identification, several spectral-based indices have been extensively explored for fast and non-destructive measurements of leaf area (Zhou et al., 2017), nitrogen content (Frels et al., 2018), photosynthetic status (Zhang et al., 2017), disease identification (AL-Saddik et al., 2017), leaf and canopy senescence (Gara et al., 2018).

Developing and computation of Vegetation Indices (VIs) is another technique for weed species discrimination. In terms of the indices, most are expressed as reflectance or first derivative at a given wavelength (R or D), simple ratios (SR), normalized differences (ND), double differences (DDn), modified simple ratios (mSR) or modified normalized differences (mND) (Sonobe & Wang, 2017). Furthermore, more complicated indices such as chlorophyll absorption ratio indices, soil line vegetation indices and the integrated forms have been used for different plant species (Wu et al., 2008). The other indices are the feature-based indices which were calculated as the sum of the reflectance at the red and infrared regions (Sonobe & Wang, 2017). However, there is no a reliable spectral index to identify glyphosate-resistant weed in the field.

Furthermore, remote sensing of the spectral reflectance using multispectral images can be a reliable way to detect changes in the physiological status of plants in response to different biotic and/or abiotic stresses, since stresses often results in the low rates of photosynthesis in the plants (Zhang et al., 2016). Glyphosate application results in a reduction of the photosynthetic

rate in susceptible plants (Gomes et al., 2017) . When the photosynthetic mechanism is less efficient, the chlorophyll and the other pigments was affected, changing the spectral reflectance in Vis/NIR range. Therefore, we hypothesized that the spectral signature of susceptible weeds should be changed in comparison with resistant weeds after glyphosate application.

This study was conducted with the objective of developing and validating spectral weed indices (SWIs) to identify glyphosate-resistant weeds from susceptible ones in selected weed species, using spectral signature 72 h after glyphosate application. We also introduced the concept of SWIs for detecting glyphosate-resistance in three weed species including waterhemp (*Amaranthus rudis*), kochia (*Kochia scoparia*), and ragweed (*Ambrosia artemisiifolia L*.), the weeds known to have glyphosate-resistance in North Dakota, US. Furthermore, the classification accuracy of the combining Relief-F and Random Forest (RF) strategy to distinguish herbicide-resistant weeds was evaluated.

3.3. Materials and Methods

3.3.1. Greenhouse Experiment

Greenhouse experiment was conducted in a greenhouse at North Dakota State University (NDSU, Fargo, ND, USA). Three different weed species including waterhemp (*Amaranthus rudis*), kochia (*Kochia scoparia*), and ragweed (*Ambrosia artemisiifolia*) were employed to assess the potential application of vegetative indices on glyphosate-resistant weeds identification. The seeds were collected from twenty different local sites in North Dakota with confirmed glyphosate-resistance and susceptible species. Weed seeds were planted in 3.81 cm diameter and 21 cm depth plastic cones to provide enough space for root growth. The cones were filled with commercial potting mix (Metro-Mix 360, Bellevue, WA) and the weeds were daily subirrigated

with water to keep the adequate soil moisture. The greenhouse day/night temperature was set at 28/22 °C with a 12 h photoperiod under sodium vapor lamps.

3.3.2. Herbicide Treatments

Three weeks after germination when waterhemp was in the four to eight leaf growth stage, kochia, and ragweed had eight to ten leaves, glyphosate was sprayed on the weeds (July 2017). The herbicide treatment was applied on the weeds with recommended full rate (1.7%) of technical grade glyphosate (glyphosateisopropylammonium, >95% purity, Chem Service, West Chester, PA, USA). A cabinet sprayer (DeVries Manufacturing, Hollandale, MN, USA) equipped with a moving boom was employed to apply herbicide on the weeds. The Tee Jet spray nozzles (8001) were mounted on the beam and the average height from nozzle to weeds was 40 cm for all samples. The spraying was conducted at 40 psi pressure and 2.23 m/s velocity.

3.3.3. Spectral Signature Recording and Datasets

A data set of spectral reflectance in the range of 450 to 920 nm was recorded using a USB2000 Vis/NIR spectrometer (MODEL + XR1-ES, Ocean Optic Inc. Dunedin, Florida, USA). The spectral signatures for each of three aforementioned weed species were collected 72 h after glyphosate application. The spectral reflectance was recorded under constant conditions in a controlled environment, and the experiments were repeated three times for each treatment.

3.3.4. Development of Specific Indices for Identifying Glyphosate-Resistant Weeds

Canopy spectral reflectance differ in weed species and some portions of the spectrum might exhibit more worth in identifying glyphosate-resistance status. A statistical algorithm was developed to compute and to evaluate spectral weed species indices (SWIs). The steps from developing spectral signatures to glyphosate-resistant weed species indices is illustrated in Figure 3.1. Developing the spectral signatures of glyphosate-resistant kochia, waterhemp, and

ragweed were the basic component in generating the SWIs. Acquired spectral reflectance data consist of a large number of continuous narrow bands from 450–920 nm. Analyzing such high dimensional data was complex and time-consuming task. The adjacent wavelengths are highly correlated to each other, therefore the spectral band interval was reduced to 20 nm to decrease computational time (Mahlein et al., 2013). In order to obtain reliable SWIs a weighted combination of single wavelength and a normalized wavelength difference was required. Single wavelengths were especially vital to differentiate samples with higher resistance degree. Normalized wavelength difference was suitable to assess changes in the hyperspectral signature caused by glyphosate application early after spraying, as the detrimental effect of glyphosate application on photosynthesis mechanism changes at different ranges on the hyperspectral signature.

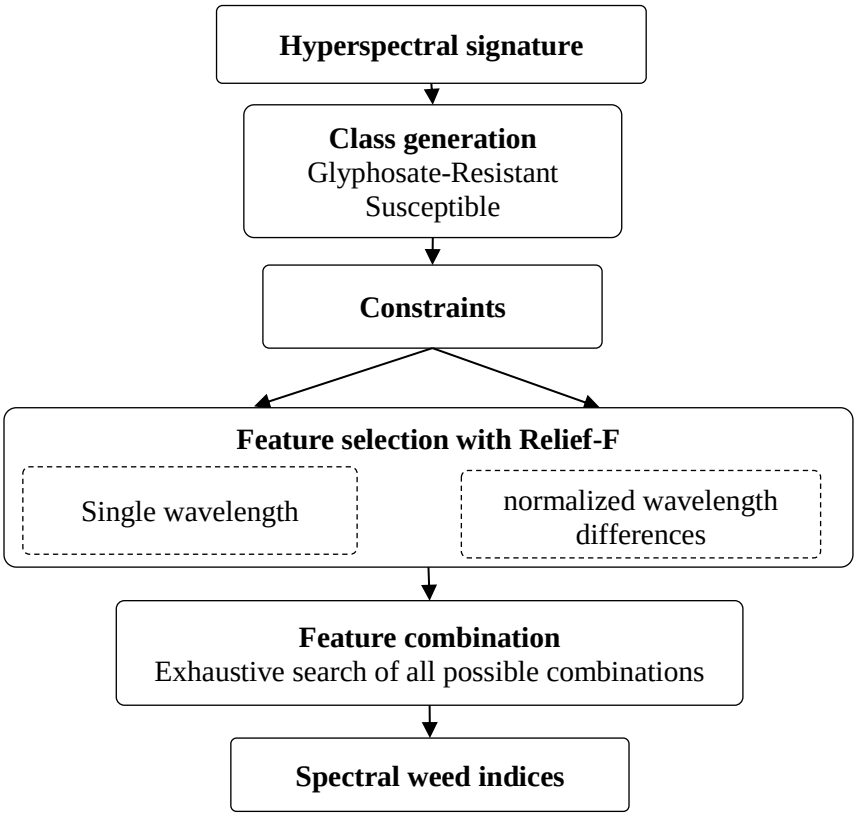

Figure 3.1. Flowchart showing the main steps involved in developing glyphosate-resistant weeds identification indices.

3.3.5. Feature Selection

The normal distribution of data was assessed since the normality is an underlying assumption in many statistical analyses. There are two main methods of assessing normality including graphically and numerically. The normality assumption of spectral signature was tested using the powerful Shapiro–Wilk test. If the Shapiro equation value is equal to one it means the data are distributed normally while small values reject the normality assumption.

This section outlines how the number of original wavelengths was narrowed down by selecting eight discriminative bands. Irrelevant wavelengths may complicate developing SWIs algorithm and leading to generate wrong results. Therefore, it is necessary to select the most relevant features based on suitable feature selection method. In this study, to reduce the computational time and effort, only eight relevant wavelengths were selected by Relief-F feature selection. The simple well-known Relief-F approach estimates the relevance of feature (wavelength) according to their goodness to separate samples of both classes, which are close to each other. Feature relevance was defined as a weight for a feature of a measurement vector. There are several advantages for the Relief-F algorithm including correct estimation of feature quality with strong dependencies, strict against outliers and nearest-neighbor classification, which made it as a widely used feature selection. The Relief-F explores the two nearest neighbors of the same class (hit) and from the different classes (miss) for a given k samples in the neighborhood. Then, the weight of a feature F_i is changed based on the absolute difference between the F_i-values of nearest hit and nearest miss. However, the sum of the Euclidean distance between nearest misses and nearest hits for all samples determines the weight (relevance) of the features (wavelengths). Pseudo code of the Relief-F algorithm for two class classification was reported by Mahlein et al. (2013).

To generate SWI, the combination of single wavelength and normalized wavelength differences were developed. Each spectral weed index included three wavelengths, and a weighting factor for single wavelength (Equation 3.1). The possible weights for single wavelength were −1, −0.5, 0.5 and 1.

$$SWI = ab + \frac{(c + d)}{(c - d)} \tag{3.1}$$

Where a, c, d are wavelengths chosen from the pool of eight selected wavelengths ($a \neq c \neq d$) and b is the weighting factor.

Since SWIs combination included multiple eight, seven and six choices for the first, second and third wavelength respectively, and four weighting factors, the totally 1344 SWIs (8×7×6×4) could be generated. However, the optimized combination of the individual wavelength and normalized wavelength difference was selected using exhaustive search by Relief-F analysis.

In order to evaluate the classification ability of developed SWIs, a 10-fold cross validation Random Forests was employed.

3.3.6. Random Forest Classifier

A Random Forest classifier (RF) is a supervised machine learning technique, which consists of multiple independent decision trees. Each individual tree randomly uses a subset of raw data, which is known as training data that contains about two-thirds of the samples. Furthermore, the split node is built by random subset of the features. The one-third of remaining data is considered to obtain a test dataset classification as well as to determine the importance of features. The predicted result is determined by a majority vote of the ensemble of decision trees leading to more accurate and stable output. There are two noticeable parameters considered by users including the number of trees (h) which are limited by prediction error, and the number of

randomly selected variables to split the nodes (k). A nested 10-fold cross validation process can minimize the estimation error and increase the performance of classifier. In respect of training data for building the classification model, we randomly selected glyphosate-resistant weed species and susceptible weeds as training set. The most significant advantage of Random Forest algorithm is preventing overfitting most of the time by generating smaller trees using random subsets of the features.

3.3.7. Classifier Performance Evaluators

The performance of RF model was evaluated through a 10-fold cross-validation method. For this purpose, data were divided randomly into two parts for training and validation, and the process was repeated for 10 times. For each fold, the RF model was built with training data set and evaluated with validation dataset. 70% of the samples were selected randomly to train the classifier and the remaining 30% was used to test the classification accuracy.

In addition to model accuracy, the model sensitivity, specificity, precision and F-measure were calculated to further evaluate model performance. Classifier performance was evaluated by two-class problems based on confusion matrix. The two classes are positive and negative and confusion matrix has four values computed based on real and predicted categories namely true positive (TP), false positive (FP), false negative (FN) and true negative (TN) values. Since the objective of classification was to identify resistant weeds, the resistant weeds (class R) was defined by a model output of positive and the susceptible weeds (Class S) was defined by a model output of negative in this study. Sensitivity and specificity were introduced to represent the proportion of real positive or negative which are correctly classified, respectively (Equation 3.3&4). The classifier evaluator F-measure defines the harmonic mean of sensitivity and precision which is the ratio of predicted positive examples which really are positive (Equation

3.6). If the β parameter on F-measure has zero value, which means that sensitivity and precision have the same importance.

$$Accuracy = \frac{TP + TN}{TP + FP + FN + TN} \tag{3.2}$$

$$Sensitivity = \frac{TP}{TP + FN} \tag{3.3}$$

$$Specificity = \frac{TN}{TN + FP} \tag{3.4}$$

$$Precision = \frac{TP}{TP + FP} \tag{3.5}$$

$$F.mea = \frac{(\beta^2 + 1) \times sens \times prec}{sens + \beta \times prec}, \qquad \beta \geq 0 \tag{3.6}$$

3.3.8. Vegetation Indices (VIs)

In this study, a total of 71 spectral-based vegetative indices were evaluated for their potential to identify glyphosate-resistant weeds based on chlorophyll content. Random Forest method was developed to find the proper indices for classifying glyphosate-resistant weed species. Cross-validation is the most common method to estimate out-of-sample prediction error. The inner evaluation of the classifiers performances was carried out by 10-fold cross-validation. Finally, we applied the RF model on unseen data samples and evaluated the prediction performance using a manually classified set of indices.

3.3.9. Software

Matlab software v8.5 (MathWorks, Natick, MA, USA) was used to build the RF classification model, and to select the significant features for modeling based on Relief-F algorithm.

3.4. Results and Discussion

3.4.1. Overview of Canopy Reflectance

Mean raw reflectance data of kochia, waterhemp, and ragweed for both resistant and susceptible species after glyphosate application are illustrated in Figure 3.2. The canopy reflectance for all three-weed species exhibited significant discrepancy in the red-edge and NIR regions which are related to chlorophyll content and cell structure of weed species, respectively. The distinguishable differences in canopy reflectance of the weed spices with different glyphosate resistance status indicated the possibility of classifying different weed species considering the spectral signature in Vis/NIR wavelengths (Figure 3.2).

All weed species exhibited the same reflectance trend. The spectral reflectance of vegetation in Vis/NIR region is characterized by very low reflectance in the red part of the spectrum followed by an abrupt increase in reflectance at 700± 740 nanometer (nm) wavelengths. However, glyphosate resistant weeds exhibited higher reflectance, in contrast to susceptible ones in different wavelengths. The most noticeable differences between resistant and susceptible weed species were observed in the wavelength of 766, 779 and above 800 nm. Particularly, resistant kochia and waterhemp weeds exhibited higher spectral reflectance as compared to susceptible species in infrared regions (>750 nm). While, in the case of ragweed more significant discrepancy between resistant and susceptible weed was happened in the wavelength of 450- 630 nm. These effects are associated with a decrease in chlorophyll content of susceptible weeds as a response of plant stress. In fact, the application of glyphosate results in lower photosynthesis rate by inhibiting chlorophyll biosynthesis. Thus, plant stresses by virtue of glyphosate application appear to be associated with an inhibition of normal shifts in the spectral reflectance towards lower values in susceptible weeds.

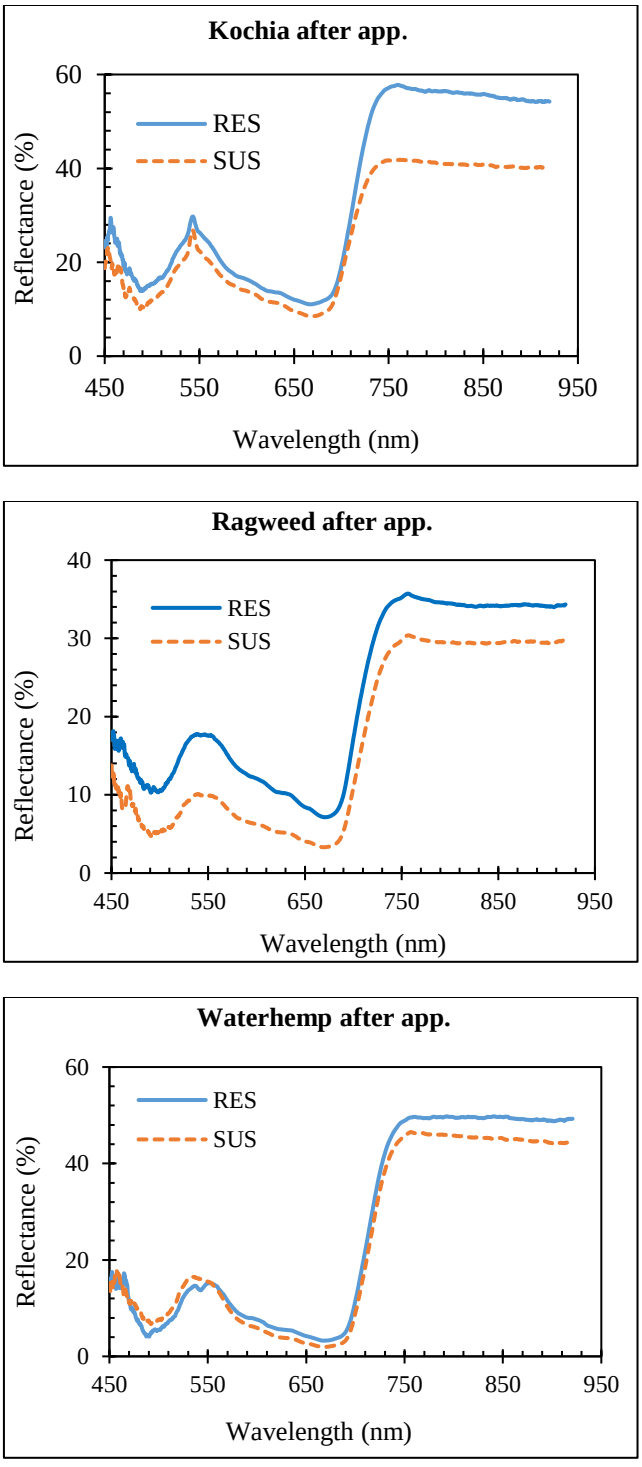

Figure 3.2. Spectral signature of three-weed species in the range of 450-920 nm.

3.4.2. Relief-F Analysis for Feature Selection

Based on the Relief-F analysis, eight discriminative wavelength features were selected to establish the combination of three wavelengths for developing the SWIs (Table 3.1). Developed spectral indices (SWIs) should able to classify glyphosate-resistant of kochia, waterhemp, and ragweed plants 72 h after herbicide application in Vis/NIR wavebands.

Table 3.1. Selected discriminative wavebands for developing SWIs.

Weed species	Discriminative Wavebands (nm)							
Kochia	550	520	670	700	640	610	460	580
Waterhemp	490	760	520	820	850	910	880	790
Ragweed	910	850	670	880	820	730	790	760

Photosynthetic pigment composition can be used as an indicator of the physiological status of a plant. The reference wavelengths at 430 and 445 nm, 531 and 570 nm is attributed to the carotenoids and xanthophylls, respectively. Xanthophyll evaluation by employing spectral reflectance can be used to assess pigment composition for determining photosynthetic efficiency. The reference wavelengths from 550 to 680 nm and red-edge region is related to chlorophyll content. Chlorophyll concentration can be derived using spectral reflectance at 675 nm and at 550 nm. For very low concentrations, the reflectance sensitivity is higher at the maximum absorption located at 675 nm and, for medium- to-high chlorophyll concentrations, reflectance sensitivity is higher around 550 nm. The red-edge region has been found to be a good indicator of chlorophyll content. The region between 700 to 800 nm stands for the brown pigments. The reference wavelengths in the range of 800 to 900 nm is called structural reference wavelengths and is sensitive to the cell organization structure (cell wall, intercellular space, etc.).

In the NIR domain (700–1300 nm), where minimum absorption and high reflectance was occurred, the magnitude of reflectance is controlled by internal leaf structure and biochemical composition. In this study, susceptible weeds exhibited lower spectral reflectance in the wavelength from 800 to 900 nm in comparison with resistant type. Glyphosate had detrimental effect on the physiological mechanisms involved in photosynthesis and other physiological processes, resulting in poor photosynthetic efficiency (Gomes et al., 2017). So, the application of glyphosate resulted in different photosynthesis performances in the plants and photosynthesis efficiency altered based on stresses. Photosynthesis efficiency of glyphosate-resistant weeds was higher than susceptible type which were affected by physiological stress.

3.4.3. Relief-F Analysis for Feature Selection

Based on the proposed combination, three wavelengths and best weighting factor for weed species were selected using Relief-F method. Consequently, the SWIs were developed for identifying glyphosate-resistant weed species (Table 3.2). The combination of wavelengths SWIs confirmed that the photosynthesis efficiency which was affected by glyphosate application played an important role for detecting glyphosate-resistant from susceptible plants. So, spectral reflectance can be used to assess pigment composition for identifying glyphosate-resistant weeds 72 h after spraying.

Table 3.2. SWIs for identifying glyphosate-resistant weeds.

Weed species	SWI
Kochia	$SWI = -R460 + \frac{(R520 + R670)}{(R520 - R670)}$
Waterhemp	$SWI = -R760 + \frac{(R490 + R790)}{(R490 - R790)}$
Ragweed	$SWI = R670 + \frac{(R790 + R760)}{(R790 - R760)}$

3.4.4. Random Forest Analysis

The test set validation results of RF analysis are shown in Table 3.3. As mentioned before, for model development, 70% of samples was used to train the classifier and 30% was selected randomly to test the classification accuracy. The number of samples in the test was 41, 33, and 33 for kochia, waterhemp, and ragweed, respectively to assess the classification accuracy of RF. Resistant kochia, ragweed and waterhemp samples were classified with 96%, 100% and 97% accuracy, respectively (Table 3.3). The specificity for ragweed was 1 while it was calculated as 0.93 and 0.92 for kochia and waterhemp, respectively (Table 3.4). The model output indicated that only one resistant sample was misclassified for waterhemp and two resistant kochia was predicted as susceptible type. (Table 3.3). In addition, RF was able to discriminate susceptible kochia, waterhemp and ragweed with 100% accuracy. The sensitivity, specificity, precision, F measure and G mean was computed as 1 (Table 3.4) for ragweed samples due to the high performance of the respective model. It means that there was a full agreement between classified glyphosate-resistant ragweed and actual class.

Table 3.3. Confusion matrix of RF classification.

		Predicted value								
		Kochia			Ragweed			Water hemp		
		SUS	RES	Total	SUS	RES	Total	SUS	RES	Total
Actual value	SUS	13	0	13	15	0	15	21	0	21
	RES	2	26	28	0	18	18	1	11	12
Total		15	26	96%	15	18	100%	22	11	97%

The overall accuracy for ragweed, waterhemp and kochia was reported as 100%, 97 % and 96% respectively (Table 3.4). Generally, in classification method, the overall accuracy higher than 85% is required to reach the commonly accepted requirements (Castillejo-González et al. 2014). The high classification accuracy for three weed species presented that SWIs were

powerful enough to identify the resistant weeds. There was no chance for happening misclassification in three-weed species due to their sensitivity value (1). Taking into consideration the model performance, RF models and SWIs presented a good assessment in identification of susceptibility and resistibility in resistant weeds.

Table 3.4. Statistical measurements of the performance of RF.

Weed Species	Kochia	Ragweed	Waterhemp
Classification accuracy, %	96	100	97
Specificity, ratio	0.93	1	0.92
Sensitivity, ratio	1	1	1
Precision, ratio	0.96	1	0.95
F Measure, ratio	0.96	1	0.98

3.4.5. Vegetation Indices (VI)

In the context of vegetation status monitoring, the plant species or specific plant stress can be identified using spectral reflectance measurement. Vegetation indices (VI) used band ratio formula to classify the spectral reflectance into weed species. This technique is based on magnifying the discrepancy between the features via manipulating spectral reflectance in one band by spectral reflectance in other bands. The most discriminative VI from 71 VIs for identifying glyphosate-resistant waterhemp, kochia and ragweed is shown in Table 3.5. The triangular vegetation index (TVI) was able to detect glyphosate-resistant waterhemp, kochia and ragweed from susceptible plants with 82%, 86% and 94% accuracy (Table 3.6). The triangular vegetation index (TVI) was calculated as the area of the triangle defined by the green peak, the chlorophyll absorption minimum, and the NIR shoulder in spectral space. Since, chlorophyll absorption cause to decrease red reflectance and leaf tissue abundance results in increasing NIR reflectance which rises the total area of the triangle (Broge & Leblanc, 2001)

Table 3.5. The most discriminative VI which identify glyphosate-resistant type of weed species.

Weed species	TVI	Overall accuracy%
Kochia	0.5×(120× (R750-R550)-200× (R670-R550))	86
Ragweed	0.5× (120× (R750-R550)-200× (R670-R550))	94
Waterhemp	0.5× (120× (R750-R550)-200× (R670-R550))	82

The TVI index could classify kochia and ragweed with accepted accuracy (> 85%). However, the classification accuracy of developed SWIs was much more than the TVI (Table 3.6). The chance of misclassification was 22%, 20% and 14% for kochia, ragweed and waterhemp.

Table 3.6. Statistical measurements of the performance of VI.

Weed Species	Kochia	Ragweed	Waterhemp
Classification accuracy %	86	94	82
specificity	0.92	1	0.75
Sensitivity	0.78	0.8	0.86
Precision	0.88	1	0.86
F Measure	0.82	0.89	0.86

3.5. Conclusion

For site specific weed management system, the difference between spectral signatures of susceptible and glyphosate-resistant weeds could be the key to identify discriminative wavelengths for detecting resistant plants. The transformation of reflectance into SWIs was a potential technique to reduce a large number of wavelengths for detecting herbicide resistant weeds. This study demonstrated that spectral weed index developed as a combination of weighted single wavelength and normalized wavelength difference were effective in identifying glyphosate-resistant weeds. The Relief-F method was employed to select 8 discriminative

wavelengths for 3 required wavelengths in SWIs and find the optimized combination from 1344 feasible combinations. Photosynthetic pigment composition region and cell structure had the most discriminative wavelengths due to detrimental effect of glyphosate application on photosynthetic mechanism and plant cell structure. The results showed machine learning Random Forest method could discriminate resistant kochia, waterhemp and ragweed with 96%, 97% and 100% accuracy respectively, based on the newly developed SWIs. The high value of sensitivity and specificity of RF models proved the ability of SWIs to identify glyphosate resistant weeds.

3.6. Acknowledgement

We thank Sandy Johnson and Mark Ciernia of NDSU greenhouse for help with the greenhouse experiment, the North Dakota Department of Commerce Research ND program for providing grant support (grant number: FAR0024073).

4. CAN CANOPY TEMPERATURE DIFFERENTIATE GLYPHOSATE-RESISTANT WEEDS IN CROP FIELDS?[1]

4.1. Abstract

The non-optimum application of herbicides with the same mode of action in crop fields results in the development of herbicide-resistant weeds. Glyphosate as a widely-used herbicide in agriculture has resulted in the development of resistant weeds. The resistance to glyphosate is the most common genetic modification (GM) in crops. In this study, the feasibility of plant canopy temperature after glyphosate application was investigated as an indicator of herbicide resistance in weeds. A greenhouse experiment was conducted on three common weed species, namely, waterhemp, kochia, and ragweed, including resistant and susceptible plants. Canopy temperature was monitored hourly using a thermal camera for up to 96 h after glyphosate application. Feature selection with stepwise regression was used to analyze the discriminative time features, and support vector machine (SVM) was used to classify resistant and susceptible weeds based on canopy temperature. Stepwise regression method indicated that the most effective time for identifying herbicide-resistant weeds was 95 h after herbicide application for waterhemp and ragweed, while, herbicide-resistant kochia was effectively identified 46 h after herbicide application. The SVM classification model achieved a classification accuracy of 97.4% for resistant Kochia, and 100% for resistant waterhemp and ragweed. The results indicated that canopy temperature after herbicide application is an excellent indicator of herbicide resistance in plants.

[1] The material in this chapter was co-authored by Alimohammad Shirzadifar, Sreekala Bajwa, Seyed Ahmad Mireei, Heather Zhang. Alimohammad Shirzadifar conceived and carried out the experiments and analyzed the observed results. Alimohammad Shirzadifar wrote this chapter in consultation with Sreekala Bajwa. Seyed Ahmad Mireei and Heather Zhang helped in data processing. Sreekala Bajwa supervised findings of this work.

Keywords: Canopy temperature, Glyphosate, Herbicide-resistance, Weeds, Support vector machine.

4.2. Introduction

Herbicide application is the most common and economical weed management strategy in the US agriculture (Zimdahl, 2018), as the economic cost of not managing weeds is estimated around $21 billion in the US (Abdul Aziz, 2015; Yontz, 2014). However, the repeated and non-optimal application of herbicides with the same mechanisms of action has caused the evolution of herbicide-resistant weeds (Green, 2018). Glyphosate [N-(phosphonomethyl)glycine)] is a widely-used herbicide in agriculture and forestry for industrial weed control in the US (Benbrook, 2016). The annual farm-sector usage of glyphosate was approximately 108.8 million kg in 2014, which is a 100-fold increase since the first decade of its use in the 1970s (Myers et al., 2016). The emerging issue of the glyphosate-resistant weeds resulting from the broad adoption of roundup ready crops has the potential to have a huge negative impact on US agriculture (Green, 2018; Myers et al., 2016).

Weed scouting is a key component of integrated weed management programs, particularly if there are resistant weeds involved. Three general characteristics used for weed species identification are biological morphology, visual texture, and spectral characteristics (Hong et al., 2012).

Glyphosate is a non-selective foliar chemical that prevents the plants from making certain proteins which are essential for plant growth (Zhong et al., 2018). This herbicide converts shikimate-3-phosphate (S-3-P) together with phosphoenolpyruvate (PEP) into enolpyruvalshikimate-3-phosphate (EPSP), leading to accumulation of shikimic acid in plant leaves (Lorentz et al., 2014). Shikimate accumulation following glyphosate application has been

used to identify glyphosate-resistance plants (Corrêa et al., 2016). However, the extraction of shikimic acid directly from the plant tissue in the lab is time-consuming and costly (Xu et al., 2017).

Glyphosate-resistant and glyphosate-susceptible weeds look alike and are not distinguishable visually. Therefore, identification of glyphosate-resistant weeds may not be accomplished using the application of common visual identification techniques. Resistance discrimination based on optical or temperature characteristics of the canopy that are not visible to the human eye has a variety of advantages such as non-contact detection, simple measurement process, fast response, and high reliability. Glyphosate-resistant and glyphosate-susceptible Palmeramaranth (*Amaranthuspalmeri S.Wats*.) was discriminated with hyperspectral imagery acquired in lab condition with the accuracy of more than 90% (Reddy et al., 2014b). However, it is difficult to translate such lab results to canopy scale in field condition due to the complex Vis/NIR optical properties of leaves, the variability introduced by varying field conditions, and the canopy structure even within the same species canopies (Roberts et al., 2004).

Remote sensing of the canopy temperature using thermal imaging can be a reliable way to detect changes in the physiological status of plants in response to different biotic and/or abiotic stresses, since abiotic or biotic stresses often result in decreased rates of photosynthesis and transpiration in the plants (Anjum et al., 2011; Zhang et al., 2016). Glyphosate application results in a reduction of the photosynthetic rate in susceptible plants (Gomes et al., 2017; Mateos-Naranjo et al., 2009; Yanniccari et al., 2012; Zobiole et al., 2012). When the photosynthetic mechanism is less efficient, more light energy becomes lost as heat, increasing canopy temperature. Therefore, we hypothesized that resistant weeds will have lower canopy temperatures in comparison with susceptible weeds immediately after glyphosate application.

Evapotranspiration of water during the photosynthesis diurnal phase has a cooling effect on the plants. However, reduced evapotranspiration rates because of reduced leaf stomatal openings lead to higher canopy temperatures. Since plant canopy temperature is a good indicator of leaf transpiration (Mangus et al., 2016), plant canopy temperature early after herbicide application could be a potential discriminative factor to identify glyphosate-resistant weeds early after herbicide spraying.

In an integrated weed management system, the optimal time for identifying glyphosate-resistance is a vital factor for timely weed management. Stepwise multiple regression analysis could select the most significant features for developing an empirical model (Bajwa & Kulkarni, 2011; Maire et al., 2015). Stepwise feature selection can be combined with support vector machine (SVM) classification method for feature selection (the optimal time), predictive modeling, and classification (Dogan & Uysal, 2018).

This study was conducted with the objective of developing and validating a method to identify the glyphosate-resistant weeds from susceptible ones in selected weed species, using canopy temperature early after glyphosate application. We also introduced the concept of thermal signature for detecting glyphosate-resistance in three weed species including waterhemp (*Amaranthus rudis*), kochia (*Kochia scoparia*), and ragweed (*Ambrosia artemisiifolia L.*), the weeds known to have glyphosate-resistance in North Dakota, US (Zollinger et al., 2006). Furthermore, the classification performance of combining stepwise regression for feature selection with SVM classification strategy to distinguish herbicide-resistant weeds was evaluated.

4.3. Materials and Methods

4.3.1. Greenhouse Experiment

To assess the influence of glyphosate application on canopy temperature, three common glyphosate-resistant weeds in the region, namely waterhemp, kochia, and ragweed were selected for a greenhouse study. The experiment was carried out in a greenhouse at North Dakota State University in Fargo, ND. A selection of weed biotypes was raised in March 2017 in the greenhouse (Figure 4.1a) from the collection of susceptible and resistant plants with approximately the same number of plants in each category.

Waterhemp plants with the smooth texture and oval leaves have reddish tinted underside and shiny surface (Figure 4.1b). Kochia leaves are elliptic, dull green above, purplish on the underside, and covered in soft hairs (Figure 4.1c). Ragweed has egg-shaped leaf outline and once or twice compounded leaves (pinnatifid) that are symmetrically distributed to either side of the hairy green stem. The leaf stem is hairy on the upper or dorsal surface and margin and densely appressed on the lower surface (Figure 4.1d). In total, 160 seeds for each species were planted in labeled SC7 cones with a cell diameter of 3.81 cm and a depth of 21 cm (Figure 4.1a). The labeled planting cones were filled with a commercial potting mix (Metro-Mix 360; Sun Gro Horticulture, Bellevue, WA) to which the seeds were planted. Plants were irrigated daily at 10 am in each individual cell, which had a center drainage hole at the bottom and four side-drain holes on the tapered end. Cone cells were arranged randomly in 70×30.5×17.15 cm3 (24"×12"×6.75") racks, with each rack holding 98 cells (Figure 4.1a). The greenhouse temperature was set at 28± 3 °C during the day, and 22 ± 3 °C during the night, with natural light supplemented by sodium vapor lamps to provide a 12 h photoperiod.

(a)

(b) (c) (d)

Figure 4.1. a) Experimental set up in the NDSU greenhouse showing cones of weed plants of the resistant and susceptible types. Three weeds addressed in this study were b) Waterhemp, c) Kochia, and d) Ragweed.

When the plant's height reached close to 10 cm, the weeds were sprayed with recommended full rate (1.7%) of glyphosate using a cabinet sprayer (DeVries Manufacturing, Hollandale, MN, USA). Spraying was done at 40 psi pressure and 2.23 m/s velocity using a model 8001 nozzle mounted on the boom 40 cm above the plants (Figure 4.2).

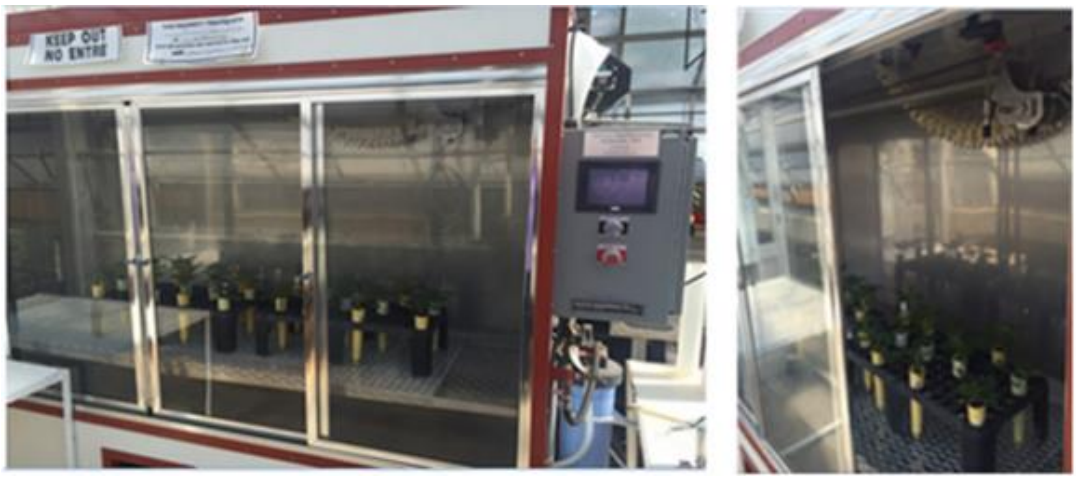

Figure 4.2. A cabinet sprayer, where weed plants are being sprayed with the recommended dose of glyphosate.

4.3.2. Thermal Images Acquisition

Thermal images of both susceptible and resistant weeds were acquired on an hourly basis during the first 96 h after herbicide application. A USB calibrated ICI thermal camera (Model 9640 P-Series Infrared Camera, ICI, Beaumont, TX, USA) was used to acquired thermal images of the weed plants. The camera was equipped with a 24.8 × 18.6 FOV lens with a focal length of 25 mm. Thermal images were acquired for a total of 418 plants including 132 waterhemp, 154 kochia, and 132 ragweed plants. The thermal camera operated in the long-wave infrared (LWIR) region of 7 to 14 µm range and recorded grey level images of 640 by 480-pixel size. The camera could operate at a temperature range of -40 to 140 °C. The grey level values of the thermal images were converted to actual temperature values using a built-in calibration function in the IR Flash software (Infrared Camera ICI. TX, USA) (Figure 4.3).

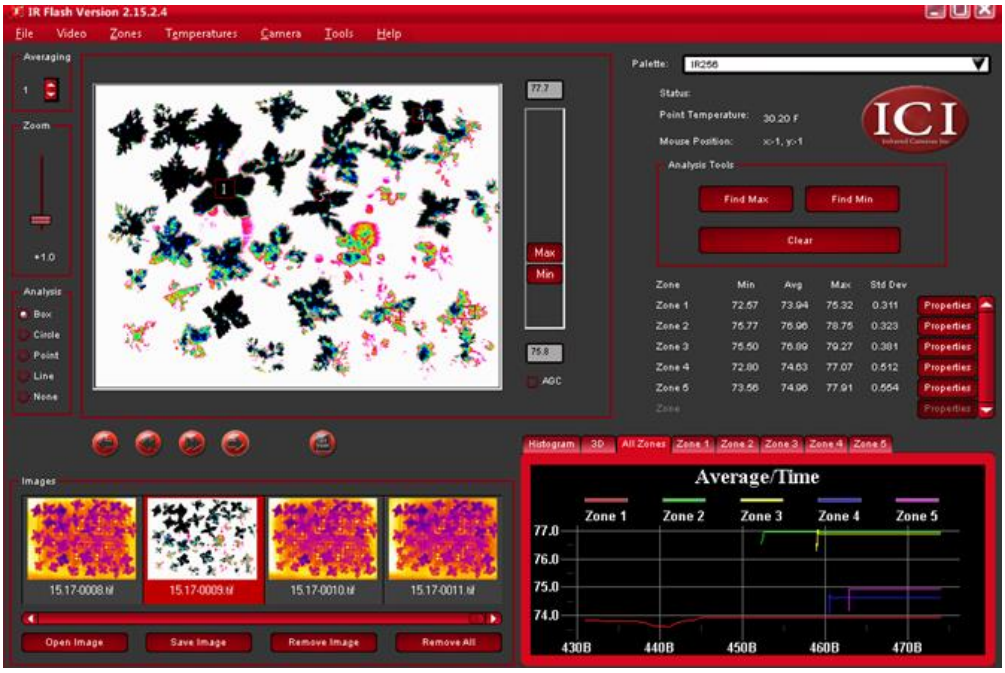

Figure 4.3. A sample thermal image of the weed plants viewed in the IR Flash software. The average temperature for the various zones can be seen on the right-hand panel.

The IR Flash software was used to control the camera operation and its settings such as the gain temperature level for the scene, hourly operation, and the specific folder where images are saved. For example, Figure 4.3 is the IR Flash window which illustrates colorized thermal image over ragweed plants. The IR256 color lookup ramp was used for visualization so that the coolest canopies were in the dark black and the hottest canopies were in the green following by pink. Before starting the image capture, a Blackbody ICI 350 portable IR calibration (ICI. TX, USA) was used to check the camera calibration. The thermal camera was mounted 1.6 m above the plants on a cross-beam (Figure 4.4) throughout the experiment, and it provided a 2.5 mm spatial resolution in the image. To account for environmental conditions, the air temperature and relative humidity in the greenhouse were recorded by a HOBO pro series sensor (Onset MA, USA), and leaf water content was recorded with a PhotosynQ (Michigan State University, USA).

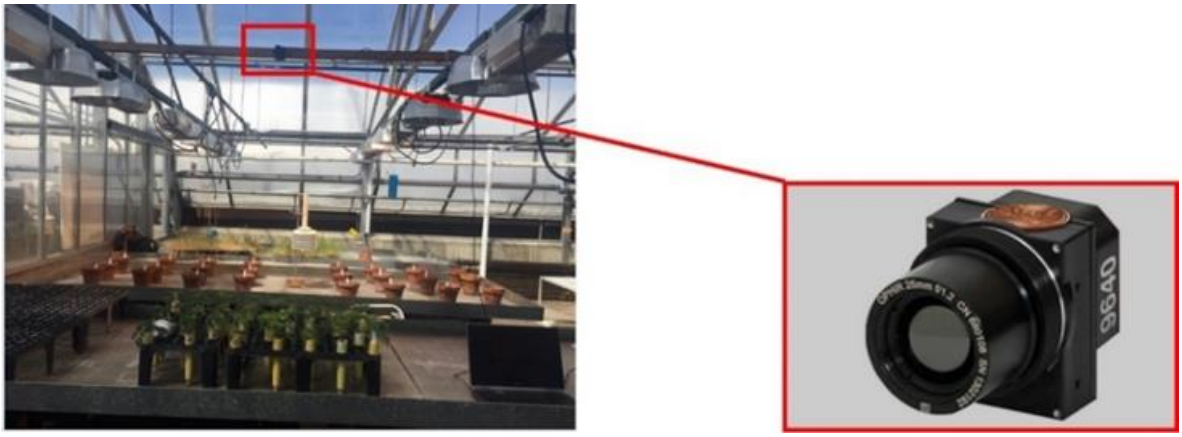

Figure 4.4. Thermal camera set up in the NDSU greenhouse, with a close-up of the thermal camera, and the plant racks placed on a table.

In this study, a novel thermal signature feature was extracted from the thermal images that was invariant to the time transition. The thermal signature describes certain characteristics of the target objects (Christiansen et al., 2014). Thermal signatures of each weed species and resistance condition were developed based on individual plant canopy temperature changes during the 96 h after herbicide application. A total of 95 thermal signatures were extracted to classify resistant weeds versus susceptible one. The signature was normalized by subtracting it with the ambient temperature. Since we aimed to compare the plant canopy temperature of resistant and susceptible weeds at the same environmental condition (greenhouse), the atmospheric relative humidity fluctuations during data collection in the greenhouse was not significant (Figure 4.5). So, the canopy temperature of resistant and susceptible weeds was normalized using T_{canopy}-T_{air} equation.

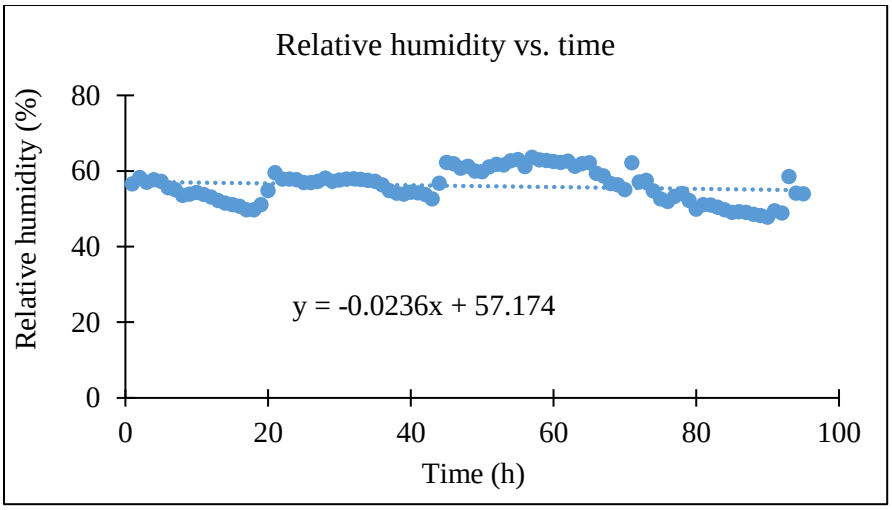

Figure 4.5. Relative humidity fluctuation during data collection in the greenhouse.

Weeds were inspected 15 days after glyphosate application and classified as resistant or susceptible based on its survival condition. Dead or dying plants 15 days after herbicide application were labeled as susceptible while green and alive plants were labeled as glyphosate-resistant weeds (Figure 4.6). Model development included feature selection by stepwise regression analysis and modeling with support vector machine (SVM).

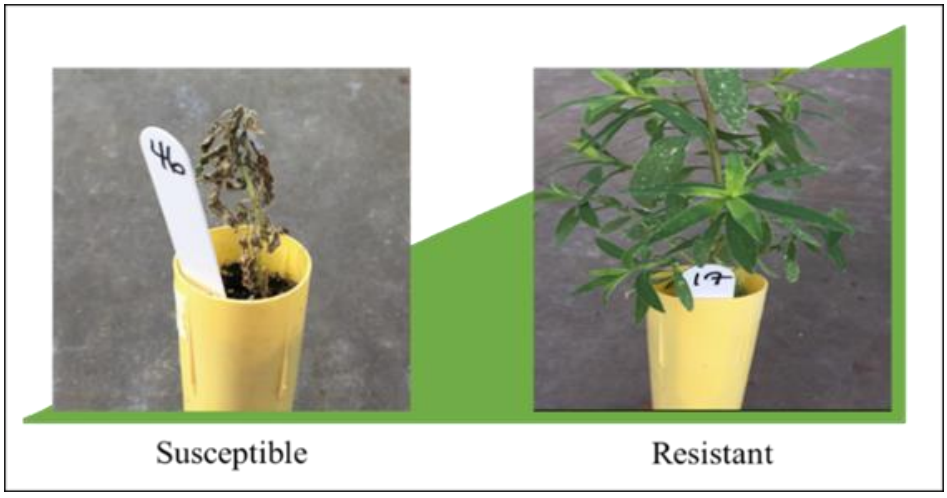

Figure 4.6. A visual illustration of resistant and susceptible weeds.

4.3.3. Measurement of Photosystem II Efficiency

Photosystem II (PSII) is where most of the energy from sunlight gets captured and used by plant to make food. PSII efficiency changes quite quickly based on plant stresses before this change is noticeable by the eye. Measurement of PSII efficiency in glyphosate-resistant and susceptible weeds in the selected three species was performed in a non-invasive method using a MultispeQ-Beta instrument (Kuhlgert et al., 2016) controlled by the PhotosynQ platform software (Michigan State University, USA). MultispeQ has four LEDs with peak emission wavelengths at 530, 605, 650 and 940 nm and a photodiode detector which is sensitive to 700–1160 nm light, making it possible to estimate a range of fluorescence-based photosynthetic parameters. Measurements were carried out 1 to 4 days after the application of glyphosate on fifteen plants of each weed type.

4.3.4. Feature Selection with Stepwise Regression Analysis

Prior to feature selection and classification, data were evaluated for normal distribution since the normality is an underlying assumption in many statistical analyses. There are two main methods of assessing normality including graphical and numerical. The normality assumption of plant canopy temperature was tested using the Shapiro–Wilk test. If the Shapiro-Wilk criterion is equal to one, it means the data are distributed normally while small values reject the normality assumption.

High-dimensional features are usually time-consuming in both features' computation and model utility. The stepwise selection process within the regression analysis was implemented in this study to select a set of features with the most discriminatory power for identifying glyphosate-resistant weeds. The stepwise regression is a technique of developing a regression

model in which the predictor variables are selected based on their ability to explain the most variability in the response variable.

In regression analysis, the regression function is the relationship between a dependent variable (Y) and one or more independent (predictor variables, X_i). A multiple linear regression model with more than one predictor variable can be presented as (Ghani & Ahmad, 2010):

$$Y = \beta_0 + \beta_1 X_1 + \beta_2 X_2 \cdots + \beta_k X_k + \varepsilon \quad (4.1)$$

Where Y is the dependent variable and represents the temperature of resistant or susceptible weed. β_0 is a constant variable, β_i denotes coefficient of i^{th} predictor variable, X_i is the temperature of weed species in i^{th} hours after glyphosate application (predictor variable), and ε represents the error.

In this research, the stepwise selection was used to find the best time after glyphosate application for identifying glyphosate-resistant weeds based on canopy temperature. Significance level for a variable to enter and stay in the model was set at P=0.05 and the criteria for features to be removed from the model was that P > 0.1.

Multiple coefficient of determination (R^2), multiple correlation coefficient (R) and adjusted R^2 were used elsewhere to interpret stepwise analysis (Darlington & Hayes, 2016). The adjusted R^2 is a modified version of R^2 that has been adjusted based on the number of predictors in the model. The adjusted R^2 increases only if the new term improves the model more than expected by chance. In contrast, it decreases when a predictor improves the model by less than expected by chance (Bates et al., 2014).

4.3.5. SVM Classification

After identifying the most discriminative features with stepwise regression method, an SVM model was used to classify glyphosate-resistant and susceptible weeds. In machine

learning theory, SVM was employed to classify the dataset into two categories, building the model as it is initially trained and consequently used to predict whether a new data point belongs to one category or the other.

4.3.6. Non-Linearly Separable Binary Classification

In SVM, all the samples, regarded as p dimensional vectors, will be divided into two classes using a (p-1) dimensional hyperplane, which is called a linear classifier. The classification problem is a set of training vector with N training samples belonging to two classes described as $\{(x_i, y_i), i = 1, 2, \ldots, N\}$, where $\boldsymbol{x_i}$ are the input vectors and y_i are the labels of class ($\boldsymbol{y_i}$ = 1 (class 1), -1 (class 2)). The classification function can be described as follows (Cristianini & Shawe-Taylor, 2000; Jayadeva et al., 2002; Jayadeva & Chandra, 2002):

$$y_i = \boldsymbol{\omega} \cdot \boldsymbol{x_i} - b \tag{4.2}$$

Where $\boldsymbol{\omega}$ is a vector normal to the hyperplane, $|b| / ||\boldsymbol{\omega}||$ is the perpendicular distance from the hyperplane to the origin (Figure 4.7), and $||\boldsymbol{\omega}||$ is the Euclidean norm of $\boldsymbol{\omega}$. Only certain data points (support vectors in SVM) influence the equation of the hyperplane while remaining data points are known as redundant data.

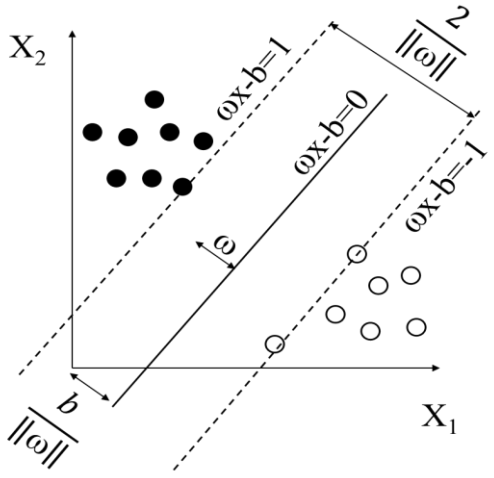

Figure 4.7. A schematic illustration of the Support Vector Machine (SVM) classification method illustrating the hyperplane classifier between two classes (Bajwa & Kulkarni, 2011).

For computing support vectors, we need to prevent data points from falling into the margin, thus one of the following constrained conditions would be required:

$$\boldsymbol{\omega} \cdot \boldsymbol{x_i} - b \geq 1, (y_i = 1) \qquad \text{for } \boldsymbol{x_{1i}} \text{ of the first class}$$

$$\boldsymbol{\omega} \cdot \boldsymbol{x_i} - b \leq -1, (y_i = -1) \qquad \text{for } \boldsymbol{x_{2i}} \text{ of the second class}$$

$[\boldsymbol{\omega}\, \boldsymbol{x} - b = 0]$ is defined as the hyperplane and the points which are on the supporting vector of $[\boldsymbol{\omega} \cdot \boldsymbol{x_i} - b = 1]$ will have a perpendicular distance from the origin of $\left[\frac{1-b}{\|\omega\|}\right]$. Similarly, those points on $[\boldsymbol{\omega} \cdot \boldsymbol{x_i} - b = -1]$ would have the distance of $\left[\frac{-1-b}{\|\omega\|}\right]$. Consequently, the distance between the two supporting planes can be obtained as $\left[\frac{2}{\|\omega\|}\right]$, which is termed as the margin of hyperplane, $\rho(\boldsymbol{\omega})$, given by:

$$\rho(\boldsymbol{\omega}) = 2/||\boldsymbol{\omega}|| \qquad (4.3)$$

For optimal classification, we need to maximize this distance via minimizing $||\boldsymbol{\omega}||$. Technically, the constrained conditions (dividing the data points into two distinct classes) are required in all classification issues. However, some of the sampled points from the two classes may overlap each other in the realistic cases. So, a relaxation for the constrained conditions is considered with the majority of points falling on the "right" side of the hyperplane and a few points falling in between the hyperplanes, which are treated as misclassifications or errors. Therefore, the optimization of the hyperplane requires maximization of the distance of the hyperplane and minimization of the errors. For this purpose, relaxation factors would be introduced to balance between distance maximization and error minimization. When the relaxation factors are introduced, the Equation 4.4 would be defined to maximized $\rho(\omega)$ (Jayadeva et al., 2002; Karimi et al., 2006).

$$\emptyset(\omega) = \|\boldsymbol{\omega}\|^2/2 + C \cdot \sum_{i=1}^{N} z_i \quad (4.4)$$

Where z_i present the relaxation factors, and *C* is the trade-off for balancing the maximized margin of the hyperplane and the minimized classification error.

The explicit solution of Equation 4.4 is rather difficult as it is a convex quadratic optimization problem. By applying Lagrangian multipliers, Equation 4.4 could be written as Equation 4.5 for the linear model (Jayadeva et al., 2002; Karimi et al., 2006).

$$\omega(\alpha) = \sum_{i=1}^{N} \alpha_i - \left(\sum_{i=1}^{N} \sum_{j=1}^{N} \alpha_i \alpha_j \, y_i y_j \boldsymbol{x_i} \cdot \boldsymbol{x_j} \right) \Big/ 2 \;, \left(\sum_{i=1}^{N} \alpha_i y_i = 0, 0 \leq \alpha_i \leq C \right) \quad (4.5)$$

In which, α_i is the positive Lagrange multipliers.

A complicated non-linear hyperplane is required to separate the class members that are not linearly separable. The SVM simplifies this problem by transforming the training points into a higher dimensional space (feature space) where the features are linearly separable. By this transformation, in the higher dimensional space, $\boldsymbol{x_i}$ and $\boldsymbol{x_j}$ are replaced by $\varphi(\boldsymbol{x_i})$ and $\varphi(\boldsymbol{x_j})$, respectively, and Equation 4.5 could be written as (Jayadeva et al., 2002; Karimi et al., 2006):

$$\omega(\alpha) = \sum_{i=1}^{N} \alpha_i - \left(\sum_{i=1}^{N} \sum_{j=1}^{N} \alpha_i \alpha_j \, y_i y_j \varphi(\boldsymbol{x_i}) \cdot \varphi(\boldsymbol{x_j}) \right) \Big/ 2 \;, \left(\sum_{i=1}^{N} \alpha_i y_i = 0, 0 \leq \alpha_i \leq C \right) \quad (4.6)$$

A "Kernel Function", $\boldsymbol{K}(\boldsymbol{x_i}, \boldsymbol{x_j})$ which is the dot product of $\varphi(\boldsymbol{x_i})$ *a*nd $\varphi(\boldsymbol{x_j})$ allows the non-feasible optimization Equation 4.6 to be solved. Three common kernel functions such as radial basis function (RBF), sigmoid, and polynomial kernels are used in SVM classifier. The RBF is the most commonly used kernel function in SVM classification problems and is described in Equation 4.7.

$$\boldsymbol{K}(\boldsymbol{x_i}, \boldsymbol{x_j}) = \boldsymbol{e}^{-\gamma(x_i - x_j)^2} \quad (4.7)$$

Where γ represents kernel parameter. Therefore, the optimization problem for non-linear cases is modified to (Jayadeva et al., 2002; Karimi et al., 2006):

$$\omega(\alpha) = \sum_{i=1}^{N} \alpha_i - \left(\sum_{i=1}^{N} \sum_{j=1}^{N} \alpha_i \alpha_j \, y_i y_j \boldsymbol{K}(\boldsymbol{x_i}, \boldsymbol{x_j}) \right) \Big/ 2 \ , (\sum_{i=1}^{N} \alpha_i y_i = 0, 0 \leq \alpha_i \leq C) \quad (4.8)$$

In which, γ and *C* are the determinants for SVM classifier evaluation. Parameter γ is the kernel parameter that defines the influence of a single training example. Parameter *C* is the penalty parameter of the error term which controls the tradeoff between smooth decision boundary and classifying the training points correctly.

4.3.7. Evaluation of SVM Classification

The performance of SVM classifier is sensitive to the C and γ parameters. A low value of C parameter makes the decision surface smooth and cause under-fitting, while a high C value aims at classifying all training examples correctly and lead to the over-fitting of the training data. Furthermore, very high γ value tries to classify single training data and causes a serious over-fitting problem (Cao & Tay, 2003).

Since there is no structured way to choose the optimum values of γ and *C* parameters in developing the SVM model, they were determined through trial and error routes in this study. The model calibration included running the model with different value sets of γ and *C* were developed using the training data set, and then building the SVM model with the optimum values. The generalization ability of the model was determined using the test data set. Finally, the performance of the SVM model was evaluated through a 10-fold cross-validation method. For this purpose, data were divided randomly into two sets for training and validation, and the process was repeated for 10 times. For each fold, the SVM model was built with training data set

and evaluated with validation data set. In this research, the optimal values of C and γ parameters were selected to be 80 and 0.07, respectively. Furthermore, 70% of the samples were selected randomly to train the classifier and the remaining 30% was used to test the classification accuracy.

In addition to model accuracy, the sensitivity of the model and kappa coefficient were calculated to further evaluate model performance. Since the objective of classification was to identify resistant weeds, the resistant weeds (class R) was defined by a model output of YES and the susceptible weeds (Class S) was defined by a model output of NO in this study. Sensitivity and specificity were introduced to represent the proportion of actual YES or NO which are correctly classified, respectively. Kappa coefficient described the performance of the model and examined the degree of agreement between the actual class and predicted class more than expected by chance. A kappa coefficient of 1 means a full agreement, and zero means full disagreement between assigned and the actual class.

4.3.8. Software

Matlab software v8.5 (MathWorks, Natick, MA, USA) and IBM SPSS Statistics 20.0 (IBM Analytics, Armonk, New York, USA) were used to build the SVM classification model, and to select the significant features for modeling.

4.4. Results and Discussion

4.4.1. Plant Canopy Temperature of Glyphosate-Resistant and Susceptible Weeds

The difference between plant canopy temperature and ambient temperature (ΔT) over the period of the experiment for resistant and susceptible weed species of kochia, waterhemp, and ragweed is illustrated in Figure 4.8. All three-weed species exhibited a higher value of ΔT for susceptible weeds 24 h after spraying glyphosate in comparison with the resistant weeds. The

temperature difference between the susceptible and resistant weeds of the same species fluctuated through 96 h after herbicide application.

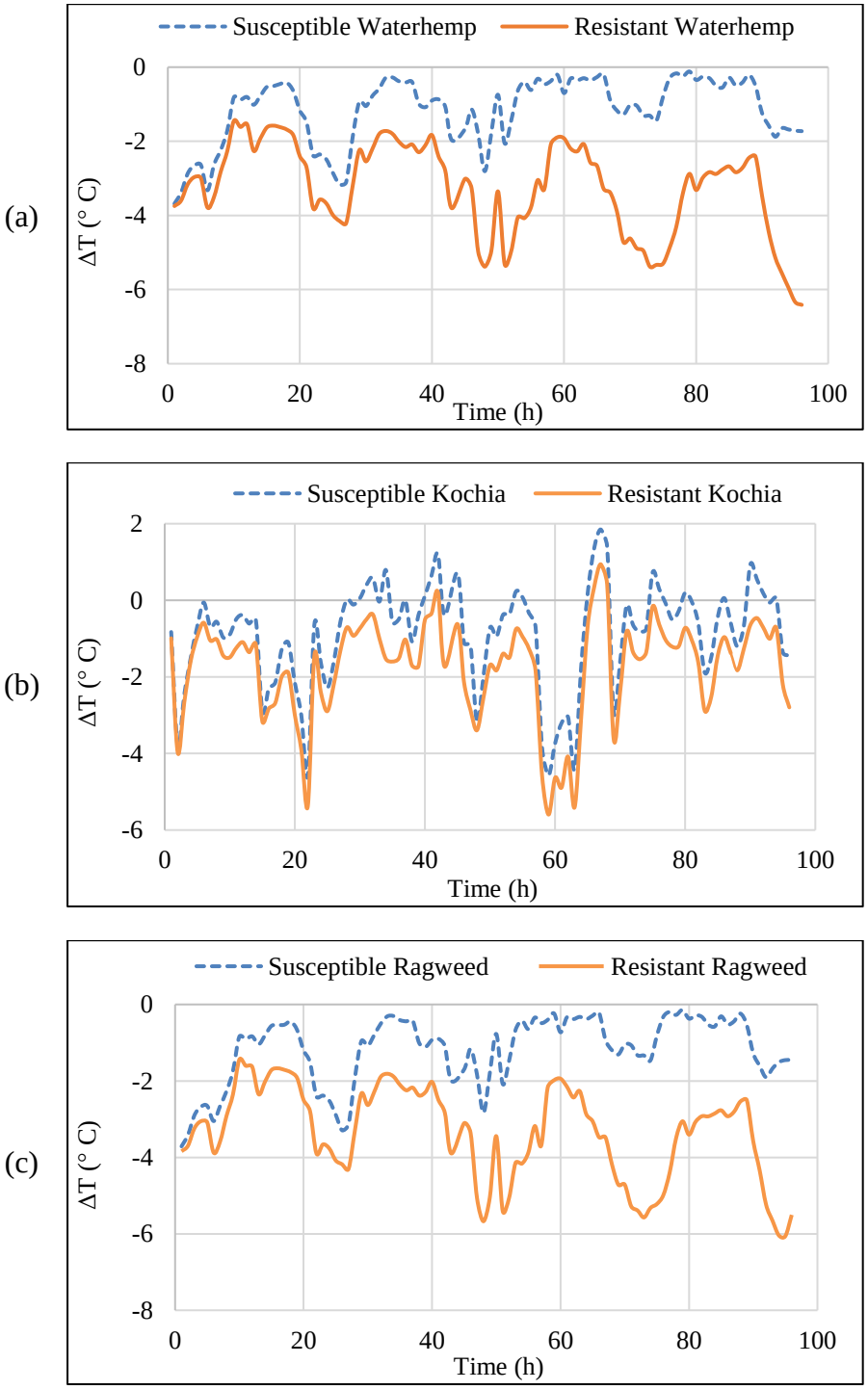

Figure 4.8. The difference between plant canopy temperature and ambient temperature (thermal signature) of resistant and susceptible three weed species (a) Waterhemp, (b) Kochia, and (c) Ragweed over time for the first 96 h after a glyphosate application.

As Figure 4.9 shows, no obvious trend was observed in ΔT as the relative humidity fluctuated, and ΔT values were not dependent on ambient relative humidity.

(a)

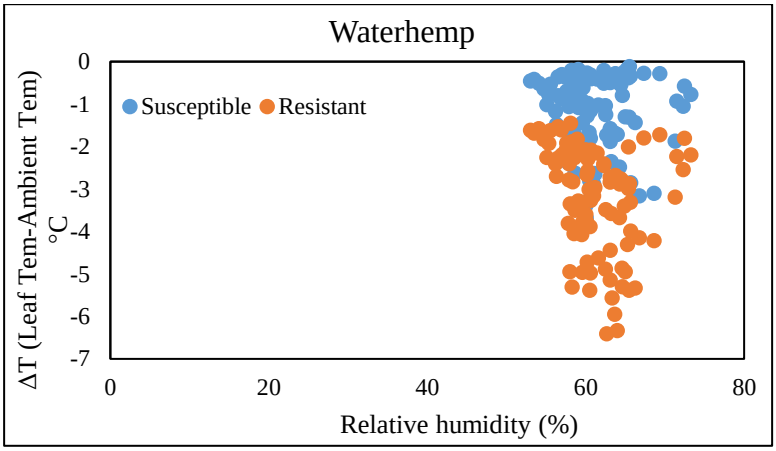

(b)

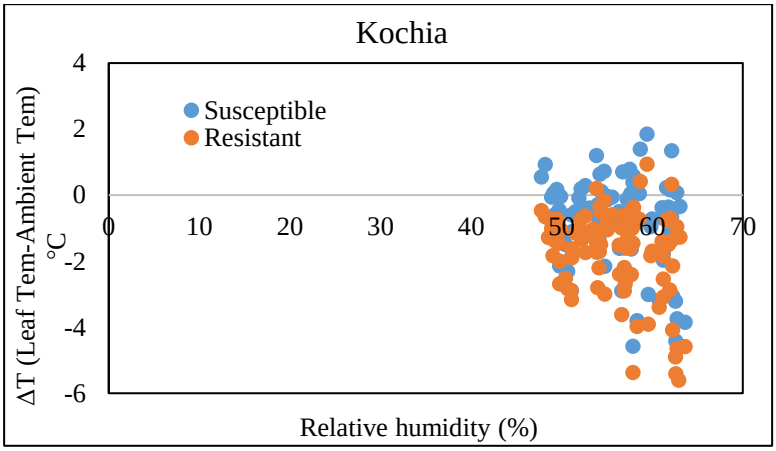

(c)

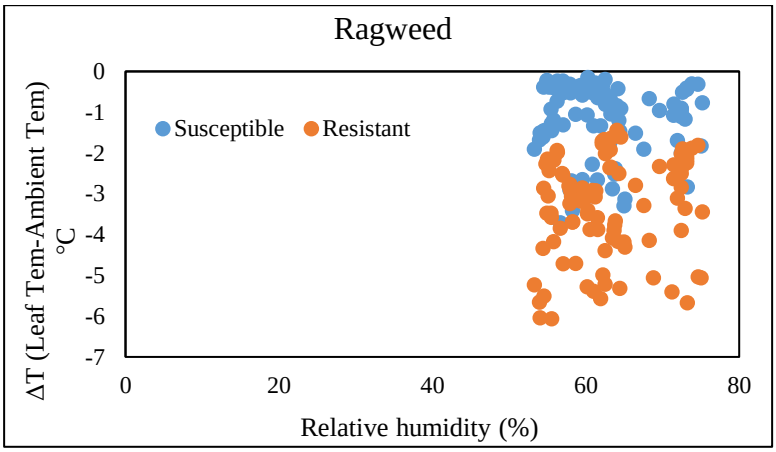

Figure 4.9. The difference between plant canopy temperature and ambient temperature of resistant and susceptible three weed species vs. relative humidity: (a) Waterhemp, (b) Kochia, and (c) Ragweed.

Furthermore, there was not significant difference between leaf water content for control and sprayed plants during four days after glyphosate application (Table 4.1).

Table 4.1. The effect of glyphosate application on leaf water content of weed species.

Weed species		No. of Days after herbicide application		
		2	3	4
Kochia	Control	78.3%+2.4[a]	78.3%+2.6[a]	78.5%+2.6[a]
	Resistant	79.1% +1.8[a]	78.5%+2.4[a]	78.3%+2.8[a]
	Susceptible	78.5% +2.7[a]	77.7%+3.1[a]	78.6%+ 2.8[a]
Waterhemp	Control	74.2%+ 3.2[b]	74.5%+3.1[b]	74.5%+ 2.9[b]
	Resistant	74.5%+3.3[b]	73.3%+3.6[b]	73.2%+3.4[b]
	Susceptible	73.3%+2.4[b]	73.2%+2.7[b]	72.5%+2.4[b]
Ragweed	Control	71.3%+4.1[c]	71.4%+3.9[c]	72.2%+3.9[c]
	Resistant	71.6%+4.2[c]	70.2%+3.5[c]	71.3%+3.1[c]
	Susceptible	71.2%+4.2[c]	71.6%+4.4[c]	70.2%+3.2[c]

* The same letters in each raw indicate a non-significant difference in the mean values at $\alpha = 0.05$.

The elevated temperature of the susceptible weeds can be explained by the fact that glyphosate is detrimental to the physiological mechanisms involved in photosynthesis and other physiological processes, resulting in poor photosynthetic efficiency. This in turn results in a significant loss of light energy as heat in the susceptible plants compared to resistant weeds (Gomes et al. 2017).

4.4.2. Stepwise Regression Analysis for Feature Selection

The stepwise regression analysis resulted in the standard error of 0.021, 0.061 and 0.009 for kochia, ragweed and waterhemp, respectively considering one discriminative feature plant canopy temperature after glyphosate application to identify resistant weeds. (Table 4.2). A slow convergence of the standard error of estimation was observed for all three-weed species by increasing the number of predictive features. Similarly, the R^2_{adj}value was improved by adding more predictive variables in kochia.

Based on the model performance, nine features including F_{46}, F_{60}, F_{91}, F_{19}, F_{15}, F_{28}, F_{44}, F_{70}, and F_{36} were selected to establish the model (Table 4.3) for classification of glyphosate-resistant kochia (subscripts indicate hours after glyphosate application). These nine variables indicated that the resistant kochia weeds could be successfully identified based on the plant canopy temperature 46, 60, 91, 19, 15, 28, 44, 70, and 36 h after glyphosate application. For identifying glyphosate-resistant ragweed and waterhemp, seven and five input features were selected, respectively (Table 4.3).

Input variables of F_{95}, F_{57}, F_{26}, F_{77}, F_{25}, F_{22}, and F_{24} were selected for the identification of resistant ragweed. The standard error of estimation started from a high value of 0.061 for one feature (F_{95}), converged fast to 0.003 with 2 features, and leveled off later. It means that the plant canopy temperature at 57, 26, 77, 25, 22, and 24 h after glyphosate application were critical to identify the resistant from susceptible ragweed with R^2_{adj} equaling to 1.

The five features selected for identifying resistant waterhemp included plant canopy temperature at 95, 57, 26, 55, and 5 h after glyphosate application. The standard error of prediction model converged from 0.009 to 0.002 with 5 selected features, resulting in R^2_{adj} equal to 1 (Table 4.2).

In fact, it is time and labor-intensive to collect plant canopy temperature at 5 to 9 times after herbicide application to identify glyphosate-resistant weeds. Therefore, the improvement in the accuracy by increasing the number of features can be neglected as the accuracy of predicted model by considering one feature was acceptable. The best feature time for the prediction of glyphosate-resistant waterhemp and ragweed was 95 h after spraying with R^2_{adj} value 1 and 0.985, respectively. In order to identify glyphosate-resistant kochia, plant canopy temperature 46 h after glyphosate spraying was the most discriminative feature with R^2_{adj} value of 0.998.

The most discriminative variable was achieved after more than 24 h after glyphosate application for all three-weed species. This result is in the agreement with the absorption pattern of glyphosate in the plants. The absorption pattern of glyphosate in the waterhemp and ragweed populations was similar up to 24 h after herbicide application for both susceptible and resistant types, however, after this time, the absorption of susceptible weeds was noticeably more than the resistant ones (Whitaker et al., 2013). The total chlorophyll and plastoquinone concentrations decrease in plant leaves after herbicide application. The carotenoid concentration was shown to decrease by 24 h after herbicide application (Gomes et al., 2017). The stepwise feature selection process confirmed the glyphosate-based herbicide mode of action interconnecting its effects on shikimate pathway, photosynthetic process, and oxidative events in plants which have been reported by Gomes et al., (2017) for the first time.

Table 4.2. Model summary of stepwise regression for feature selection.

NO	Adjusted R^2			Std. error of the estimate		
	Waterhemp	Ragweed	Kochia	Waterhemp	Ragweed	Kochia
1	1	.985	.998	.009	.061	0.021
2	1	.999	.999	.003	.003	0.018
3	1	1	.999	.003	.003	0.017
4	1	1	.999	.002	.002	0.016
5	1	1	.999	.002	.002	0.015
6		1	.999		.002	0.014
7		1	.999		.002	0.013
8			.999			0.012
9			1.000			0.011

An analysis of canopy temperatures at the time points identified in stepwise regression process revealed that the largest temperature difference in kochia was observed at 46 h after

glyphosate application (Figure 4.10a), which matched well with the feature selection results from the stepwise model (Table 4.3).

(a)

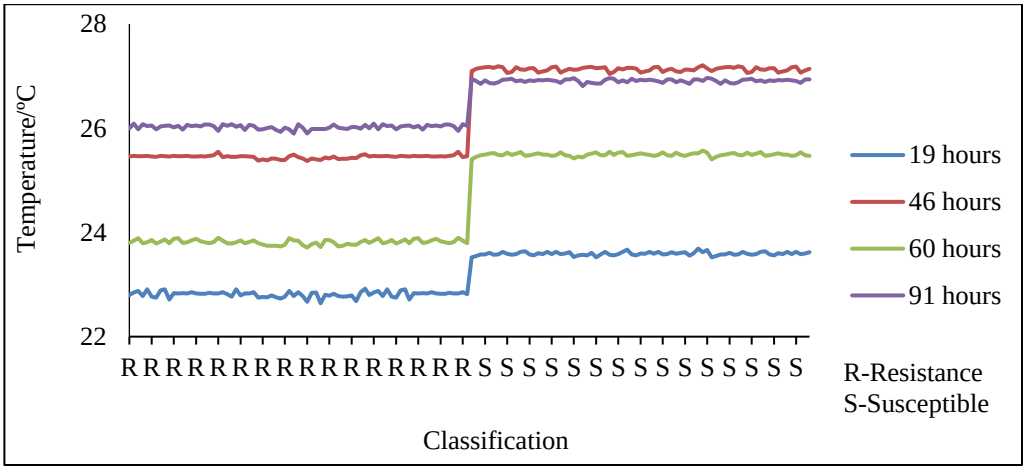

(b)

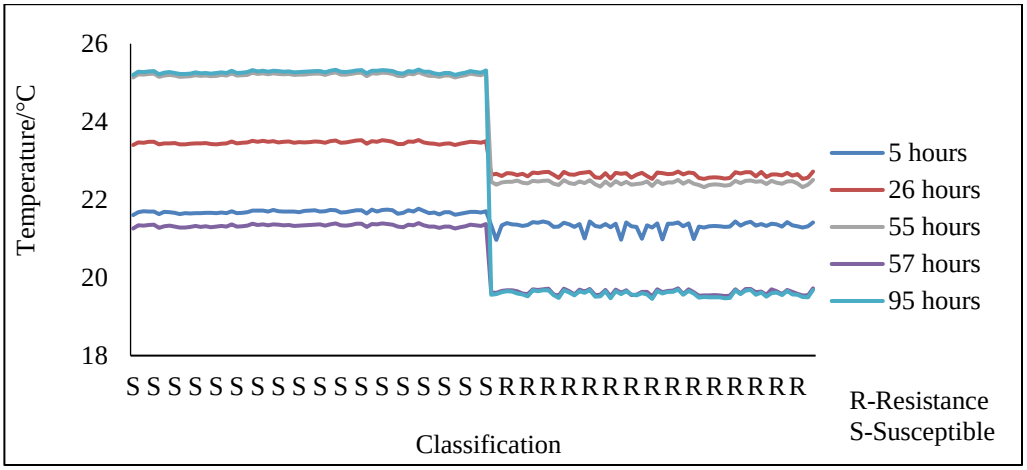

(c)

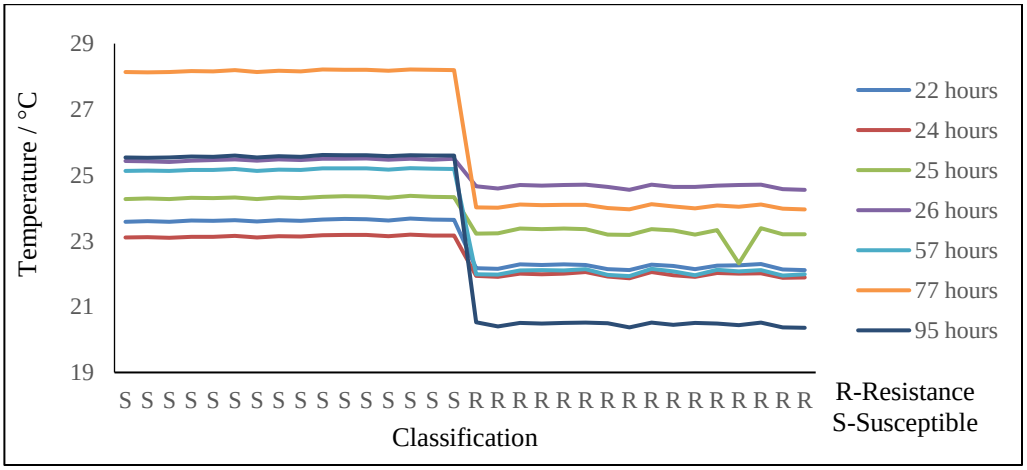

Figure 4.10. Features selected by the stepwise regression process plotted for resistant and susceptible plants of a) Kochia, b) Waterhemp, and c) Ragweed.

The largest temperature difference in waterhemp and ragweed was achieved at 95 h after the herbicide application (Figure 4.10b and 10c). This is consistent with the finding that glyphosate activations rapidly reduces photosynthesis activity, and it is translocated with photosynthesis from the leaves to the meristematic tissue to reach the target-site, achieving maximum uptake at 96 h after treatment (Alcántara-de la Cruz et al., 2016).

The stepwise regression model to predict the plant canopy temperature of selected weed species was developed based on the most discriminative features for identifying glyphosate-resistant weeds (Table 4.3).

Table 4.3. Stepwise regression model developed from thermal signatures weeds.

Weed species	Model[a]
Kochia	$Y = 12.073-0.293*F_{46}-0.354*F_{60}-0.05*F_{91}+0.102*F_{19}+0.021*F_{15}+0.268*F_{28}-0.135*F_{44}+0.255*F_{70}-0.137*F_{36}$
Ragweed	$Y = 1.808-0.191*F_{95}+0.173*F_{57}+0.102*F_{26}0.106*F_{77}+0.006*F_{25}+0.065*F_{22}-0.05*F_{24}$
Waterhemp	$Y = 2.000-0.191*F_{95}+0.182*F_{57}+0.105*F_{26}-0.115*F_{55}+0.017*F_{5}$

[a] F_i (i = 1,2, …) = plant canopy temperature i^{th} after glyphosate application.
Y is dependent variable and represents the temperature of resistant or susceptible weed.

4.4.3. Measurement of Photosystem II Efficiency

The application of glyphosate can affect photosynthesis in the plants, and photosynthesis efficiency alters based on stresses. Photosynthesis efficiency of glyphosate-resistant weeds is much higher than susceptible weeds from one to four days after spraying (Figure 4.11).

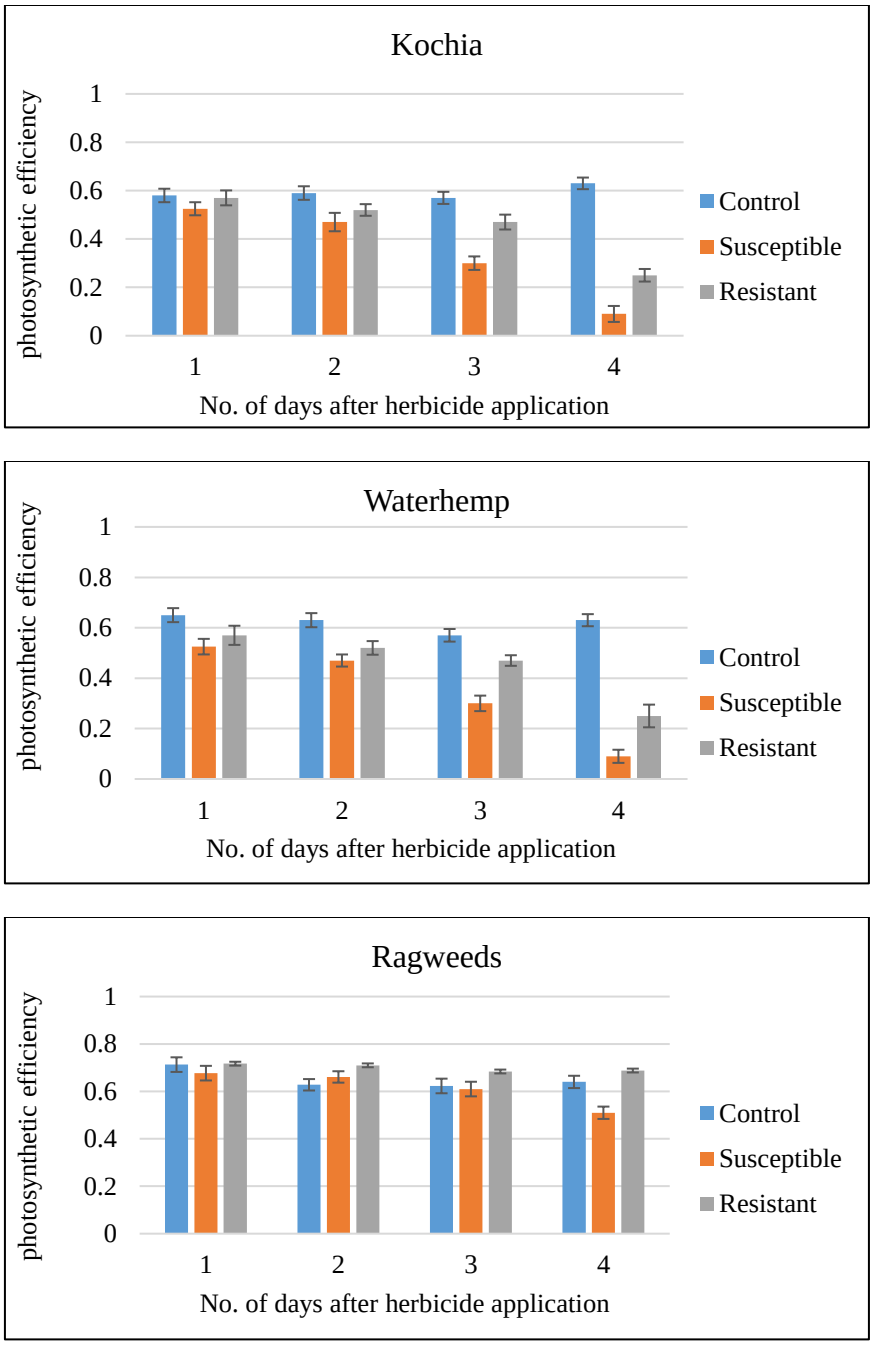

Figure 4.11. Comparison of photosynthesis's performance measured from 1 to 4 days after glyphosate application on the weeds (Error bars represent the standard deviations). No significant difference was observed in the photosynthetic efficiency for different weed species in the first day. However, resistant weeds exhibited significantly higher photosynthetic efficiency than susceptible weeds two days after herbicide application.

.

4.4.4. SVM Analysis

Resistant kochia samples were successfully classified with 100% accuracy, while the waterhemp and ragweed resistant weeds were classified with 97.4% accuracy (Table 4.4). The specificity of the classification model was 1 for all three-weed species. The model output indicated that only one resistant sample was misclassified for waterhemp and ragweed (Table 4.4). In addition, SVM was able to discriminate susceptible weeds with 100% accuracy for all three-weed species. The maximum kappa coefficient was computed as 1 (Table 4.4) for kochia samples which was due to the high performance of the respective model. It means that there was a full agreement between classified glyphosate-resistant kochia and actual class.

Table 4.4. Confusion matrix of SVM classification.

		Predicted value								
		Kochia			Ragweed			Water hemp		
		NO	YES	Total	NO	YES	Total	NO	YES	Total
Actual value	NO	23	0	23	19	0	19	21	0	21
	YES	0	23	23	1	18	19	1	16	17
Total		23	23	100%	20	18	97.4%	22	16	97.4%

The kappa coefficients for waterhemp and ragweed were reported as 0.947 and 0.948, respectively (Table 4.5). This strong degree of agreement between actual and predicted classes for three weed species presented that thermal features after herbicides application were powerful enough to identify the resistant weeds. Misclassifications occurred in both ragweed and waterhemp discrimination with the sensitivity values of 0.947 and 0.941, respectively (Table 4.5), indicating that resistant weeds could be misidentified by chance of 5.3% and 5.9%. Taking into consideration the limited number of sample data and weed species, SVM models and

thermal features of weeds presented a good performance in identification of susceptibility and resistibility in weeds.

Table 4.5. Statistical measurements of the performance of SVM.

Weed Species	Kochia	Ragweed	Waterhemp
Classification accuracy %	100	97.4	97.4
specificity	1	1	1
Sensitivity	1	0.947	0.941
Kappa Coefficient	1	0.948	0.947

4.5. Conclusion

The study demonstrated the feasibility of stepwise regression-based feature selection and SVM classifier to identify resistant weeds based on weed species' thermal signature. The stepwise regression method was able to select the optimum time after glyphosate application to identify the glyphosate-resistant type of kochia, ragweed, and waterhemp. The strong degree of agreement between actual resistant type and predicted resistant plant for three weed species revealed that thermal features after herbicides application were powerful enough to identify the resistant weeds with high accuracy. Based on the test set validation results, SVM machine learning classified glyphosate-resistant weed species with more than 97 % accuracy. The most effective features to obtain high accuracy classification were more than 24 h after glyphosate application in this study. According to the stepwise regression model results, 95 h after spraying was the most discriminative time to identify glyphosate-resistant ragweed and waterhemp with reliable accuracy. Resistant kochia weeds could be identified based on plant canopy temperature 46 h after glyphosate application. The results of this study exhibited a novel approach to identify glyphosate-resistant weeds based on canopy temperature in support of SSWM.

4.6. Acknowledgment

We thank Sandy Johnson and Mark Ciernia from NDSU greenhouse for their help with the greenhouse experiment. The authors would like to thank the North Dakota Agricultural Experiment Station, North Dakota Soybean Council, and the North Dakota Department of Commerce for providing grant support to conduct this research.

5. FIELD IDENTIFICATION OF WEED SPECIES AND GLYPHOSATE-RESISTANT WEEDS BASED ON UAS IMAGERY IN EARLY GROWING SEASON[1]

5.1. Abstract

Accurate weed mapping in early growing season is an essential step in a site-specific weed management (SSWM) system. This study focuses on validating the potential application of high resolution multispectral and thermal UAS images in classification of weed species and glyphosate-resistant weeds at an early phenological stage. A field experiment was conducted to evaluate supervised classification methods to identify three-weed species including waterhemp, kochia, and ragweed. The accuracy of six classification algorithms namely Parallelepipeds (P), Mahalanobis Distance (MD), Maximum Likelihood (ML), Spectral Angle Mapper (SAM), Support Vector Machine (SVM) and Decision Tree (DT) implemented at pixel level and object-level for weed species classification were studied. Thermal infrared imagery was also used to assess the canopy temperature variance within the weed species to identify the glyphosate-resistance status in detected weeds. The object-based algorithms developed with mosaicked imagery effectively classified weed species with the overall accuracy and Kappa coefficient values greater than 86% and 0.77, respectively. The lowest accuracy and Kappa coefficient (67% and 0.58) were observed for pixel-based MD algorithm. The canopy temperature-based classification of susceptible and resistant weeds resulted in discrimination accuracies of 88%, 93% and 92% in glyphosate-resistant kochia, waterhemp and ragweed.

[1] The material in this chapter was co-authored by Alimohammad Shirzadifar, Sreekala Bajwa, and John Nowatzki. Alimohammad Shirzadifar developed the idea and processed the experimental data. Alimohammad Shirzadifar performed the analysis, drafted the manuscript and designed the figures. Sreekala Bajwa provided critical feedback and supervised the project. John Nowatzki helped supervise the project.

Keywords: Weed species; Glyphosate-resistant weeds; UAS imagery; Object-based classification.

5.2. Introduction

Weeds are considered as the most serious threat to agricultural crop production as they compete with crops for water, nutrients, and light, resulting in yield reduction. Currently, herbicide application is the most common weed management technology in the US (Benbrook, 2018), where weed control is achieved through a uniform herbicide application across the entire field (Kunz et al., 2018). However, weed species and populations across the field are highly variable (Lambert et al., 2018). Chemical weed management is of great interest owing to increased concern over environmental protection as well as the emergence of herbicide resistant weeds as a result of sub-optimal application of chemicals (Schütte et al., 2017).

In the context of precision agriculture, site-specific weed management (SSWM) is an emerging strategy, confining the application of herbicides to weed infested areas to improve crop protection efficacy (Pflanz et al., 2018). The SSWM strategy includes four steps of weed monitoring, decision making, herbicide application, and evaluation and documentation. Weed mapping as the first step is a key element in SSWM, collecting data for field survey and weed distribution either by ground sampling or remote detection. Remote sensing that captures the whole field offers particular advantages for weed mapping over traditional ground survey methods including large area coverage, facile data collection, and time-efficient process (Gålfalk et al., 2018).

The recent advances in Unmanned Aerial System (UAS) facilitate the application of time-efficient field mapping in large scale in modern agriculture. Small UAS with light weight and high level of maneuverability are capable of carrying deferent sensors and flying at low

altitude over agricultural fields (Sosnowski et al., 2018). Very high ground resolution (pixel<5cm) UAS images can be used to identify and map the spatial distribution of weeds within crop fields when spectral differences among weeds, crop and soil are present and quantifiable (Castillejo-González et al., 2014). Although Garcia-Ruiz et al. (2013) used low attitude UAS equipped with multi spectral camera to detect different plants, traditional pixel-based image analysis cannot effectively detect weeds in crop fields during early growth stages due to spectral similarity of crop and weed pixels, and the variability in spectral characteristics of similar plants caused by field variability.

The application of supervised classification methods using ground-based imaging devices has shown promise for weed classification (Pérez-Ortiz et al., 2015). Remote sensing-based high-resolution UAS imagery in combination with supervised classification holds the potential to identify weed species. Supervised pixel-based classifiers use prior knowledge to identify spectral similarity in image pixels to assign each pixel to the most similar class. Supervised classification methods include the simplest distance- or angular-based classifiers (Mahalanobis Distance and Spectral Angel Mapper) to the most complex probability-based (maximum likelihood) or machine learning (support vector machine and decision tree) algorithms. Each classifier has its own strengths and limitations, and the selection of a classifier for specific site study requires the consideration of many factors, including data distribution, classification accuracy, algorithm performance and computational resources.

In UAS-based remote sensing, object-based image analysis (OBIA) and pixel-based image analysis (PBIA) are two categories of image classification. In conventional PBIA supervised weed classification, each pixel could potentially include a mixture of soil, plant leaves, residue and shadow. The variability in target spectral reflectance introduced by mixing of

target classes can limit the classification accuracy. In contrast, the geographic OBIA recognizes spatially and spectrally homogenous objects through a segmentation process based on different attributes, such as size, texture, shape, and spatial and spectral distribution (Liu & Abd-Elrahman, 2018). These factors can be combined with contextual and hierarchy procedures to give an accurate classification in OBIA (Pena et al., 2013). A comparative study on the performances of PBIA and OBIA to discriminate weeds and sorghum plant indicated higher accuracy for OBIA (Che'Ya, 2016).

The visual similarity between herbicide-resistant and susceptible weeds limits the identification accuracy of herbicide resistance status, and SSWM may not be effectively accomplished using the application of common visual plant species identification techniques. It was reported that the application of herbicide can cause stress in plants and this, in turn, can reduce the rates of photosynthesis and transpiration in the plants. Reduced transpiration rate is accompanied by elevated temperatures in stressed plants (Zhang et al., 2016). Therefore, we hypothesized that the canopy temperature after spraying can be a reliable indicator to detect resistant weeds.

This research aims at exploring the potential of multispectral imagery captured by UAS over crop fields for weed species identification, followed by the application of thermal images for the identification of herbicide resistant weeds. Field experiment was conducted with the objective of identifying and validating the best PBIA and OBIA supervised classification methods to identify three weed species including waterhemp (*Amaranthus rudis*), kochia (*Kochia scoparia*), and ragweed (*Ambrosia artemisiifolia L.*). The detected weeds were then classified into glyphosate resistant and susceptible categories by the application of canopy temperature after an herbicide application.

5.3. Materials and Methods

5.3.1. Study Site and Field Experiment Design

A field-scale study was conducted on a 680 m^2 soybean crop field at NDSU Research Farm located at Carrington, North Dakota, USA (Figure 5.1). The Roundup ready Nutech Soybean (Glycine max) was planted on May 22nd, 2017 at 403845 seeds/ha. For field experiment, two common types of weeds (kochia and waterhemp) were grown in the greenhouse in separate pots, and the pots were transferred into the field at 5-7 leaf stage (Figure 5.2). The weed plants were transplanted randomly in the fields to create a mix of main crop with two weed species. The seeds for the weeds were collected randomly from different parent plants to provide a collection of resistant and susceptible plants.

Field data were also collected from a 400 m^2 research field located at Mayville (Figure 5.1). The field was naturally infested with glyphosate-resistant and susceptible lambsquarters, and ragweed (Figure 5.2). Weeds on the fields were manually identified and tagged with their species and geographic coordinates through field scouting. When the weeds were approximately 7.6 cm tall, glyphosate [N-(phosphonomethyl) glycine] of 1.7% concentration was applied to the fields at a uniform rate.

Figure 5.1. Field sites: a) Google Maps® inset showing the general location of the study sites with blown up views of fields at b) Carrington, c) Mayville.

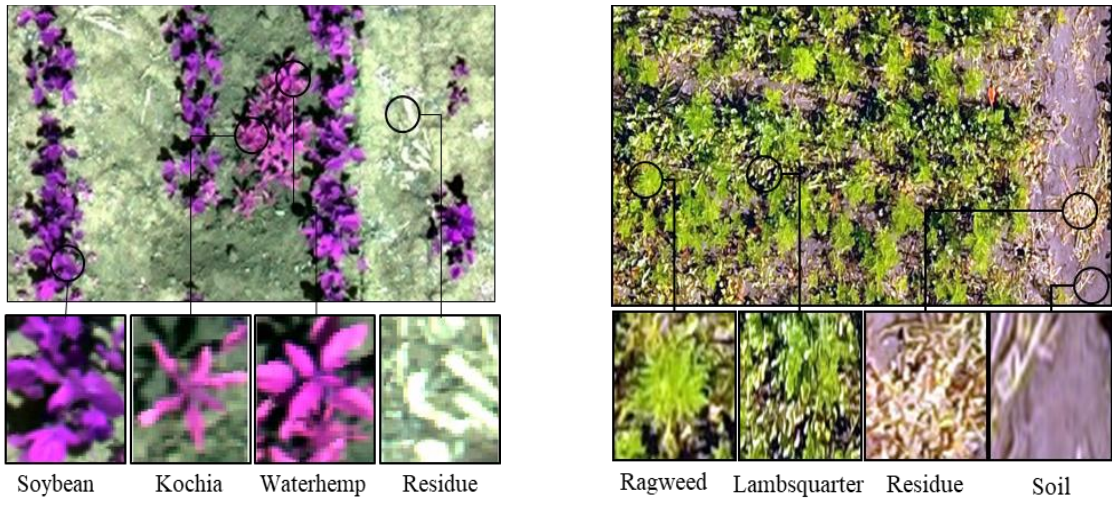

(a) (b)

Figure 5.2. A multispectral image illustrating the target classes in the two study sites: a) Carrington (false color image), b) Mayville (RGB image).

5.3.2. Data Collection

The aerial data acquisition system was composed of a multispectral camera (Quad sensor, Sentera, Minnesota, USA) and a thermal camera (Infrared Camera Inc. Texas, USA), mounted separately on two types of small UAS. Two Quad-copters namely Phantom3 and DJI S1000 (SZ, DJI Technology Co., Ltd., Shenzhen, China) were used to fly the cameras over the experimental fields for collecting multispectral and thermal images, respectively (Table 5.1). Multispectral images were used to classify weed species. Thermal images were captured 4 days after glyphosate application and were used to identify herbicide resistance status in the weeds. Direct georeferencing of acquired images with the accuracy of 20 centimeter was provided by dual on-board navigation-grade GPS and GLONASS receiver.

Table 5.1. Summary of used cameras and flight procedures in the study.

Item	Camera type	
	Multispectral	Thermal
UAS	Phontom3	S1000
Sensor name	Sentera Quad	9640 P-Series USB
Sensor type	CMOS	UFPA (VO×)
Max-pixels	10.5 MP RGB, 3×1.2MP	640×480
Length of focus	6.05 mm	25mm
Sensor size	56×96×52 mm	34×30×34 mm
Channels	RGB,670,710,730	7µm-14µm
Average wind speed	4.5 m/s	3.2 m/s
Average altitude	10.1 m	8 m
Average pixel size on the ground	6.14 mm	5.5mm
Forward overlap	60	65
Side overlap	70	80
FOV[a]	44° H	24.8 × 18.6

UAS images were captured at low flying altitudes of 8 m for thermal, and 10.1 m for multispectral. Therefore, the area covered by each single still image was limited. The still images collected from the UAS at 60-65% forward overlap, and 70-80% side overlap were mosaicked to obtain an image covering the whole study area. In total, 420 multispectral images were captured over the study field located at Mayville and 750 multispectral images were recorded for the soybean farms at NDSU Research Center.

Five ground control points including four points at the field corners and a coordinate close to the field center point were marked for bundle block adjusting. The flight route was programmed using DJI GS PRO app to allow the UAS to acquire data automatically at pre-set waypoints. In addition, the flight altitude and required image overlapping for mosaicking process was also managed using DJI GS PRO app.

5.3.3. Image Calibration

During data collection, a standard spectralon split gray level panel reference (Labsphere Inc., North Sutton, NH, USA) was placed in the middle of the field to calibrate spectral data. Digital images captured by multispectral camera were spectrally corrected by applying an empirical linear calibration method (Hunt et al., 2010). The mean values of three bands (blue, green, and red) in an image before and after correction is shown in Figure 5.3.

5.3.4. Image Mosaicking

Prior to implementing image processing steps to identify weeds, the individual images were mosaicked to create a single image representing the whole field. Agisoft Photoscan Professional Edition (Agisoft LLC, St. Petersburg, Russia) software was employed to orthorectify and mosaic the collected images. A point cloud model was developed by finding the geographical position and principal axes (roll, pitch and yaw) of the camera in each acquired

image and aligning the images automatically with the Agisoft Photoscan software. Then, the individual images were projected over a geometry of 3D construction to generate an orthophoto map. The final step was developing a single image representing the whole study site.

5.3.5. Spectral Separability Analysis

The application of supervised classification methods on large image sets is time and effort- intensive to identify the best method. The feasibility of classifications algorithms in field target class detection was evaluated based on the visual differences in spectral signature, principal component analysis (PCA), and scatter plots of spectral reflectance for target classes. Spectral signature of plant species of interest, bare soil and residue were developed to determine the possibility of weed species classification. The PCA is a statistical method that uses orthogonal transformation to transform a set of observations of possibly correlated variables into a set of values of linearly uncorrelated variables called principal components (Voyant et al., 2017) . Due to the high degree of spatial similarity between spectral signatures, PCA is used to identify the most significant variance in the spectral reflectance of target classes. The scatter plot of target spectral reflectance in the first two PC space can illustrate the separability of target classes.

(a)

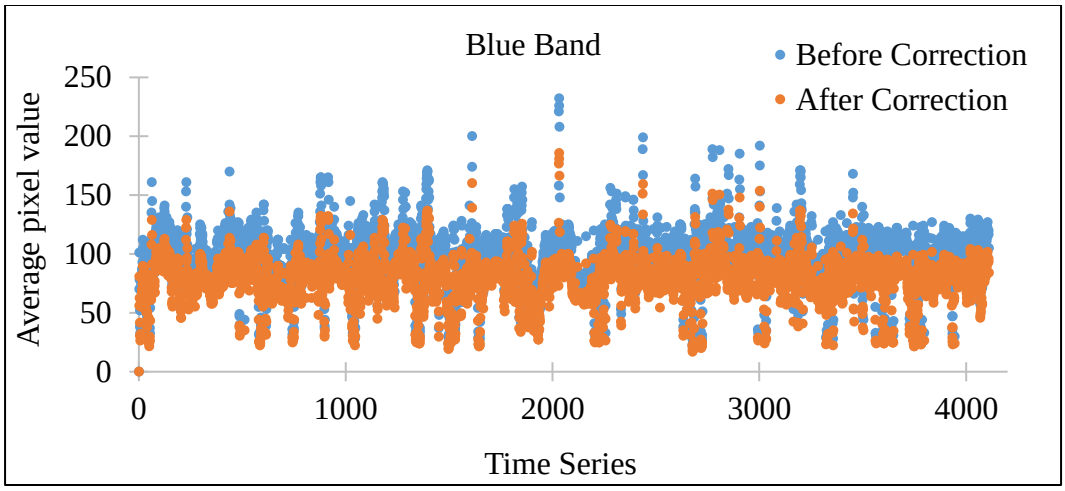

(b)

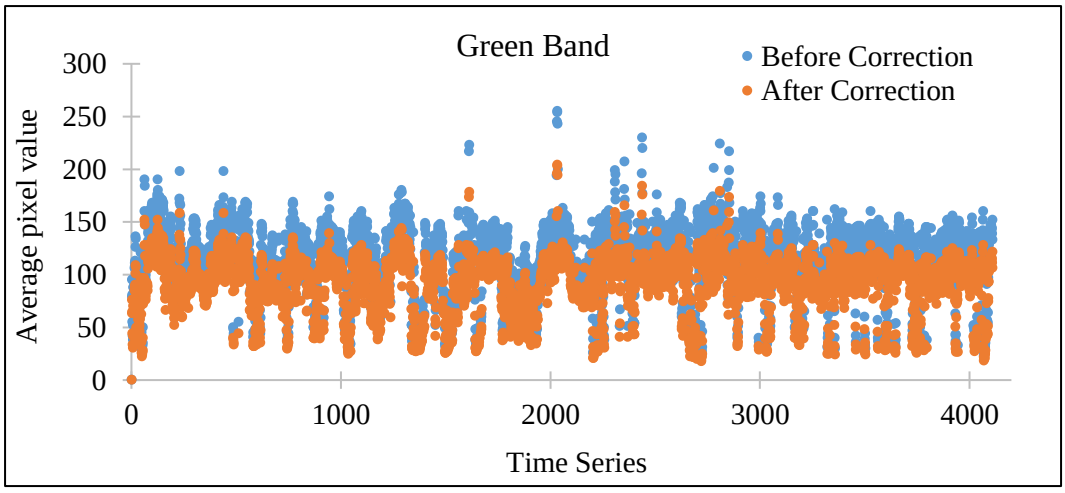

(c)

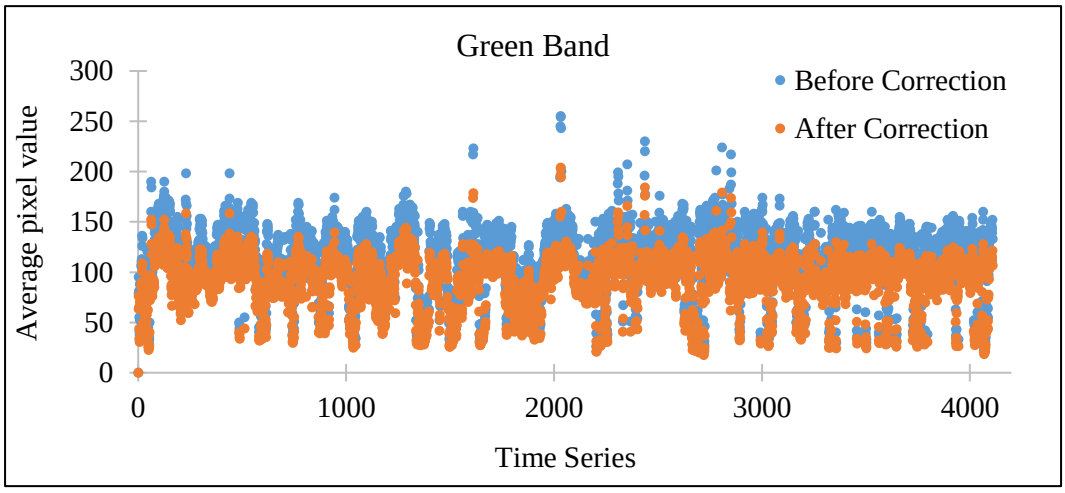

Figure 5.3. Calibrating RGB band Digital Numbers (DNs), in an empirical line correction approach. a) Blue band, b) Green band, c) Red band.

5.3.6. Segmentation Procedure

Segmentation is a key factor in the OBIA classification methods. The images were segmented using a multi-resolution algorithm to create homogeneous multi-pixel objects corresponding to crop, weed species, bare soil and residue. The multi-resolution segmentation method minimizes the average heterogeneity and produces highly homogeneous image objects at an arbitrary resolution. The image objects were generated from the spectrally and spatially similar pixels based on a set of input parameters including shape, smoothness, compactness, etc (Table 5.2). The OBIA method designed for the weed mapping objectives was developed using the commercial software eCognition Developer 8.9 (Trimble GeoSpatial, Munich, Germany).

Table 5.2. The input information used for segmenting field image into objects for object-based classification.

Target	Compactness	Smoothness	Shape index	Roundness	Asymmetry	Elliptic fit	Density	Border index
Soybean	0.23	0.77	2.68	1.43	0.25	0.31	1.8	2.68
Waterhemp	0.5	0.5	1.4	0.75	0.69	0.54	2.31	1.25
Kochia	0.52	0.38	1.37	0.19	0.75	0.36	1.89	1.2
Ragweed	0.34	0.76	2.27	0.81	0.74	0.67	2.1	2.15
Lambsquarters	0.16	0.84	1.38	0.31	0.22	0.76	1.62	1.42
Residue	0.44	0.56	1.39	0.36	0.9	0.68	1.2	3.69

5.3.7. Image Classification

Weed species, crop and soil were classified using six supervised classification algorithms with both PBIA and OBIA methods. Six supervised classifiers with strong conceptual and mathematical differences including Parallelepiped (P), Maximum Likelihood (ML), Mahalanobis Distance (MD), Support Vector Machine (SVM), Spectral Angle Mapper (SAM), and Decision Tree (DT) were examined to select the optimum method for weed species classification (Castillejo-González et al., 2014). To evaluate the normality of UAS images data, the histogram

graphical visual inspection with skewness and kurtosis parameters were used. Exploratory data analysis showed that image data were normally distributed and meets the normality assumption for methods such as ML.

The P classification method also known as the box decision rule, recognizes each class by defining square areas based on minimum and maximum reflectance values into spectral measures of training classes. The MD and SAM algorithms calculate the spectral distance and the spectral angle from each pixel to the spectral average of each class, respectively. The ML algorithm is a parametric supervised classifier based on the Bayes theorem and classifies the objects by considering the variance– covariance within the class distributions.

The SVM is a supervised learning algorithm that analyzes data as points in a feature space and identifies the pattern for classification. This model divides the data into separate categories by defining a clear gap between the categories as wide as possible. In this study, the linear SVM method was used due to obtaining more accurate result than non-linear functions. The DT is a predictive model that maps observations to their target values or labels. DT method makes classification rules by recursively partitioning the data into increasingly homogenous groups (Stephens & Diesing, 2014). In this study, the DT method was applied using the C5 algorithm (Pandya & Pandya, 2015) that expands nodes in depth-first order in each step by the divide-and-conquer strategy. Mosaicked multispectral images were classified in ENVI 5.3 (Broomfield County, Colorado, US) software equipped with image processing toolbox.

The accuracy of each classification method was evaluated by developing the numerical confusion matrix (error matrix) and computing the kappa coefficient. The confusion matrix provides the overall accuracy of the classification by comparing the percentage of classified pixels of each class with the verified ground truth class. The Kappa coefficient is a measure of

how the classification results compare to class labels assigned by chance. It can take values from 0 to 1, and the value of 0 indicates that there is no agreement between the classified image and the reference image. If kappa coefficient equals to 1, then the classified image and the ground truth image are totally identical.

5.3.8. Glyphosate-Resistant Weed Identification

After weed species identification step, herbicide resistance status was studied by comparing the canopy temperature 4 days after glyphosate application. Canopy temperature was obtained from thermal images using a 9640 P-Series Infrared Camera (ICI, Beaumont, TX, USA) with 7–14 μm spectral response and ±1°C accuracy. Thermal camera was mounted on DJI S1000 and images were processed using IR Flash software (Infrared Camera ICI. TX, USA) to identify glyphosate-resistant kochia and waterhemp in Carrington site, and resistant-ragweed in Mayville field. Before capturing the images, a Blackbody ICI 350 portable IR calibration (ICI. TX, USA) was used to check the camera calibration. Thermal images were captured in low altitude to develop high resolution (5.5 mm) images for classifying resistant versus susceptible weeds. Each individual thermal image covered a relatively small area of 1.6 m^2 in the field. This analysis assumed that the variations in thermal signature due to soil moisture content was negligible in a small field. Furthermore, atmospheric condition in each image was the same for both susceptible and resistant weeds (data were collected between 12 to 2 pm and the sky was clear) (Table 5.3). Therefore, the comparison of plant canopy temperature could lead to classify resistant versus susceptible weeds in each individual thermal image. Before starting the image capture, a Blackbody ICI 350 portable IR calibration (ICI. TX, USA) was used to check the camera calibration.

Table 5.3. Atmospheric conditions during the period of data collection in Carrington (S1) and Mayville (S2) study sites.

Study site	Data collection time	Air temperature (°C)	Relative humidity (%)
S1	12:15-12:30	32.13±0.01	48.32±0.00
S2	13:05-13:23	33.37±0.02	54.12±0.01

To identify glyphosate-resistant weeds based on canopy temperature, 16 thermal images captured form each field were analyzed separately by threshholding and segmentation in IR Flash software. The results were compared with the ground truth data to evaluate the accuracy, sensitivity, specificity, and precision through counting the false positives and the false negatives for herbicide resistance. Classifier performance was evaluated as two-class problems based on the confusion matrix. There are two classes namely positive and negative for herbicide resistance. Confusion matrix consists of true positive (TP), false positive (FP), false negative (FN) and true negative (TN) values. Since the objective of classification was to identify resistant weeds, the resistant weed (class R) was defined by a model output of positive and the susceptible weed (Class S) was defined by a model output of negative in this study. False positive represents the number of susceptible weeds which were identified as resistant. In contrast, false negative indicates the number of resistant weeds which were classified as susceptible ones. Accuracy was the ratio of correct decisions made by a classifier (Equation 5.1). Sensitivity and specificity were introduced to represent the proportion of actual resistant (Equation 5.2) or susceptible (Equation 5.3) species which are correctly classified, respectively. Precision was defined as the ratio of predicted positive examples which really were positive (Equation 5.4).

$$Accuracy = \frac{TP + TN}{TP + FP + FN + TN} \tag{5.1}$$

$$Sensitivity = \frac{TP}{TP + FN} \tag{5.2}$$

$$Specificity = \frac{TN}{TN + FP} \tag{5.3}$$

$$Precision = \frac{TP}{TP + FP} \tag{5.4}$$

The ground truth data were collected 15 days after glyphosate application to visually detect the resistant weeds. Glyphosate-resistant weeds on the field were identified and labeled with their geographic coordinates throughout the field.

An overview of weed species classification and identifying glyphosate-resistant weeds in this study is illustrated in Figure 5.4.

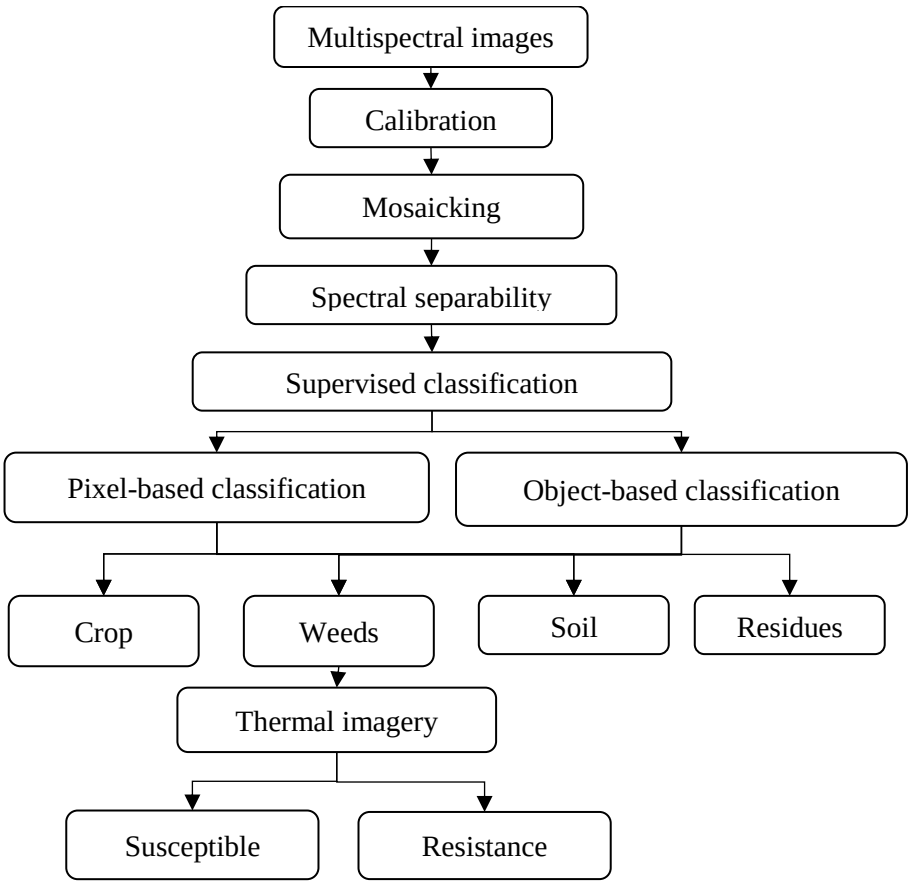

Figure 5.4. Flowchart of recognition algorithms applied for object classification and weed species detection and glyphosate resistant weeds.

5.4. Results and Discussion

5.4.1. Spectral Reflectance Separability

The distinct spectral signatures for field components in both field studies are illustrated in Figures 5.5a and 5.5a. The scatter plot of spectral reflectance in the first two PC indicated that soybean and weed species in Carrington could be discriminated into separate classes considering spectral signature in red and blue wavebands (Figure 5.5).

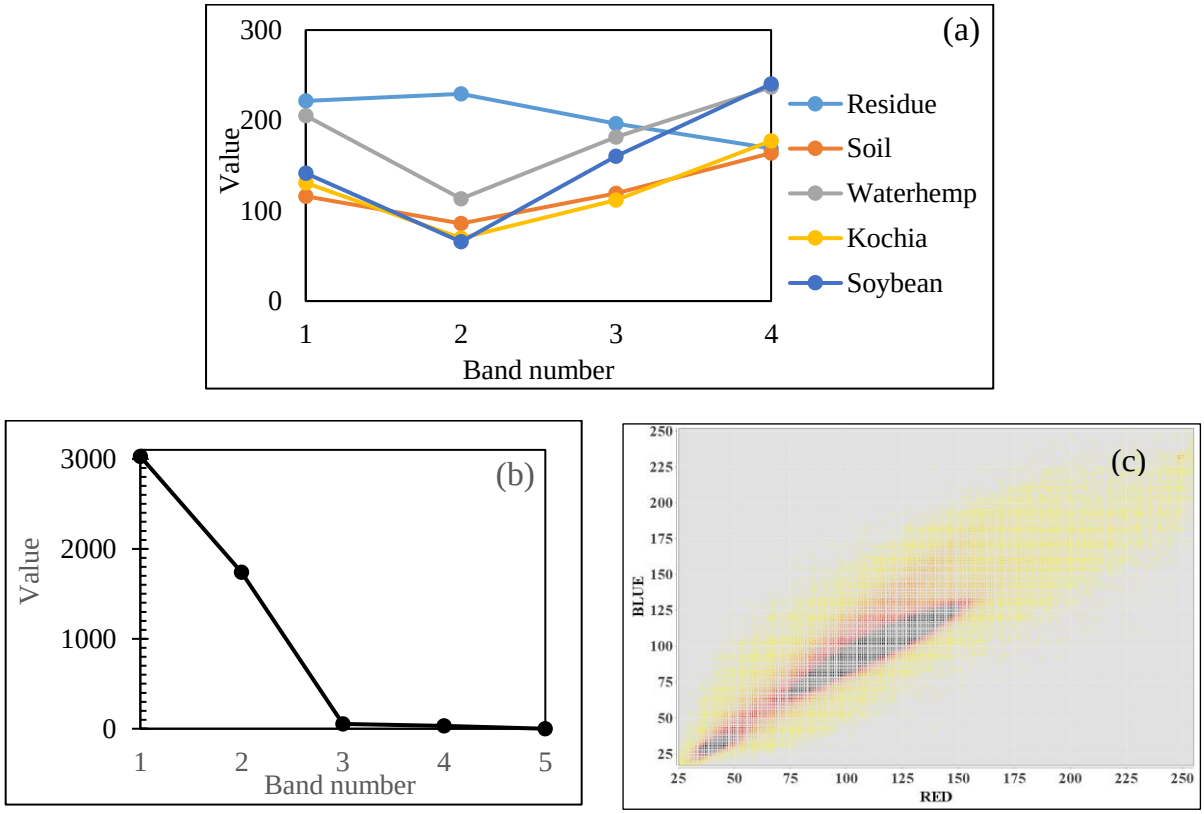

Figure 5.5. Assessment of feasibility of field components classification in Carrington study site: a) Spectral signature, b) PC plane, and c) Scatterplot of spectral reflectance. Band number 1 through 4 are RGB, 670,710,730 nm.

Similarly, the separable scatterplots in the discriminative range of green and red wavebands (Figure 5.6) confirmed the possibility of weed species classification in Mayville research site. In general, the differences in the spectral responses between crop and weed species

in visible blue, green and red wavebands can be attributed to variations caused by the differences in the chlorophyll content of the plants.

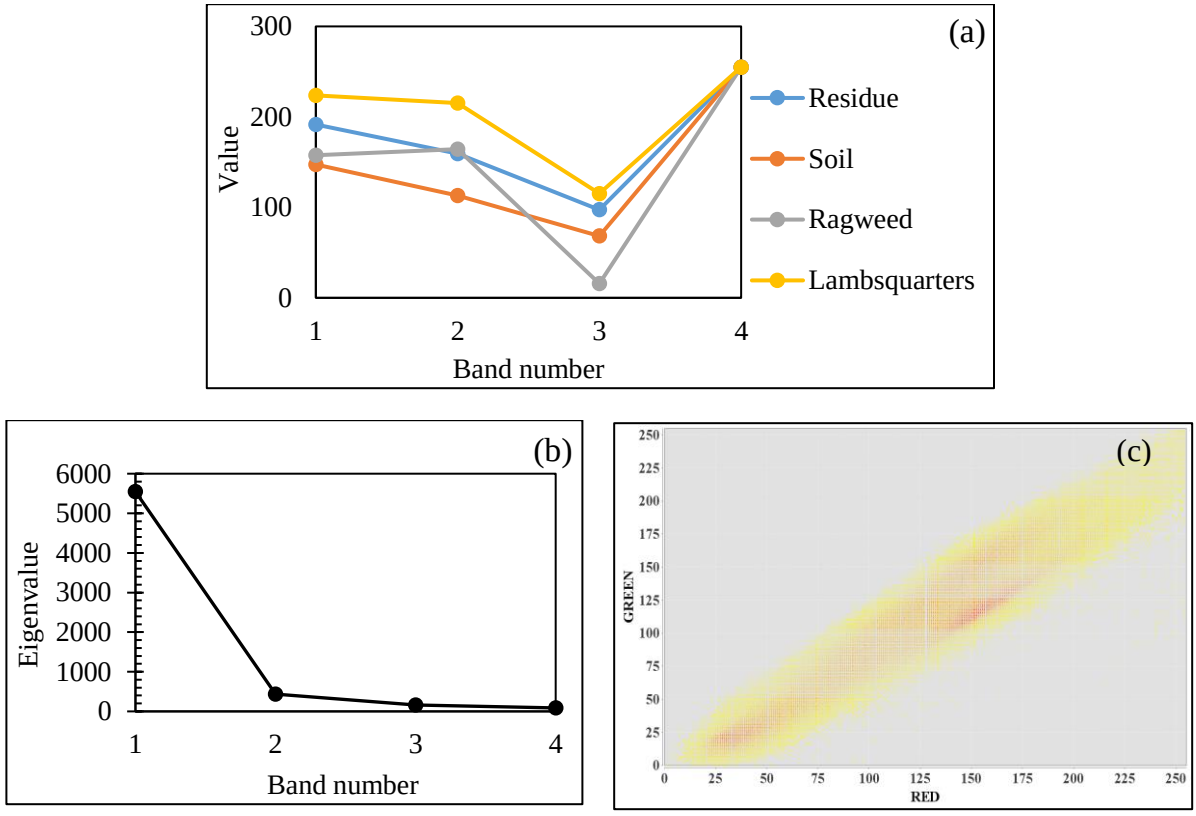

Figure 5.6. Assessment of feasibility of field components classification in Mayville study site: a) Spectral signature, b) PC plane, and c) Scatterplot of spectral reflectance. Band number 1 through 4 are RGB, 670,710,730 nm.

5.4.2. Crop and Weed Species Classification Accuracy

At high spatial resolution, it is possible to distinguish the different leaf shapes and textures for the different target classes. The accuracy of classifying the target classes (main crop, weed species, soil and residue) in the experimental fields using OBIA and PBIA classification algorithms is listed in Table 5.4. All six classification algorithms resulted in lower the overall accuracies and Kappa coefficients under the pixel-based analysis, compared to object-based analysis. Lower accuracies of PBIA methods indicate that soil background, residue, and shadow in mixed-pixel may cause variabilities that reduce the classification accuracy.

The SVM method resulted in the highest classification accuracy of 98-99%, and kappa coefficient of 0.99-1 under object-based classification. In OBIA method, all classification methods except MD algorithm exhibited high classification accuracies with overall accuracies greater than 86% and Kappa coefficients greater than 0.77. A supervised classification strategy is considered acceptable if the overall classification accuracy higher than 85%, and Kappa coefficient higher than 0.75 (Castillejo-González et al., 2014). Therefore, the OBIA classification with P, ML, SVM, SAM, DT methods exhibited accuracies higher than the minimum acceptable levels (Table 5.4). However, the MD classifier with the overall accuracy of 74% and Kappa coefficient of 0.6 didn't reach the commonly accepted requirements. This observation might be attributed to the disability of simple MD analysis to detect small variations in spectral reflectivity (Morozova et al., 2013).

Table 5.4. Classification accuracy of weed species using different supervised classification algorithms at Carrington (S1) and Mayville (S2) study sites.

Supervised classification method	Pixel-based				Object-based			
	OA[a] (%)		*K*[b]		OA (%)		*K*	
	S_1[c]	S_2[d]	S_1	S_2	S_1	S_2	S_1	S_2
Parallelepiped (P)	78	86	0.69	0.78	85	90	0.77	0.82
Maximum Likelihood (ML)	83	87	0.65	0.86	91	97	0.86	0.94
Mahalanobis Distance (MD)	67	85	0.58	0.85	74	95	0.6	0.93
Support Vector Machine (SVM)	92	93	0.87	0.9	99	98	1	0.96
Spectral Angle Mapper (SAM)	87	85	0.8	0.83	92	91	0.86	0.81
Decision Tree (DT)	88	89	0.87	0.92	94	97	0.91	0.95

OA[a]: overall accuracy, *K*[b]: Kappa coefficient

In PBIA method, the most comparable classification results were observed with SVM method. The SVM classifier exhibited the overall accuracy and Kappa coefficient of 92-93% and

0.87-0.9, respectively. While, MD classification algorithm resulted in the lowest overall accuracy of 67% and Kappa value 0.58 for the Carrington location.

The distribution of soybean crops, waterhemp and kochia weed species, soil and the other field components in Carrington field in multispectral image were analyzed using all the classification algorithms evaluated with the PBIA and OBIA methods (Figure 5.7.).

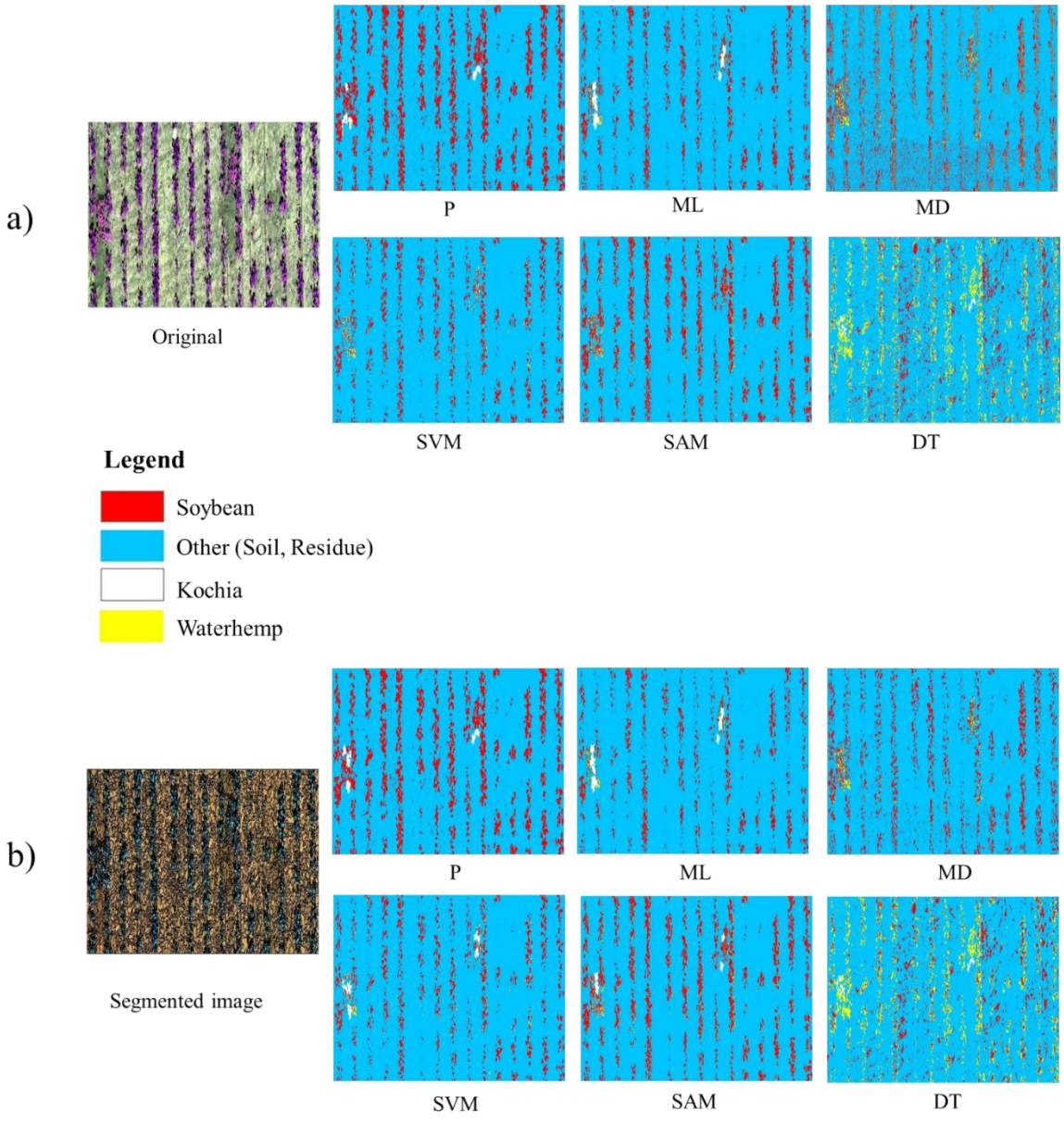

Figure 5.7. Comparison of a) PBIA and b) OBIA classification algorithms in Carrington study site.

Similarly, the results of classified images for two weed species including lambsquarters and ragweed, bare soil and residue in Mayville research site using all the classification algorithms through PBIA and OBIA methods are illustrated in Figure 5.8.

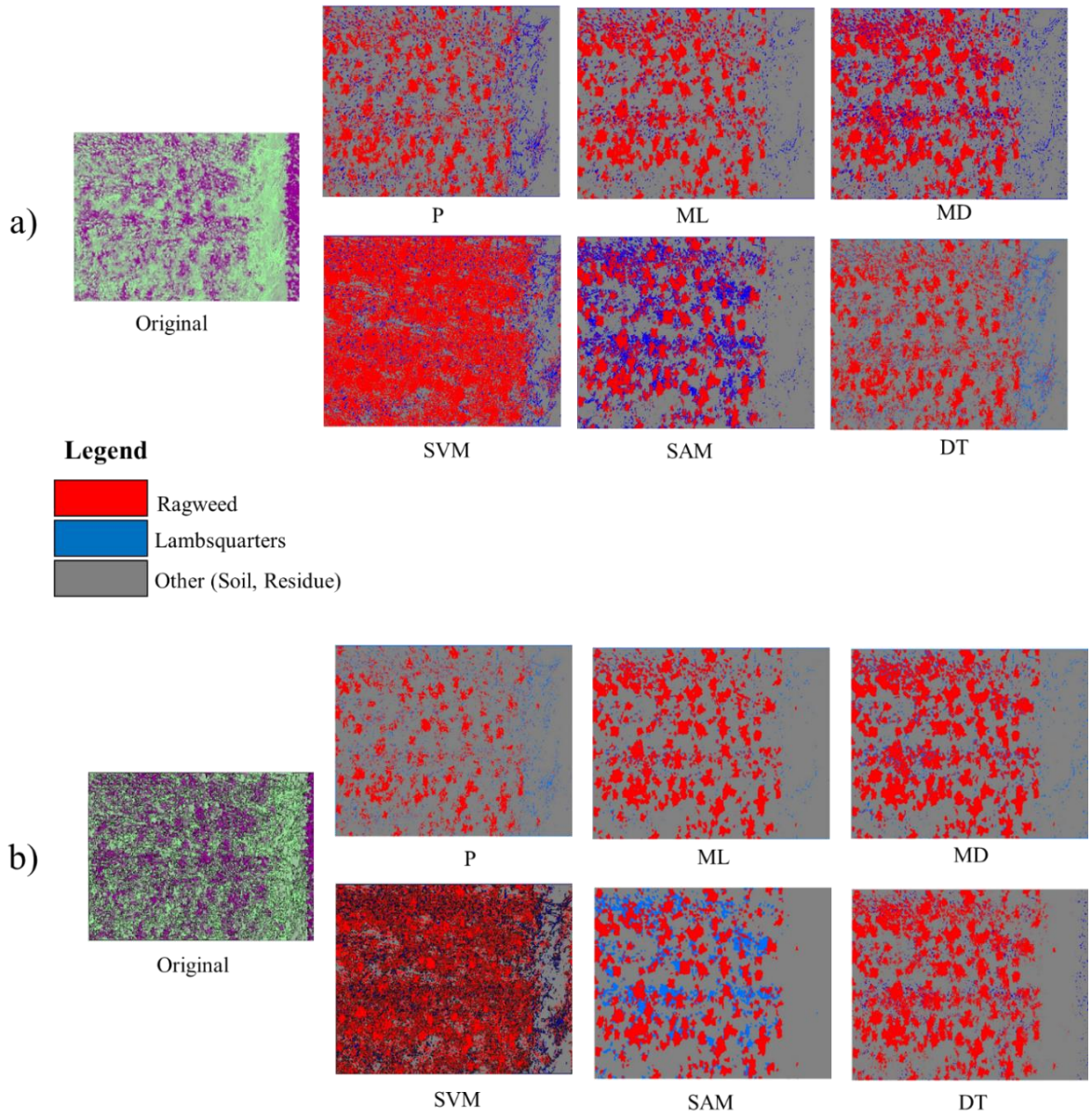

Figure 5.8. Comparison of a) pixel- and b) object-based classification algorithms in Mayville study site.

All classifiers under PBIA and OBIA exhibited higher overall accuracy in Mayville field in comparison to Carrington site. This observation was related to the reduction of crop-plant

detection ability in the multispectral images as a classified object. Furthermore, the relatively higher phenological difference between lambsquarters and ragweeds in Mayville field than soybean and weed species (waterhemp and kochia) in Carrington might be another factor in enhancing weed detection accuracy in Mayville. This fact confirmed that the spectral reflectance similarity between plant species in early growth season is a limiting factor in PBIA. However, OBIA methods by segmenting the images into groups of adjacent pixels with homogenous spectral values displayed higher detection accuracy for weed species by reducing some of the pixel to pixel variability.

Although all the classifiers worked with the same data, SVM and DT algorithms required longer processing times. More complicated computational processing made SVM and DT more sensitive and accurate in comparison to MD, ML and p algorithms with a fast and facile procedure for weed species classification early after plant germination. The two simple MD and ML algorithms yielded very accurate results in Mayville site where there were two weed species for discriminating, while their classification accuracy was lower in Carrington site in which soybean was added to classified objects.

Clear difference was observed between the OBIA and PBIA classifications in all supervised classification methods evaluated in this study. The integration of segmented objects in the studied classifiers resulted in an increase in overall accuracy in OBIA classification methods. The ML classifier exhibited 10% higher overall accuracy through OBIA classification platform in comparison with PBIA method in Carrington site study. While, the least growth in overall accuracy was seen in P with 4% increase in OBIA with segmentation in Mayville site. Similar observation was reported by López Granados (2011). On one hand, a high spatial resolution of the remote images is required for weed detection, however, the higher spatial

resolution is penalised with lower spectral resolutions limited to the visible and NIR spectral regions. The similar morphology between plant species in early growing season cause low spectral differentiation between weed species and main crop. Therefore, the combination of spectral and spatial characteristics produced a significant improvement over the precision obtained in the object-based classifications. Although, OBIA was more time and effort- intensive due to the initial segmentation process for which more expert knowledge and more specialised software were required, the overall classification accuracy exceeded the performance achieved using PBIA algorithm. Therefore, in this study the object-based had great potential and advantages for weed species detection in early growth stage.

5.4.3. Glyphosate-Resistant and Glyphosate-Susceptible Weed Accuracy

The plant canopy temperature extracted from the thermal images indicated that the temperature of susceptible weeds increased after glyphosate application. The resistant weeds in Carrington and Mayville exhibited much lower canopy temperature in comparison with the susceptible weeds for all three-weed species (Table 5.5).

Table 5.5. Mean values of canopy temperatures in Carrington (S1) and Mayville (S2) study sites.

Study site	Weed species	Canopy temperature (°C)	
		Resistant weeds	Susceptible weeds
S1	Kochia	26.12 ±0.11	27.95± 0.25
	Waterhemp	27± 0.18	28.85±0.19
S2	Ragweed	28.04 ±0.21	29.96±0.33

The temperature variance in weed species with different level of susceptibility is a result of physiological mechanism involved in the photosynthesis process. The application of herbicide leads to a poor photosynthetic efficiency accompanied by a significant loss of light energy as

heat in the susceptible plants (Gomes et al., 2017). The IR Flash window which illustrates the colorized thermal image over weed plants is shown in Figure 5.9 and 10. The IR256 color lookup ramp was used for temperature variance visualization, in which the area with lower temperatures were displayed in blue and the hottest canopies were presented in red and followed by green. Glyphosate-resistant waterhemp weeds are shown by green color (27.18 °C) in the Carrington experimental field in comparison with susceptible weeds which were shown in red (28.99°C). In Mayville, the resistant-ragweed plants are revealed by the blue color (28.14 °C) in IR Flash window while susceptible are displaced in green (30.06 °C).

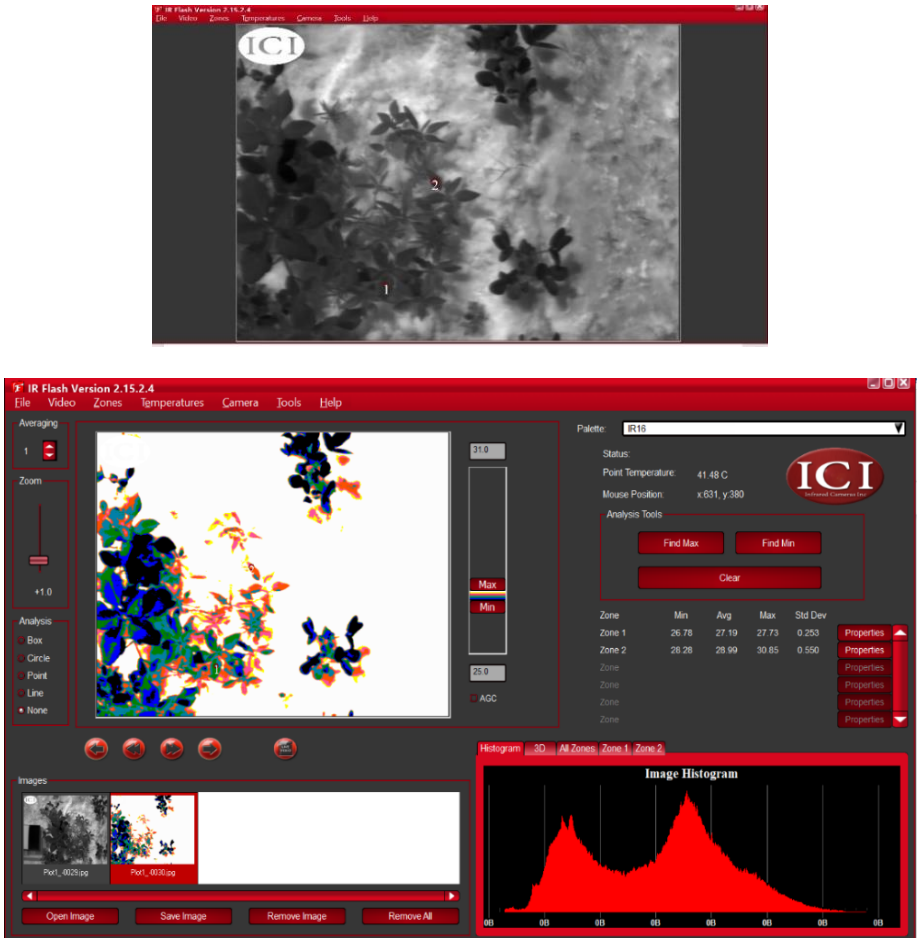

Figure 5.9. A thermal image of the waterhemp plants (Carrington study site) in IR Flash software. Zone 1(green) indicates Resistant waterhemp. And Zone 2 (red) indicates susceptible waterhemp. The average temperature for the various zones can be seen on the right-hand panel.

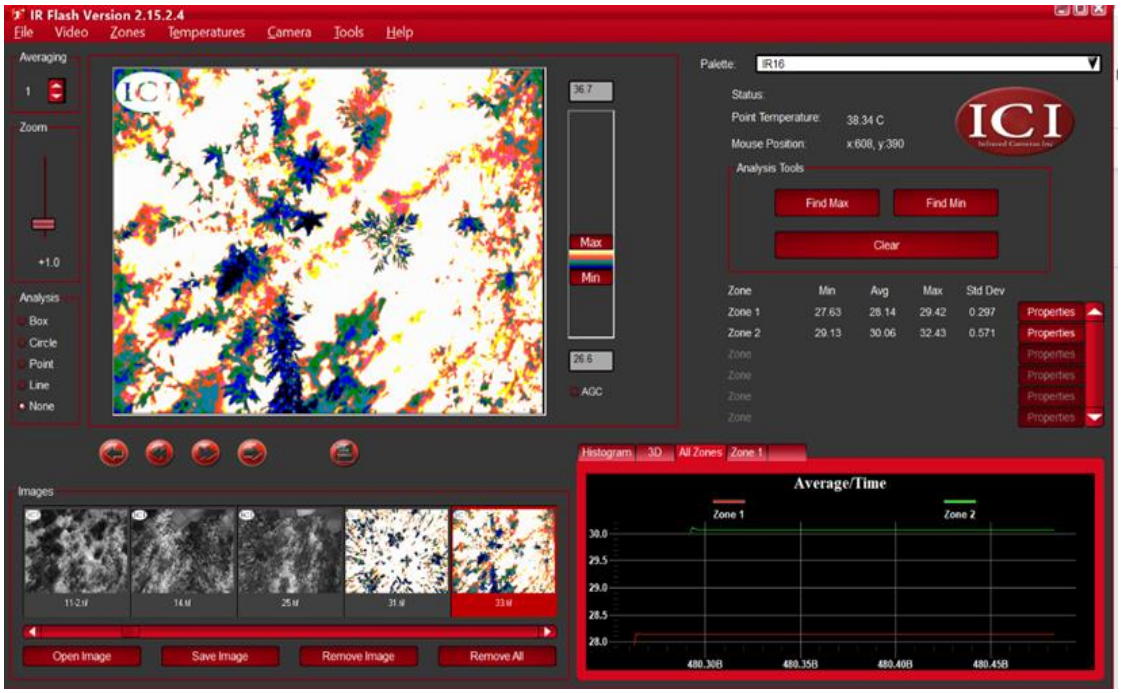

Figure 5.10. The thermal image of the ragweed plants (Mayville study site) in IR Flash software. Zone 1 (blue) # Resistant ragweed. Zone 2 (green) # susceptible ragweed. The average temperature for the various zones can be seen on the right-hand panel.

The results were compared with the ground truth data after observing the death symptoms in susceptible weeds. (Table 5.6).

Table 5.6. Summary of glyphosate-resistant weed classification accuracy at Carrington (S1) and Mayville (S2) study sites.

Study site	Weed species	Weed No.		Resistant weed classification accuracy			
		Resistant	Susceptible	Accuracy %	Sensitivity	Specificity	Precision
S1	Kochia	25	36	88	0.83	0.92	0.87
	Waterhemp	27	41	93	0.91	0.95	0.90
S2	Ragweed	56	21	92	0.89	0.95	0.88

The overall accuracy was 88%, 93% and 92% for kochia and waterhemp in Carrington site, and ragweed in Mayville research field, respectively. The high accuracy for all three-weed species in two different locations indicated that plant canopy temperature can be a reliable discriminative feature for identifying glyphosate-resistant weeds early after spraying, and even before observing stress symptom on plants. The false positive and negative errors were interpreted by the fact that weeds varied in their level of susceptibility to glyphosate. In fact, there were some actual resistant weeds while their temperature raised early after spraying. However, they were survived after 15 days when the drying symptom was observed on susceptible weeds.

5.5. Conclusions

In this field study, the potential application of supervised classification methods and canopy temperature in weed species and glyphosate-resistant weed detection. Supervised object-based and pixel-based image analysis strategies were employed to assess six different classification methods that included Parallelepipeds (P), Mahalanobis Distance (MD), Maximum Likelihood (ML), Spectral Angle Mapper (SAM), Support Vector Machine (SVM) and Decision Tree (DT). The object-based algorithms developed with mosaicked imagery effectively classified weed species with the overall accuracy and Kappa coefficient values greater than 86% and 0.77,

respectively. However, the performance of pixel-based classification methods was limited in early growth stages due to the high similarity between weed species. The canopy temperature variation within the crop species provided a novel approach for identifying glyphosate-resistant weeds with the accuracy of 88%, 93% and 92.6% for kochia, waterhemp and ragweed. The results of this study can be used in support of SSWM to inhibit the distribution of resistant weeds across the fields.

5.6. Acknowledgment

We thank Dr. Zollinger and Dr. Ostlie from NDSU for their help with the field experiment. The authors would like to thank the North Dakota Agricultural Experiment Station, North Dakota Soybean Council, and the North Dakota Department of Commerce for providing grant support to conduct this research.

6. SUMMARY AND CONCLUSIONS

The main goal of this dissertation was to classify selected weed species and to specifically identify glyphosate-resistance in those weeds for a site-specific weed management system (SSWM). This dissertation aimed at contributing to issues such as 1) protecting the environment by site-specifically applying the herbicide based on weed maps, 2) reducing chemical application cost through a need-based herbicide application, 3) preventing the distribution of glyphosate-resistant weeds, and 5) increasing farmers profits by SSWM. In this study, different weed species were classified based on spectral reflectance. Glyphosate-resistant weeds were identified using plant canopy temperature and spectral reflectance in greenhouse and field scale experiments.

In chapter 2, spectral signature of three common and challenging weed species in ND, USA, namely waterhemp (*Amaranthus rudis*), kochia (*Kochia scoparia*), and lambsquarters (*Chenopodium album*) were collected and analyzed to classify weed species. Results showed noticeable differences between spectral signatures of the three-weed species, especially in the red and red-edge regions and in several parts of the NIR region. The combination of a second-derivative of spectral reflectance in NIR (920-2500 nm) with the supervised SIMCA model could classify weed species with 100% accuracy. The SIMCA model on NIR bands showed a lower risk for misclassification compared to visible region.

In chapter 3, the spectral based weed indices (SWIs) were developed to identify glyphosate-resistant weeds after herbicide application. The indices generated included a combination of weighted single wavelengths and normalized wavelength differences for identifying glyphosate-resistant weeds. The Relief-F algorithm selected 8 discriminative wavelengths on 550-680 nm for 3 required wavelengths and found an optimized combination for

the SWIs. The wavelengths selected for the SWI were sensitive to the photosynthetic pigments and plant cell structure that affected by the detrimental effect of glyphosate application. The model validation indicated that machine learning Random Forest (RF) classifier could discriminate resistant kochia, waterhemp and ragweed with 96%, 97% and 100% accuracy, respectively, based on developed SWIs. The high accuracy of the RF model showed that the selected wavebands can be employed in multispectral camera for weed mapping.

Chapter 4 focused on introducing a new concept for identifying glyphosate-resistant weeds based on plant canopy temperature. Thermal images of both susceptible and resistant types of waterhemp (*Amaranthus rudis*), kochia (*Kochia scoparia*) and ragweed (*Ambrosia artemisiifolia*) were acquired on an hourly basis for the first 96 hours after a glyphosate application. The exploratory analysis of the thermal data indicated that the canopy temperatures of susceptible weeds increase after glyphosate application, which could be attributed to the damages to the physiological mechanism such as photosynthesis caused by herbicide spraying. Significant thermal features for identifying resistant weeds were selected with stepwise regression. The most discriminative thermal feature to identify glyphosate-resistant ragweed and waterhemp was canopy temperature 95 h after spraying while, resistant kochia plants could be identified at 46, 60, 91, 15, 28, 70, and 36 h after a glyphosate application. Furthermore, an SVM model developed to discriminate resistant weeds species based on the plant canopy temperature showed more than 95% accuracy. The high accuracy in identifying glyphosate resistance in three weed species indicated that thermal features of plants after herbicides application were powerful enough to identify the herbicide resistance in different weed species. We recommend that analyzing thermal images 46-95 h after glyphosate application is a potential way to discriminate resistant from susceptible weeds with reliable accuracy.

In chapter 5, a field scale experiment was conducted at research site in Carrington and Mayville, ND, USA to evaluate the greenhouse results on weed species and herbicide resistance identification at field scale. Six supervised classifiers methods including Parallelepipeds (P), Mahalanobis Distance (MD), Maximum Likelihood (ML), Spectral Angle Mapper (SAM), Support Vector Machine (SVM) and Decision Tree (DT) were implemented at pixel level and object level for weed species classification in early growing season. Then, the feasibility of identifying glyphosate-resistant weeds based on canopy temperature was evaluated at field scale.

The object-based algorithms applied on a mosaicked multispectral UAS image effectively classified weed species with the overall accuracy and Kappa coefficient values greater than 86% and 0.77, respectively. The performance of pixel-based classification methods was limited in early growth stages due to the large level of variability in mixed-object pixels. The glyphosate-resistant kochia, waterhemp and ragweed were identified from thermal imagery based on canopy temperature with 88%, 93% and 92% accuracy, respectively.

Currently, there is no cost-effective method to identify and map the distribution of herbicide resistant weeds on large fields. Developing a method and an algorithm to identify weed species and major glyphosate-resistant weeds in the field using UAS imagery in early growing season can support sustainable agriculture by using SSWM.

Remote sensing provides an inexpensive and more efficient method for mapping weed infestations than ground surveys. Timely and efficient classification herbicide resistant weeds allows growers to effectively manage these weeds by using alternative methods before developing multi resistant weeds. Also, the same methodology would be applicable to identify invasive species and weeds in parks, highway sides, and other state properties before they seed and spread. This project has positive impact on crop agriculture across the state and around the

world by identifying herbicide resistant weeds and thereby allowing proper management before they become a major disaster.

6.1. Future Work

Although the research studies and methodologies in this dissertation covered a relatively wide area of identifying weed species and glyphosate-resistant weeds using different methods, future research should aim at further improving the weed identification efficiency. Here are a few recommendations for future research:

1) Identifying glyphosate-resistant weeds considering different degrees of resistance in resistant weeds. This research currently does not consider plants with different levels of herbicide resistance.
2) Perhaps, the research should be expanded to include additional weed species, and resistance to other herbicides.
3) Developing online processing website to generate weed map for creating herbicide application map
4) Conducting field experiment to assess the developed spectral weed indices.

REFERENCES

Abdul Aziz, A. 2015. Integrating a REDD+ Project into the management of a production mangrove forest in Matang Forest Reserve, Malaysia.

Aiello, G., Giovino, I., Vallone, M., Catania, P., Argento, A. 2018. A decision support system based on multisensor data fusion for sustainable greenhouse management. *Journal of Cleaner Production*, **172**, 4057-4065.

AL-Saddik, H., Simon, J.-C., Cointault, F. 2017. Development of Spectral Disease Indices for 'Flavescence Dorée'Grapevine Disease Identification. *Sensors*, **17**(12), 2772.

Alcántara-de la Cruz, R., Fernández-Moreno, P.T., Ozuna, C.V., Rojano-Delgado, A.M., Cruz-Hipolito, H.E., Domínguez-Valenzuela, J.A., Barro, F., De Prado, R. 2016. Target and non-target site mechanisms developed by glyphosate-resistant hairy beggarticks (Bidens pilosa L.) populations from Mexico. *Frontiers in plant science*, **7**, 1492.

Andújar, D., Ribeiro, Á., Fernández-Quintanilla, C., Dorado, J. 2011. Accuracy and Feasibility of Optoelectronic Sensors for Weed Mapping in Wide Row Crops. *Sensors*, **11**(3), 2304.

Andújar, D., Rueda-Ayala, V., Moreno, H., Rosell-Polo, J.R., Escolà, A., Valero, C., Gerhards, R., Fernández-Quintanilla, C., Dorado, J., Griepentrog, H.-W. 2013. Discriminating Crop, Weeds and Soil Surface with a Terrestrial LIDAR Sensor. *Sensors (Basel, Switzerland)*, **13**(11), 14662-14675.

Andújar, D., Weis, M., Gerhards, R. 2012. An Ultrasonic System for Weed Detection in Cereal Crops. *Sensors*, **12**(12), 17343.

Anjum, S.A., Xie, X.-y., Wang, L.-c., Saleem, M.F., Man, C., Lei, W. 2011. Morphological, physiological and biochemical responses of plants to drought stress. *African Journal of Agricultural Research*, **6**(9), 2026-2032.

Bajwa, S.G., Kulkarni, S.S. 2011. *Hyperspectral data mining*. Boca Raton, London, New York: CRC Press/Taylor and Francis Group.

Bates, D., Maechler, M., Bolker, B., Walker, S. 2014. lme4: Linear mixed-effects models using Eigen and S4. *R package version*, **1**(7), 1-23.

Ben-Gal, A., Agam, N., Alchanatis, V., Cohen, Y., Yermiyahu, U., Zipori, I., Presnov, E., Sprintsin, M., Dag, A. 2009. Evaluating water stress in irrigated olives: correlation of soil water status, tree water status, and thermal imagery. *Irrigation Science*, **27**(5), 367-376.

Benbrook, C.M. 2016. Trends in glyphosate herbicide use in the United States and globally. *Environmental Sciences Europe*, **28**(1), 3.

Benbrook, C.M. 2018. Why Regulators Lost Track and Control of Pesticide Risks: Lessons From the Case of Glyphosate-Based Herbicides and Genetically Engineered-Crop Technology. *Current environmental health reports*, **5**(3), 387-395.

Berni, J., Zarco-Tejada, P., Suárez, L., González-Dugo, V., Fereres, E. 2009. Remote sensing of vegetation from UAV platforms using lightweight multispectral and thermal imaging sensors. *Int. Arch. Photogramm. Remote Sens. Spatial Inform. Sci*, **38**(6).

Biller, R.H. 1998. Reduced Input of Herbicides by Use of Optoelectronic Sensors. *Journal of Agricultural Engineering Research*, **71**(4), 357-362.

Blackburn, G.A. 2006. Hyperspectral remote sensing of plant pigments. *Journal of experimental botany*, **58**(4), 855-867.

Bonny, S. 2016. Genetically modified herbicide-tolerant crops, weeds, and herbicides: overview and impact. *Environmental management*, **57**(1), 31-48.

Brereton, R.G. 2003. Pattern Recognition. in: *Chemometrics*, John Wiley & Sons, Ltd, pp. 183-269.

Broge, N.H., Leblanc, E. 2001. Comparing prediction power and stability of broadband and hyperspectral vegetation indices for estimation of green leaf area index and canopy chlorophyll density. *Remote sensing of environment*, **76**(2), 156-172.

Burgos-Artizzu, X.P., Ribeiro, A., Guijarro, M., Pajares, G. 2011. Real-time image processing for crop/weed discrimination in maize fields. *Computers and Electronics in Agriculture*, **75**(2), 337-346.

Burns, D.A., Ciurczak, E.W. 2007. *Handbook of Near-Infrared Analysis, Third Edition*. CRC Press.

Cao, L.-J., Tay, F.E.H. 2003. Support vector machine with adaptive parameters in financial time series forecasting. *IEEE Transactions on neural networks*, **14**(6), 1506-1518.

Cardina, J., Doohan, D.J. 2000. Weed biology and precision farming. In: Site-Specific Management Guidelines, SSMG-25. *Purdue University, Indiana, USA.*

Castillejo-González, I.L., Pena-Barragán, J.M., Jurado-Expósito, M., Mesas-Carrascosa, F.J., López-Granados, F. 2014. Evaluation of pixel-and object-based approaches for mapping wild oat (Avena sterilis) weed patches in wheat fields using QuickBird imagery for site-specific management. *European Journal of Agronomy*, **59**, 57-66.

Che'Ya, N.N. 2016. Site-Specific Weed Management Using Remote Sensing.

Christensen, S., SØGaard, H.T., Kudsk, P., NØRremark, M., Lund, I., Nadimi, E.S., JØRgensen, R. 2009. Site-specific weed control technologies. *Weed Research*, **49**(3), 233-241.

Christiansen, P., Steen, K.A., Jørgensen, R.N., Karstoft, H. 2014. Automated detection and recognition of wildlife using thermal cameras. *Sensors*, **14**(8), 13778-13793.

Colbach, N., Fernier, A., Le Corre, V., Messéan, A., Darmency, H. 2017. Simulating changes in cropping practises in conventional and glyphosate-tolerant maize. I. Effects on weeds. *Environmental Science and Pollution Research*, **24**(12), 11582-11600.

Corrêa, E.A., Dayan, F.E., Owens, D.K., Rimando, A.M., Duke, S.O. 2016. Glyphosate-Resistant and Conventional Canola (Brassica napus L.) Responses to Glyphosate and Aminomethylphosphonic Acid (AMPA) Treatment. *Journal of agricultural and food chemistry*, **64**(18), 3508-3513.

Costa, J.M., Grant, O.M., Chaves, M.M. 2013. Thermography to explore plant–environment interactions. *Journal of experimental botany*, **64**(13), 3937-3949.

Cristianini, N., Shawe-Taylor, J. 2000. *An introduction to support vector machines and other kernel-based learning methods*. Cambridge university press.

Darlington, R.B., Hayes, A.F. 2016. *Regression analysis and linear models: Concepts, applications, and implementation*. Guilford Publications.

Davis, C., Busch, K., Rabbe, D., Busch, M., Lusk, J. 2015. Rapid, non-destructive, textile classification using SIMCA on diffuse near-infrared reflectance spectra. *Journal of Modern Physics*, **6**, 711-718.

de Castro, A.-I., Jurado-Expósito, M., Gómez-Casero, M.-T., López-Granados, F. 2012. Applying neural networks to hyperspectral and multispectral field data for discrimination of cruciferous weeds in winter crops. *The Scientific World Journal*, **2012**.

Dogan, T., Uysal, A.K. 2018. The Impact of Feature Selection on Urban Land Cover Classification. *International Journal of Intelligent Systems and Applications in Engineering*, **6**(1), 59-64.

Eddy, P., Smith, A., Hill, B., Peddle, D., Coburn, C., Blackshaw, R. 2008. Hybrid segmentation–artificial neural network classification of high resolution hyperspectral imagery for site-specific herbicide management in agriculture. *Photogrammetric Engineering & Remote Sensing*, **74**(10), 1249-1257.

Eddy, P., Smith, A., Hill, B., Peddle, D., Coburn, C., Blackshaw, R. 2014. Weed and crop discrimination using hyperspectral image data and reduced bandsets. *Canadian Journal of Remote Sensing*, **39**(6), 481-490.

Esbensen, K.H., Guyot, D., Westad, F., Houmoller, L.P. 2002. *Multivariate data analysis - in practice: An introduction to multivariate data analysis and experimental design*. Camo Process AS, Trondheim, Norway.

Espinoza, C.Z., Sankaran, S., Pumphrey, M.O., Miklas, P.N., Carter, A.H., Vandemark, G.J., Knowles, N.R., Khot, L.R., Jarolmasjed, S., Sathuvalli, V.R. 2015. Low-altitude, high-resolution aerial imaging systems for row and field crop phenotyping: A review.

Evans, F.H., Diggle, A.J. 2008. A spatio-temporal modelling framework for assessing the impact of weed management technologies on the spread of herbicide resistance. *Proceedings of the 16th Australian Weeds Conference, Cairns Convention Centre, North Queensland, Australia, 18-22 May, 2008*. Queensland Weed Society. pp. 218-220.

Everitt, J.H., Yang, C., Summy, K.R., Glomski, L.M., Owens, C.S. 2011. Evaluation of hyperspectral reflectance data for discriminating six aquatic weeds. *Journal of Aquatic Plant Management*, **49**, 94-100.

FAOSTAT. 2014. Statistical year book of FAO, available at http://faostat.fao.org.

Ferguson, R., Rundquist, D. 2018. Remote sensing for site-specific crop management. *Precision agriculture basics*(precisionagbasics), 103-118.

Frels, K., Guttieri, M., Joyce, B., Leavitt, B., Baenziger, P.S. 2018. Evaluating canopy spectral reflectance vegetation indices to estimate nitrogen use traits in hard winter wheat. *Field Crops Research*, **217**, 82-92.

Gålfalk, M., Karlson, M., Crill, P., Bousquet, P., Bastviken, D. 2018. A simple approach for efficient collection of field reference data for calibrating remote sensing mapping of northern wetlands. *Biogeosciences*, **15**(5), 1549.

Gara, T.W., Darvishzadeh, R., Skidmore, A.K., Wang, T. 2018. Impact of vertical canopy position on leaf spectral properties and traits across multiple species. *Remote sensing*, **10**(2), 346.

Garcia-Ruiz, F., Sankaran, S., Maja, J.M., Lee, W.S., Rasmussen, J., Ehsani, R. 2013. Comparison of two aerial imaging platforms for identification of Huanglongbing-infected citrus trees. *Computers and Electronics in Agriculture*, **91**, 106-115.

Garcia-Ruiz, F.J., Wulfsohn, D., Rasmussen, J. 2015. Sugar beet (Beta vulgaris L.) and thistle (Cirsium arvensis L.) discrimination based on field spectral data. *Biosystems Engineering*, **139**, 1-15.

Ghani, I.M.M., Ahmad, S. 2010. Stepwise multiple regression method to forecast fish landing. *Procedia-Social and Behavioral Sciences*, **8**, 549-554.

Gianessi, L., Reigner, N. 2006. The value of herbicides in US crop production. 2005 Update. Croplife Foundation. *Crop Protection Research Institute (CPRI)*.

Gil, Y., Sinfort, C. 2005. Emission of pesticides to the air during sprayer application: A bibliographic review. *Atmospheric Environment*, **39**(28), 5183-5193.

Gomes, M.P., Le Manac'h, S.G., Maccario, S., Labrecque, M., Lucotte, M., Juneau, P. 2016. Differential effects of glyphosate and aminomethylphosphonic acid (AMPA) on

photosynthesis and chlorophyll metabolism in willow plants. *Pesticide biochemistry and physiology*, **130**, 65-70.
Gomes, M.P., Manac'h, L., Sarah, G., Hénault-Ethier, L., Labrecque, M., Lucotte, M., Juneau, P. 2017. Glyphosate-dependent inhibition of photosynthesis in willow. *Frontiers in plant science*, **8**, 207.
Gray, C.J., Shaw, D.R., Bruce, L.M. 2009. Utility of Hyperspectral Reflectance for Differentiating Soybean (Glycine max) and Six Weed Species. *Weed Technology*, **23**(1), 108-119.
Green, J.M. 2018. The rise and future of glyphosate and glyphosate-resistant crops. *Pest management science*, **74**(5), 1035-1039.
Gutjahr, C., Gerhards, R. 2010. Decision rules for site-specific weed management. in: *Precision Crop Protection-the Challenge and Use of Heterogeneity*, Springer, pp. 223-239.
Hadoux, X., Gorretta, N., Roger, J.-M., Bendoula, R., Rabatel, G. 2014. Comparison of the efficacy of spectral pre-treatments for wheat and weed discrimination in outdoor conditions. *Computers and Electronics in Agriculture*, **108**, 242-249.
Haff, R.P., Slaughter, D.C., Jackson, E.S. 2011. X-Ray based stem detection in an automatic tomato weeding system. *Transactions of the ASABE*, **27**(5), 803-810.
Harker, K., O'Donovan, J., Blackshaw, R., Hall, L., Willenborg, C., Kutcher, H., Gan, Y., Lafond, G., May, W., Grant, C. 2013. Effect of agronomic inputs and crop rotation on biodiesel quality and fatty acid profiles of direct-seeded canola. *Canadian journal of plant science*, **93**(4), 577-588.
He, K.S., Bradley, B.A., Cord, A.F., Rocchini, D., Tuanmu, M.-N., Schmidtlein, S., Turner, W., Wegmann, M., Pettorelli, N. 2015. Will remote sensing shape the next generation of species distribution models? *Remote Sensing in Ecology and Conservation*, **1**(1), 4-18.
Hong, S., Minzan, L., Zhang, Q. 2012. Detection system of smart sprayers: Status, challenges, and perspectives. *International Journal of Agricultural and Biological Engineering*, **5**(3), 10.
Hunt, E.R., Hively, W.D., Fujikawa, S.J., Linden, D.S., Daughtry, C.S., McCarty, G.W. 2010. Acquisition of NIR-green-blue digital photographs from unmanned aircraft for crop monitoring. *Remote Sensing*, **2**(1), 290-305.
Jackson, J.E. 2004. Linear Models I: Regression; PCA of Predictor Variables. in: *A User's Guide to Principal Components*, John Wiley & Sons, Inc., pp. 263-300.
Jayadeva, Deb, A.K., Chandra, S. 2002. Binary classification by SVM based tree type neural networks. *Proceeding of the 2002 International Joint Conference on Neural Networks, Vols 1-3*, 2773-2778.
Jayadeva, A.K.D., Chandra, S. 2002. Binary classification by SVM based tree type neural network. *Proc. Int. Conf. Neural Netw*. pp. 2773-2778.
Jayasumana, C., Gunatilake, S., Senanayake, P. 2014. Glyphosate, hard water and nephrotoxic metals: are they the culprits behind the epidemic of chronic kidney disease of unknown etiology in Sri Lanka? *International journal of environmental research and public health*, **11**(2), 2125-2147.
Jones, H. 1999. Use of thermography for quantitative studies of spatial and temporal variation of stomatal conductance over leaf surfaces. *Plant, Cell & Environment*, **22**(9), 1043-1055.
Karimi, Y., Prasher, S., Patel, R., Kim, S. 2006. Application of support vector machine technology for weed and nitrogen stress detection in corn. *Computers and electronics in agriculture*, **51**(1-2), 99-109.

Kuhlgert, S., Austic, G., Zegarac, R., Osei-Bonsu, I., Hoh, D., Chilvers, M.I., Roth, M.G., Bi, K., TerAvest, D., Weebadde, P. 2016. MultispeQ Beta: a tool for large-scale plant phenotyping connected to the open PhotosynQ network. *Royal Society open science*, **3**(10), 160592.

Kunz, C., Weber, J.F., Peteinatos, G.G., Sökefeld, M., Gerhards, R. 2018. Camera steered mechanical weed control in sugar beet, maize and soybean. *Precision Agriculture*, **19**(4), 708-720.

Laliberte, A.S., Herrick, J.E., Rango, A., Winters, C. 2010. Acquisition, orthorectification, and object-based classification of unmanned aerial vehicle (UAV) imagery for rangeland monitoring. *Photogrammetric Engineering & Remote Sensing*, **76**(6), 661-672.

Lambert, J., Hicks, H., Childs, D., Freckleton, R. 2018. Evaluating the potential of Unmanned Aerial Systems for mapping weeds at field scales: a case study with Alopecurus myosuroides. *Weed research*, **58**(1), 35-45.

Lee, W., Alchanatis, V., Yang, C., Hirafuji, M., Moshou, D., Li, C. 2010. Sensing technologies for precision specialty crop production. *Computers and electronics in agriculture*, **74**(1), 2-33.

Lehmann, J., Große-Stoltenberg, A., Römer, M., Oldeland, J. 2015. Field spectroscopy in the VNIR-SWIR region to discriminate between Mediterranean native plants and exotic-invasive shrubs based on leaf tannin content. *Remote Sensing*, **7**(2), 1225.

Lin, C. 2010. A support vector machine embedded weed identification system.

Liu, B., Fang, J., Liu, X., Zhang, L., Zhang, B., Tong, Q. 2010. Research on crop-weed discrimination using a field imaging spectrometer. *Guang pu xue yu guang pu fen xi= Guang pu*, **30**(7), 1830-1833.

Liu, T., Abd-Elrahman, A. 2018. Multi-view object-based classification of wetland land covers using unmanned aircraft system images. *Remote Sensing of Environment*, **216**, 122-138.

Livingston, M., Fernandez-Cornejo, J., Unger, J., Osteen, C., Schimmelpfennig, D., Park, T., Lambert, D.M. 2015. The economics of glyphosate resistance management in corn and soybean production.

López Granados, F., Peña Barragán, J.M., Jurado-Expósito, M., Francisco-Fernández, M., Cao, R., Alonso-Betanzos, A., Fontela-Romero, Ó. 2008. Multispectral classification of grass weeds and wheat (Triticum durum) using linear and nonparametric functional discriminant analysis and neural networks. *Weed Research*, **37**, 28-37.

Lorentz, L., Gaines, T.A., Nissen, S.J., Westra, P., Strek, H.J., Dehne, H.W., Ruiz-Santaella, J.P., Beffa, R. 2014. Characterization of glyphosate resistance in Amaranthus tuberculatus populations. *Journal of agricultural and food chemistry*, **62**(32), 8134-8142.

Mahlein, A.-K., Rumpf, T., Welke, P., Dehne, H.-W., Plümer, L., Steiner, U., Oerke, E.-C. 2013. Development of spectral indices for detecting and identifying plant diseases. *Remote Sensing of Environment*, **128**, 21-30.

Maire, V., Wright, I.J., Prentice, I.C., Batjes, N.H., Bhaskar, R., van Bodegom, P.M., Cornwell, W.K., Ellsworth, D., Niinemets, Ü., Ordonez, A. 2015. Global effects of soil and climate on leaf photosynthetic traits and rates. *Global Ecology and Biogeography*, **24**(6), 706-717.

Mangus, D.L., Sharda, A., Zhang, N. 2016. Development and evaluation of thermal infrared imaging system for high spatial and temporal resolution crop water stress monitoring of corn within a greenhouse. *Computers and Electronics in Agriculture*, **121**, 149-159.

Mateos-Naranjo, E., Redondo-Gómez, S., Cox, L., Cornejo, J., Figueroa, M.E. 2009. Effectiveness of glyphosate and imazamox on the control of the invasive cordgrass Spartina densiflora. *Ecotoxicology and Environmental Safety*, **72**(6), 1694-1700.
Morozova, M., Elizarova, T., Pleteneva, T. 2013. Discriminant analysis and Mahalanobis distance (NIR diffuse reflectance spectra) in the assessment of drug's batch-to-batch dispersion and quality threshold establishment. *European Scientific Journal, ESJ*, **9**(27).
Myers, J.P., Antoniou, M.N., Blumberg, B., Carroll, L., Colborn, T., Everett, L.G., Hansen, M., Landrigan, P.J., Lanphear, B.P., Mesnage, R. 2016. Concerns over use of glyphosate-based herbicides and risks associated with exposures: a consensus statement. *Environmental Health*, **15**(1), 19.
Oerke, E.-C. 2006. Crop losses to pests. *The Journal of Agricultural Science*, **144**(1), 31-43.
Pandya, R., Pandya, J. 2015. C5. 0 algorithm to improved decision tree with feature selection and reduced error pruning. *International Journal of Computer Applications*, **117**(16), 18-21.
Pantazi, X.-E., Moshou, D., Bravo, C. 2016. Active learning system for weed species recognition based on hyperspectral sensing. *Biosystems Engineering*, **146**, 193-202.
Pena, J.M., Torres-Sánchez, J., de Castro, A.I., Kelly, M., López-Granados, F. 2013. Weed mapping in early-season maize fields using object-based analysis of unmanned aerial vehicle (UAV) images. *PloS one*, **8**(10), e77151.
Peña, J.M., Torres-Sánchez, J., de Castro, A.I., Kelly, M., López-Granados, F. 2013. Weed mapping in early-season maize fields using object-based analysis of unmanned aerial vehicle (UAV) images. *PloS one*, **8**(10), e77151.
Pérez-Ortiz, M., Peña, J., Gutiérrez, P.A., Torres-Sánchez, J., Hervás-Martínez, C., López-Granados, F. 2015. A semi-supervised system for weed mapping in sunflower crops using unmanned aerial vehicles and a crop row detection method. *Applied Soft Computing*, **37**, 533-544.
Pflanz, M., Nordmeyer, H., Schirrmann, M. 2018. Weed Mapping with UAS Imagery and a Bag of Visual Words Based Image Classifier. *Remote Sensing*, **10**(10), 1530.
Pimentel, D., Acquay, H., Biltonen, M., Rice, P., Silva, M., Nelson, J., Lipner, V., Giordano, S., Horowitz, A., D'Amore, M. 1992. Environmental and Economic Costs of Pesticide Use. *BioScience*, **42**(10), 750-760.
Piron, A., van der Heijden, F., Destain, M.F. 2011. Weed detection in 3D images. *Precision Agriculture*, **12**(5), 607-622.
Pollegioni, L., Schonbrunn, E., Siehl, D. 2011. Molecular basis of glyphosate resistance–different approaches through protein engineering. *The FEBS journal*, **278**(16), 2753-2766.
Primicerio, J., Di Gennaro, S.F., Fiorillo, E., Genesio, L., Lugato, E., Matese, A., Vaccari, F.P. 2012. A flexible unmanned aerial vehicle for precision agriculture. *Precision Agriculture*, **13**(4), 517-523.
Qin, Z., Wei, D., Xiu, W., Chun-jiang, W. 2013. Research on spectra recognition method for cabbages and weeds based on PCA and SIMCA. *Spectroscopy and Spectral Analysis* (10), 2745-2750.
Rabatel, G., Ougache, F., Gorretta, N., Ecarnot, M. 2011. Hyperspectral imagery to discriminate weeds in wheat. *Robotics and associated High technologies and Equipment for Agriculture (RHEA-2011)*. Pablo Gonzalez de Santos & Gilles Rabatel. pp. p. 35-p. 46.
Radwan, D., Fayez, K. 2016. Photosynthesis, antioxidant status and gas-exchange are altered by glyphosate application in peanut leaves. *Photosynthetica*, **54**(2), 307-316.

Rao, A., Singh, R.G., Mahajan, G., Wani, S. 2018. Weed research issues, challenges, and opportunities in India. *Crop Protection*.

Reddy, K.N., Huang, Y., Lee, M.A., Nandula, V.K., Fletcher, R.S., Thomson, S.J., Zhao, F. 2014a. Glyphosate-resistant and glyphosate-susceptible Palmer amaranth (Amaranthus palmeri S. Wats.): hyperspectral reflectance properties of plants and potential for classification. *Pest Manag Sci*, **70**(12), 1910-7.

Reddy, K.N., Huang, Y., Lee, M.A., Nandula, V.K., Fletcher, R.S., Thomson, S.J., Zhao, F. 2014b. Glyphosate-resistant and glyphosate-susceptible Palmer amaranth (Amaranthus palmeri S. Wats.): hyperspectral reflectance properties of plants and potential for classification. *Pest management science*, **70**(12), 1910-1917.

Roberts, D.A., Ustin, S.L., Ogunjemiyo, S., Greenberg, J., Dobrowski, S.Z., Chen, J., Hinckley, T.M. 2004. Spectral and structural measures of northwest forest vegetation at leaf to landscape scales. *Ecosystems*, **7**(5), 545-562.

Rogalski, A. 2003. Infrared detectors: status and trends. *Progress in Quantum Electronics*, **27**(2–3), 59-210.

Schütte, G., Eckerstorfer, M., Rastelli, V., Reichenbecher, W., Restrepo-Vassalli, S., Ruohonen-Lehto, M., Saucy, A.-G.W., Mertens, M. 2017. Herbicide resistance and biodiversity: agronomic and environmental aspects of genetically modified herbicide-resistant plants. *Environmental Sciences Europe*, **29**(1), 5.

Scotford, I.M., Miller, P.C.H. 2005. Applications of Spectral Reflectance Techniques in Northern European Cereal Production: A Review. *Biosystems Engineering*, **90**(3), 235-250.

Shapira, U., Herrmann, I., Karnieli, A., Bonfil, D.J. 2013. Field spectroscopy for weed detection in wheat and chickpea fields. *International Journal of Remote Sensing*, **34**(17), 6094-6108.

Shirzadifar, A., Bajwa, S., Mireei, S.A., Howatt, K., Nowatzki, J. 2018. Weed species discrimination based on SIMCA analysis of plant canopy spectral data. *Biosystems Engineering*, **171**, 143-154.

Singh, A., Ganapathysubramanian, B., Singh, A.K., Sarkar, S. 2016. Machine learning for high-throughput stress phenotyping in plants. *Trends in plant science*, **21**(2), 110-124.

Slaughter, D.C., Giles, D.K., Downey, D. 2008. Autonomous robotic weed control systems: A review. *Computers and Electronics in Agriculture*, **61**(1), 63-78.

Smith, A.M., Blackshaw, R.E. 2003. Weed–crop discrimination using remote sensing: a detached leaf experiment. *Weed Technology*, **17**(4), 811-820.

Sonobe, R., Wang, Q. 2017. Hyperspectral indices for quantifying leaf chlorophyll concentrations performed differently with different leaf types in deciduous forests. *Ecological Informatics*, **37**, 1-9.

Sosnowski, T., Bieszczad, G., Madura, H., Kastek, M. 2018. Thermovision system for flying objects detection. *2018 Baltic URSI Symposium (URSI)*. IEEE. pp. 141-144.

Stephens, D., Diesing, M. 2014. A comparison of supervised classification methods for the prediction of substrate type using multibeam acoustic and legacy grain-size data. *PloS one*, **9**(4), e93950.

Sui, R., Thomasson, J.A., Hanks, J., Wooten, J. 2008. Ground-based sensing system for weed mapping in cotton. *Computers and Electronics in Agriculture*, **60**(1), 31-38.

Testi, L., Goldhamer, D., Iniesta, F., Salinas, M. 2008. Crop water stress index is a sensitive water stress indicator in pistachio trees. *Irrigation Science*, **26**(5), 395-405.

Thorp, K.R., Tian, L.F. 2004. A Review on Remote Sensing of Weeds in Agriculture. *Precision Agriculture*, **5**(5), 477-508.
Tian, L. 2002. Development of a sensor-based precision herbicide application system. *Computers and Electronics in Agriculture*, **36**(2–3), 133-149.
Torres-Sánchez, J., López-Granados, F., De Castro, A.I., Peña-Barragán, J.M. 2013. Configuration and specifications of an unmanned aerial vehicle (UAV) for early site specific weed management. *PloS one*, **8**(3), e58210.
Van der Wal, T., Abma, B., Viguria, A., Prévinaire, E., Zarco-Tejada, P., Serruys, P., van Valkengoed, E., van der Voet, P. 2013. Fieldcopter: unmanned aerial systems for crop monitoring services. in: *Precision agriculture'13*, Springer, pp. 169-175.
Von Bueren, S., Burkart, A., Hueni, A., Rascher, U., Tuohy, M., Yule, I. 2015. Deploying four optical UAV-based sensors over grassland: challenges and limitations. *Biogeosciences*, **12**(1), 163.
Voyant, C., Notton, G., Kalogirou, S., Nivet, M.-L., Paoli, C., Motte, F., Fouilloy, A. 2017. Machine learning methods for solar radiation forecasting: A review. *Renewable Energy*, **105**, 569-582.
Vrindts, E., De Baerdemaeker, J., Ramon, H. 2002. Weed Detection Using Canopy Reflection. *Precision Agriculture*, **3**(1), 63-80.
Wang, N., Zhang, N., Dowell, F.E., Peterson, D.E. 2001. Design of an optical weed sensor using plant spectral characteristics. *Transactions of the ASAE*, **44**(2), 409-419.
Weis, M., Gutjahr, C., Rueda Ayala, V., Gerhards, R., Ritter, C., Schölderle, F. 2008. Precision farming for weed management: techniques. *Gesunde Pflanzen*, **60**(4), 171-181.
Weis, M., Sökefeld, M. 2010. Detection and Identification of Weeds. in: *Precision Crop Protection - the Challenge and Use of Heterogeneity*, (Eds.) E.-C. Oerke, R. Gerhards, G. Menz, R.A. Sikora, Springer Netherlands. Dordrecht, pp. 119-134.
Westwood, J.H., Charudattan, R., Duke, S.O., Fennimore, S.A., Marrone, P., Slaughter, D.C., Swanton, C., Zollinger, R. 2018. Weed Management in 2050: Perspectives on the Future of Weed Science. *Weed Science*, **66**(3), 275-285.
Whitaker, J.R., Burton, J.D., York, A.C., Jordan, D.L., Chandi, A. 2013. Physiology of glyphosate-resistant and glyphosate-susceptible palmer amaranth (Amaranthus palmeri) biotypes collected from North Carolina. *International journal of agronomy*, **2013**.
Wilson, J.H., Zhang, C., Kovacs, J.M. 2014. Separating crop species in northeastern Ontario using hyperspectral data. *Remote Sensing*, **6**(2), 925-945.
Wold, S., Esbensen, K., Geladi, P. 1987. Principal component analysis. *Chemometrics and Intelligent Laboratory Systems*, **2**(1), 37-52.
Wu, C., Niu, Z., Tang, Q., Huang, W. 2008. Estimating chlorophyll content from hyperspectral vegetation indices: Modeling and validation. *Agricultural and forest meteorology*, **148**(8-9), 1230-1241.
Xu, S., Hossain, M.M., Lau, B.B., To, T.Q., Rawal, A., Aldous, L. 2017. Total quantification and extraction of shikimic acid from star anise (llicium verum) using solid-state NMR and cellulose-dissolving aqueous hydroxide solutions. *Sustainable Chemistry and Pharmacy*, **5**, 115-121.
Yadav, T., Chopra, N.K., Chopra, N., Kumar, R., Soni, P. 2018. Assessment of critical period of crop-weed competition in forage cowpea (Vigna unguiculata) and its effect on seed yield and quality. *INDIAN SOCIETY OF AGRONOMY*, 124.

Yang, C., Everitt, J.H. 2010. Mapping three invasive weeds using airborne hyperspectral imagery. *Ecological informatics*, **5**(5), 429-439.
Yang, C., Lee, W.S., Williamson, J.G. 2012. Classification of blueberry fruit and leaves based on spectral signatures. *Biosystems Engineering*, **113**(4), 351-362.
Yanniccari, M., Tambussi, E., Istilart, C., Castro, A.M. 2012. Glyphosate effects on gas exchange and chlorophyll fluorescence responses of two Lolium perenne L. biotypes with differential herbicide sensitivity. *Plant Physiology and Biochemistry*, **57**, 210-217.
Yontz, M. 2014. Weeds and income. *Farm Futures*, 12.
Zhang, C., Filella, I., Garbulsky, M.F., Peñuelas, J. 2016. Affecting factors and recent improvements of the photochemical reflectance index (PRI) for remotely sensing foliar, canopy and ecosystemic radiation-use efficiencies. *Remote Sensing*, **8**(9), 677.
Zhang, C., Filella, I., Liu, D., Ogaya, R., Llusià, J., Asensio, D., Peñuelas, J. 2017. Photochemical reflectance index (PRI) for detecting responses of diurnal and seasonal photosynthetic activity to experimental drought and warming in a mediterranean shrubland. *Remote Sensing*, **9**(11), 1189.
Zhong, G., Wu, Z., Liu, N., Yin, J. 2018. Phosphate alleviation of glyphosate-induced toxicity in Hydrocharis dubia (Bl.) Backer. *Aquatic Toxicology*.
Zhou, Z., Plauborg, F., Thomsen, A.G., Andersen, M.N. 2017. A RVI/LAI-reference curve to detect N stress and guide N fertigation using combined information from spectral reflectance and leaf area measurements in potato. *European journal of agronomy*, **87**, 1-7.
Zimdahl, R.L. 2018. *Fundamentals of weed science*. Academic Press.
Zobiole, L.H.S., Kremer, R.J., de Oliveira Jr, R.S., Constantin, J. 2012. Glyphosate effects on photosynthesis, nutrient accumulation, and nodulation in glyphosate-resistant soybean. *Journal of Plant Nutrition and Soil Science*, **175**(2), 319-330.
Zollinger, R. 2016. North Dakota Weed Control Guide. *NDSU Extension Service*.
Zollinger, R., Christoffers, M., Endres, G., Gramig, G., Howatt, K., Jenks, B., Lym, R., Stachler, J., Thostenson, A., Valenti, H. 2006. North Dakota weed control guide. *Fargo, ND, North Dakota State University Extension Service Publication W-253*.